UNIVERSITÀ DI PARMA

UNIVERSITA' DEGLI STUDI DI PARMA

DOTTORATO DI RICERCA IN

"Ingegneria Industriale"

CICLO XXXVII°

Development and Validation of In-Situ Acoustic Characterization Methods: A Comparative Analysis of Innovative Measurement Techniques for Complex Materials

Coordinatore:

Chiar.mo Prof. ROYER CARFAGNI Gianni

Tutore:

Chiar.mo Prof. FARINA ANGELO

Dottoranda: FERRARI JESSICA

Anni Accademici 2021/2022 – 2023/2024

1. STUDY OF THE SOUND ABSORPTION COEFFICIENT OF MATERIALS

1.1 INTRODUCTION TO FUNDAMENTAL ACOUSTIC PHENOMENA (STATE OF THE ART)

Applied acoustics, particularly the study and characterization of acoustic materials, represents a fundamental field for understanding and optimizing noise control systems. To fully understand the acoustic behavior of materials, it is essential to analyze three fundamental parameters that are closely interconnected: acoustic absorption, acoustic reflection and acoustic impedance.

1.1.1 The Acoustic Absorption Phenomenon

Acoustic absorption is a complex physical phenomenon that occurs when a sound wave interacts with a surface or material. During this interaction, part of the incident sound energy is transformed into other forms of energy, mainly thermal, through three main mechanisms that operate simultaneously:

1. Viscous dissipation:
    - The sound wave induces vibration of air particles within the material's pores.
    - Friction between moving air and pore walls converts sound energy into heat.
    - This mechanism is particularly effective in porous materials like mineral wools and foams.
    - Efficiency depends on pore size and material flow resistivity.
2. Membrane Resonance Dissipation:
    - The material vibrates as a membrane under the action of the sound wave.
    - Material deformations cause energy dissipation through mechanical hysteresis.
    - This mechanism is particularly effective for thin panels and stretched membranes.
    - Resonance frequency depends on mass and material stiffness.
3. Cavity Resonance Dissipation:
    - Based on the Helmholtz resonator principle.
    - Air in a closed volume acts like a spring when excited.
    - Particularly effective for selective absorption at specific frequencies.
    - Resonance frequency tuning depends on cavity dimensions.

1.1.2 Acoustic Absorption Coefficient

The acoustic absorption coefficient α represents the quantitative measure of a material's effectiveness in absorbing sound energy. It is defined as the ratio between absorbed energy and incident energy on the material surface:

$$\alpha = \frac{Absorbed\ energy}{Incident\ energy}$$

This coefficient varies between 0 (total reflection) and 1 (total absorption) and depends on:

- Frequency of incident sound;
- Angle of incidence;
- Physical characteristics of the material (pore size, open or closed cell, etc.);
- Material thickness;
- Mounting method.

It is fundamental to distinguish between absorption and acoustic isolation, two phenomena often confused but substantially different in their nature and application.

Acoustic absorption, which manifests through the transformation of sound energy into thermal energy, requires materials with specific characteristics: a porous or fibrous structure that allows sound wave penetration, low density to favor fiber vibrations, and high flow resistance to maximize energy dissipation. Materials like rock wool, glass wool or open-cell polyurethane foams represent excellent examples of sound-absorbing materials, each with its own specific performance characteristics at different frequencies.

Acoustic isolation, on the other hand, is based on completely different principles. The mass law, which governs the behavior of sound insulating materials, requires high surface mass and air impermeability. Materials such as cement, high-density plasterboard or lead sheets perfectly exemplify these characteristics. Their effectiveness in reducing sound transmission between environments is based on their ability to oppose inertial resistance to the vibration induced by the sound wave.

1.1.3 Reflection Coefficient

When discussing acoustic absorption, it is fundamental to clearly distinguish it from acoustic isolation, another phenomenon often confused with absorption but substantially different. While absorption concerns a material's ability to transform sound energy into other forms of energy, isolation refers to the ability to prevent sound transmission between two environments. The reflection coefficient R remains however closely linked to the absorption coefficient and is a complex number that includes information about both amplitude and phase of the reflected wave compared to the incident wave. It is expressed as:

$$R = \frac{p_r}{p_i}$$

where:

- p_r is the pressure of the reflected wave;
- p_i is the pressure of the incident wave.

The fundamental relationship between absorption and reflection is:

$$\alpha = 1 - |R|^2$$

Thus, a high reflection coefficient indicates that the material reflects most of the sound energy, while a low reflection coefficient indicates that the material absorbs or transmits most of the sound energy.

1.1.4 Acoustic Impedance

Acoustic impedance Z represents the resistance that a material opposes to the passage of sound waves (i.e. to sound propagation). Therefore, impedance define the ease with which the particles of the medium can be set in motion and is defined as the ratio between sound pressure and particle velocity:

$$Z = \frac{p}{u}$$

where:

- p is a scalar quantity that indicates sound pressure in Pascal [Pa]. Sound pressure represents the local variation of air pressure relative to atmospheric pressure caused by acoustic wave propagation. It is typically measured with condenser microphones.
- u is a vector quantity (having both amplitude and direction) that indicates particle velocity in meters per second [m/s]. Particle velocity represents the oscillation velocity of air molecules around their equilibrium position during the passage of a sound wave. It is important to note that this is not the net movement of air (like in wind), but a local oscillation, therefore it varies with position in space and distance from the source. It can be measured with a hot-wire anemometer as in the case of the Microflown probe, or with microphone arrays like the Sonocat probe, or with a velocity sensor such as a LDV laser [1] [2].

Therefore, high acoustic impedance (also called characteristic impedance) indicates that the material reflects most of the sound energy, while low impedance indicates that the material absorbs or transmits most of the sound energy.

In a progressive plane wave in free field, sound pressure and particle velocity are characterized by:

- being in phase with each other;
- a constant ratio of their amplitudes;
- ratio equal to the characteristic impedance of the medium (ρc).

In real situations, this relationship becomes more complex. It is important to analyze three particular situations that are frequently encountered in practical applications: the near field, standing waves and the diffuse field.

The near field represents the region of space immediately adjacent to the sound source, typically within a distance equal to a few wavelengths. In this region, sound propagation presents peculiar and complex characteristics. The relationship between pressure and velocity becomes particularly complex: the phase between these two quantities is no longer constant as in the far field, but varies continuously in space. Also the ratio between pressure and velocity amplitudes undergoes significant variations with position,

making acoustic impedance a complex quantity that changes point by point. This complexity makes measurements in the near field particularly delicate and requires specific instrumentation and analysis techniques.

Standing waves occur when sound waves propagating in opposite directions interfere with each other, a common situation in closed environments like rooms or ducts. In this case, sound pressure and particle velocity present a particular phase relationship, being 90 degrees out of phase. This means that when pressure reaches its maximum or minimum, particle velocity is zero, and vice versa. This results in the presence of nodes and antinodes, points in space where pressure and velocity reach their respective maximum and minimum values, but in different positions. Consequently, acoustic impedance is not constant but varies significantly with position in space, making the acoustic characterization of the environment more complex.

The diffuse field represents a situation where sound waves come from all directions with equal probability and intensity, as typically occurs in a reverberation chamber or in highly reverberant environments. In these conditions, the relationship between pressure and velocity loses its regularity and becomes statistically random. Acoustic impedance is no longer a deterministic quantity but varies both in space and time in a random manner. This statistical randomness makes the diffuse field particularly interesting for certain applications, such as testing acoustic materials, but requires specific approaches for its characterization and measurement.

The importance of understanding these different acoustic field conditions lies in their practical implications. Measurement techniques, instrumentation used, and interpretation of results must be adapted to the type of field present. For example, near field measurements require particular attention to the exact position of sensors, standing waves require consideration of node and antinode positions, while the diffuse field requires a statistical approach to data analysis. The correct identification of the present field type and understanding of its characteristics are therefore fundamental for obtaining accurate and significant measurements of the acoustic properties of materials and environments.

In the characterization of porous materials, it is also useful to calculate normalized acoustic impedance, which is determined through the transfer function method, and the propagation constant [3]. The transfer function method, also known as the Chung & Blaser method, uses two fixed microphones inside an impedance tube and a broadband signal to separate the incident and reflected sound wave components.

The propagation constant, on the other hand, describes how the sound wave attenuates and changes phase while propagating through the material. It is a complex number that accounts for both attenuation and phase variation of the sound wave. Propagation constant and characteristic impedance can be calculated for example with the two-cavity method [4]. This method involves measuring the acoustic impedance of a material sample positioned in front of two air cavities of different thickness. The difference between the two measurements allows obtaining the necessary information to calculate characteristic impedance and propagation constant.

Only after fully understanding these fundamental concepts can we move on to the analysis of specific measurement methods, which represent the practical application of these theoretical principles.

1.2 MEASUREMENT METHODS

In this study, we decided to focus on material characterization through the acoustic absorption coefficient, a choice motivated by both scientific and practical reasons. From a scientific perspective, this coefficient allows understanding the physical mechanisms of sound-material interaction, validating theoretical models, and developing new materials. From a design perspective, it enables predicting in-service performance, optimizing solutions, and selecting the most suitable materials for specific applications. Such characterization becomes even more important when dealing with multilayer materials, where the complexity of interactions between different layers requires a deep understanding of the phenomena involved. In these cases, the absorption coefficient not only provides information about the overall system performance but also allows understanding the interaction between different layers, identifying resonance and interference phenomena, and optimizing layer sequence for maximizing acoustic performance. The importance of correct acoustic characterization of materials through the absorption coefficient becomes particularly evident when considering the different measurement methodologies available. Each technique presents specific peculiarities that make it more or less suitable for some applications.

1.2.1 Traditional Method: Reverberation Chamber

Two of the most common methods are the reverberation chamber and the Kundt tube: both are considered valid approaches for obtaining the absorption coefficient in material characterization and both are regulated by standards.

A reverberation chamber is an environment designed to have a diffuse sound field, that is, a field where sound waves propagate in all directions with equal intensity. This effect is achieved through highly reflective walls and diffusion elements, such as irregularly shaped panels or diffusers, which promote multiple sound reflection. Its ability to create a diffuse sound field makes it ideal for simulating real environmental conditions compared to other measurement methods.

The geometric design of a reverberation chamber follows very specific criteria:

- Walls are not parallel to each other to avoid standing waves.
- Volume is generally large (typically over 200 m^3).
- Shape is irregular to promote sound diffusion.
- Surfaces are highly reflective (often constructed of smooth concrete or similar materials).
- The chamber is completely isolated from the external environment through thick and heavy walls, a floating floor to prevent structural transmissions and special acoustic doors.
- During measurements, temperature (15-30°C) and relative humidity (30-90%) are carefully controlled and recorded.

The measurement follows a precise protocol established by ISO 354 standard [5]: the material sample is positioned on the chamber floor, with a significant surface area (typically 10-12 m^2). A sound field is generated through speakers and the reverberation time is measured with (T_2) and without (T_1) the sample. Measurements are taken in different positions - minimum 2 source positions and 3 microphone positions for each source position. Once the reverberation time variations have been measured, the absorption coefficient is calculated through Sabine's formula:

$$T_{60} = 0.161 * \frac{V}{A}$$

where V is the chamber volume and A is the equivalent acoustic absorption area. Although internationally recognized as a reference standard method, the reverberation chamber has several limitations. Construction is expensive and requires significant space, as well as specific technical expertise for realization. Measurement preparation is laborious, the diffuse sound field is never perfect, and it is difficult to obtain significant results at low frequencies. Furthermore, edge effects can occur on samples that influence results. These limitations become particularly critical when testing multilayer materials or complex composite systems, where correct characterization of interactions between layers requires very controlled measurement conditions.

1.2.2 Traditional Method: Kundt Tube

The Kundt tube represents another traditional method that allows measurements under controlled conditions. It is a cylindrical device closed at one end by a sample of the material under examination. A speaker at the other end generates a standing sound wave. By measuring sound pressure at different points along the tube, it is possible to determine the reflection coefficient and, consequently, the absorption coefficient of the material. The officiality of this method is validated by the presence of two governing standards: ISO 10534-1 and ISO 10534-2 [6] [7]. These standards, while aiming at the same objective, follow methodologically different paths, each with its own peculiarities and optimal application areas. ISO 10534-1 describes the traditional method, which we could define as "historical", based on the use of a single microphone that is mechanically moved along the tube to identify points of maximum and minimum sound pressure. It is a process where a single microphone is mechanically moved along the tube's axis to measure sound pressure variations. The speaker generates a sinusoidal sound wave at a specific frequency, and the mobile microphone detects pressure maxima and minima. This approach presents some significant limitations:

- Requires separate measurements for each frequency.
- Needs a precise mechanical system for microphone movement.
- Measurements are relatively slow.
- Precision can be compromised in determining maximum and minimum points.

In contrast, ISO 10534-2 represents the modern Chung & Blaser approach, exploiting the potential of the digital signal processing through the use of two fixed microphones in the tube. Instead of generating single pure frequencies, broadband noise is used, and through analysis of the transfer function between the two

microphones, information is simultaneously obtained across the entire spectrum of frequencies of interest. It's like moving from analog to digital photography: everything becomes faster, more precise, more repeatable. The difference between the two methods is also manifested in the required instrumentation: the modern method needs more sophisticated electronics for signal acquisition and processing, but the mechanical part is much simpler, as there are no moving parts. In terms of precision and repeatability, the modern method offers significant advantages. While in the traditional method the quality of measurements strongly depends on the operator's skill and experience, the transfer function method provides more objective and consistent results. It's like comparing a measurement made by eye with one made with a digital precision instrument. The measurement times represent perhaps the most evident difference: what requires hours with the traditional method can be completed in a few minutes with the modern method. This speed, combined with high precision, makes the ISO 10534-2 method particularly suitable for industrial applications and quality control. This efficiency becomes crucial especially in the characterization of multilayer materials, where numerous measurements are needed to fully understand the complex interactions between different layers. Although the traditional method maintains its validity in specific research and development contexts, ISO 10534-2 represents today's state of the art in acoustic characterization of materials, combining speed of execution, precision and repeatability of measurements.

However, both methods share some intrinsic limitations of the Kundt tube. First, the sample to be analyzed must always be resized to the tube's dimension, therefore it must be cut or cored from the original sample. This makes the method destructive, resulting in loss of money and time. Furthermore, measurements must be made inside a laboratory and not directly in the place where the sample is located or where it will be installed, resulting in non-representative conditions of real conditions. The sample dimensions, limited to the tube diameter, in turn limit the maximum measurable frequency, making comparison with free field measurements difficult. The mounting of the sample inside the tube is another critical aspect and requires particular attention to avoid measurement errors such as airtightness problems between the sample in the tube that can influence results especially at low frequencies. Results can also be influenced by sample vibrations inside the tube, conditioned by the rigid boundary conditions of the tube, another disadvantage coupled with the fact that only locally reactive materials can be measured accurately.

1.2.3 Innovative Methods: In Situ Technique

Traditional techniques like the reverberation chamber and Kundt tube present several limitations that have pushed towards the development of innovative measurement methods. These new approaches offer numerous advantages over classical methodologies while still maintaining reliability and repeatability of results:

- preservation of sample integrity;
- evaluation in real conditions;
- speed and flexibility;
- measurement of irregular surfaces;
- real-time quality control.

One of the most significant benefits is the ability to keep the sample intact during analysis. Take for example a car seat leather covering: when it undergoes coring for the Kundt tube, it loses the original surface tension maintained by the stitching, thus altering its acoustic properties. In situ measurements completely avoid this problem, allowing analysis of the material in its real conditions of use. Moreover, cutting the sample for measurement in the Kundt tube has no standardized method for precise cutting to have perfect adhesion of the sample to the tube walls (if undersized it allows air passage that is measured creating an error in sample measurement). In situ this kind of error does not interfere with the measurement as there is no need to insert the sample in an instrument. The environment in which an acoustic material is used can significantly influence its behavior. Factors like temperature, humidity and presence of other materials can alter the acoustic properties of the material. In situ measurements take these factors into account, providing a more realistic evaluation of material behavior in its actual context of use, maintaining its physical and structural characteristics unaltered, without the need to use controlled environments like anechoic chambers. In situ measurements, like the surface impedance technique, are generally faster to execute compared to traditional methods. They do not require sample preparation or use of specialized structures like reverberation chambers. This flexibility allows measurements to be taken at different points and in different conditions, obtaining a more complete acoustic characterization of the material. In addition to allowing wide-band measurements, capable of providing results in a fairly extensive frequency range (will depend on the type of probe used). Traditional methods, like the Kundt tube, are suitable for measuring homogeneous materials with flat surfaces. In situ measurements, instead, allow analysis of irregular surfaces or non-homogeneous materials as well, offering greater versatility in evaluating acoustic properties. Furthermore, they can be used for real-time quality control during

production or installation of acoustic materials. This allows identification and correction of any problems at an early stage, ensuring material compliance with required specifications. However, these methods also present limitations, as will be seen from this study. Measurement of highly reflective surfaces can be difficult and show insignificant results, especially at low frequencies, due to low particle velocity near the surface. In the presence of highly reflective surfaces, the technique is also sensitive to phase errors. A certain precision is required in probe position relative to the sample to be measured and speaker position (which must be in line with probe and sample as will be seen in next chapters). Edge effects also come into play: based on probe and speaker dimensions, reduced sample dimensions can cause edge effects that influence material acoustic behavior. When sample dimensions are below a certain threshold, edge effects become significant, leading to deviations in surface impedance measurements. So while coring the sample is not necessary, it must still have a minimum size below which not to go. Experiments conducted on samples of varying dimensions have shown that reducing sample dimensions can lead to an underestimation of absorption coefficient, especially at high frequencies (the edge effect incorporates reflection phenomena in the absorption value that interfere with absorption value). A critical aspect of in situ techniques is the absence of an official standard regulating their application. This lack of standardization makes it difficult to guarantee repeatability and robustness of measurements. The present study therefore aims to develop a unified methodology accessible to all operators in the sector, with the goal of making results obtained more reliable and comparable. In the long term, this work could form the basis for developing an official standard dedicated to this non-destructive and non-invasive technique. The standardization of a method that allows measurements in real conditions would indeed represent an important step forward in acoustic characterization of materials, opening new possibilities in numerous application areas.

1.3 OBJECTIVE OF IN SITU METHOD STUDY

This doctoral thesis aims to demonstrate the superiority of in situ techniques compared to traditional methods of acoustic characterization, such as the reverberation chamber and Kundt tube. The objective is to highlight how these innovative techniques maintain high standards of repeatability and robustness in measurements, while offering significant advantages: these methods preserve sample integrity by avoiding alterations due to cuts or coring, and allow analysis both in laboratory and directly in the material's context of use. This operational flexibility, combined with the non-invasive nature of the

method, represents an important step forward in acoustic characterization of materials. The definition of a standardized and replicable methodology forms the basis for future official recognition of these techniques, paving the way for their inclusion in sector standards for result certification, on par with traditional methods currently in use.

2. DEVELOPMENT OF IN SITU METHODOLOGY FOR ACOUSTIC ABSORPTION COEFFICIENT MEASUREMENTS

The definition of in situ methodology requires a systematic approach in selecting materials to study. The starting point was identified in two materials with distinctly different characteristics: Basotect and EPS (expanded polystyrene). The choice of Basotect is strategic as it is a widely documented material, with a well-characterized acoustic absorption coefficient and supported by an extensive database provided directly by the manufacturer. EPS, on the contrary, being a predominantly reflective material and little used for acoustic absorption, serves as a validation element for the accuracy of measurement probes, allowing verification of their ability to discriminate between absorbing and reflecting materials. The research then evolves towards the analysis of more complex and inhomogeneous materials, particularly multilayer or composite structures. This progression reflects the real application conditions of in situ techniques, where isolated materials like in laboratory are rarely encountered. A significant example is the study of automotive seats, a choice that intersects with the current interest of the automotive sector in optimizing vehicle interior acoustics.

The choice of measurement instruments followed a well-defined evolutionary path. The first phase saw the use of a PU probe (pressure-velocity), the Microflown, particularly suitable for acoustic absorption measurements thanks to its ability to simultaneously detect pressure and particle velocity. This probe integrates a microphone, a hot-wire anemometer and a spherical speaker in a single system. Initially, the complete system provided by the manufacturer was used, but subsequently the use of only the probe was opted for, connecting it to a Zoom F8 audio card. This choice allowed focusing the study on the probe's performance itself, with the future goal of developing a proprietary system. Data processing was transferred from native Microflown software to a combination of Adobe Audition and MATLAB. The second phase of research was oriented towards a technologically more robust solution, eliminating the anemometer, a component particularly sensitive to environmental conditions such as temperature and wind. The choice fell on systems based exclusively on microphones, particularly microphone arrays. Among these, special attention was dedicated to the Sonocat spherical microphone array. The study was then extended to comparison with other types of arrays, to evaluate their respective peculiarities and performance.

Defining the measurement setup represented a fundamental aspect of the research. The first experiments were conducted in a controlled laboratory environment, to minimize the influence of external

environmental variables and establish optimal operating conditions. Through these tests, the crucial importance of the distance between probe and sample emerged: for Microflown, an optimal range between 0.5 and 1 centimeter was identified, while for Sonocat the ideal distance settles around 0.5 centimeters. Particular attention was also dedicated to sample positioning, evaluating two configurations: placement on a completely reflective surface (like a tiled floor) and sample suspension, the latter aimed at simulating conditions closer to real usage scenarios.

The study also investigated the influence of the sound source, analyzing various aspects: the type of signal (comparing white noise and sine sweep), the impact of distance between source and probe, and positioning relative to the sample. The post-processing phase focused on defining the most appropriate methods for calculating acoustic absorption coefficient, calibration procedures, and interpretation of obtained results.

A crucial stage of the research concerned the validation of laboratory measurements through comparison with the standardized Kundt tube method, performed at the University of Trieste. Although it was not possible to perform direct coring of the automotive seat to preserve its integrity, an alternative approach was adopted: samples were created and tested that replicated the layering of materials present in the seat. This allowed validating the proposed methodology by comparing results obtained with in situ techniques with those of the standardized method, thus confirming the validity of the non-destructive approach.

To complete the validation of the methodology, tests were also conducted in outdoor environment, thus approaching real conditions of technique usage.

2.1 MATERIALS USED

When we talk about acoustic control, it is fundamental to understand the distinction between sound-absorbing and sound-insulating materials, as these respond to two completely different needs in sound treatment. While the former transform sound energy into thermal energy, the latter act as barriers to prevent sound transmission between different environments.

Sound-absorbing materials represent an ingenious solution for sound control within an environment. Their effectiveness is based on a porous or fibrous structure characterized by high porosity and a complex network of interconnected pores. This structure, typically open-celled, allows the sound wave to

penetrate the material, where energy is dissipated through multiple friction mechanisms. Imagine observing materials like rock wool, glass wool, or open-cell polyurethane foams under a microscope: we would see a structure similar to a sponge, where air can move freely through a labyrinth of fibers or cells. When a sound wave enters this labyrinth, energy is progressively converted into heat through air friction with fibers or cell walls. The effectiveness of these materials increases with thickness and manifests primarily at high frequencies, where the sound wavelength is comparable with pore dimensions. It is interesting to note how even the mounting method can significantly influence performance: a compressed sound-absorbing material or installed incorrectly can lose much of its effectiveness. In this study the focus is on porous and mixed type sound-absorbing materials. The effectiveness of porous materials is strongly linked to the $\lambda/4$ principle, where λ is the sound wavelength: a porous material absorbs effectively when its thickness is at least equal to a quarter of the wavelength of the frequency to be treated. We will see in the Comsol simulation how this factor will be important for PML determination.

In stark contrast, sound-insulating materials follow a completely different philosophy. Instead of "capturing" sound, these materials try to block its transmission through a dense and compact structure. Their effectiveness is mainly based on the mass law: the heavier and more rigid the material, the greater its ability to acoustically isolate. Materials like cement, high-density plasterboard or laminated glass work as true acoustic barriers. Their compact structure and high surface mass make them particularly effective in blocking low frequencies, which are typically the most difficult to control. Air impermeability is another fundamental characteristic: even a small crack can significantly compromise insulation performance.

It is fascinating to observe how these two types of materials show almost complementary performance in terms of frequency. Sound-absorbing materials excel at high frequencies, where their porous structure can effectively interact with shorter sound waves. In contrast, sound-insulating materials are particularly effective at low frequencies, where their high mass can effectively oppose the movement of longer sound waves. This complementarity explains why in many practical applications combinations of both types of materials are used. For example, in a theater we might find heavy sound-insulating walls to prevent entry of external noise, internally lined with sound-absorbing materials to control sound reflections inside the hall.

The choice between sound-absorbing and sound-insulating materials, or their combination, derives from specific application requirements. In the context of this research, attention is primarily focused on sound-absorbing materials, with a dual objective. Firstly, to identify the correct methodology to characterize and understand the acoustic behavior of materials used in automotive seats; secondly, to identify with the

same methodologies the behavior at low frequencies of materials and possibly find that material capable of absorbing significantly even at low frequencies (traditionally more critical area for absorbing materials). This extension of the absorption band represents a challenge in the field of applied acoustics, particularly relevant in the automotive context where noise control covers a very wide frequency spectrum.

2.1.1 Basotect and EPS

Basotect, a melamine foam with excellent acoustic absorption properties, and EPS (Synthetized Expanded Polystyrene), a predominantly reflective material, are the known materials used in this study. This dichotomy in acoustic properties presents on one hand a highly absorbent material with coefficients approaching unity, on the other a material that tends to reflect almost completely the incident sound energy.

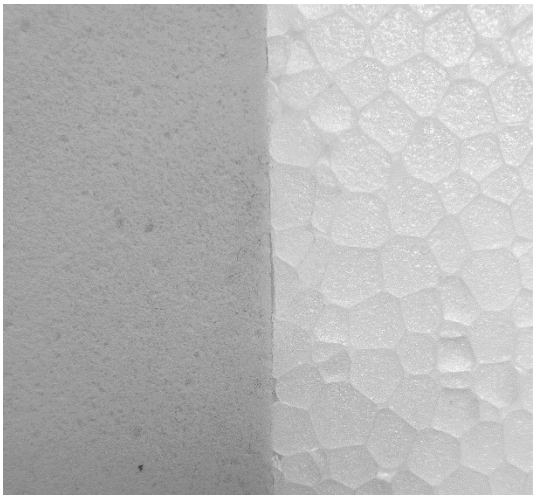

Figure 1: The image compares the two materials under study: on the left Basotect, characterized by an open-cell structure, and on the right EPS, characterized by a closed-cell structure. The morphological difference is clearly visible.

Basotect represents one of the most interesting materials in the field of architectural and industrial acoustics. It is a melamine foam produced by BASF, characterized by a particular microscopic structure: it consists of thin intertwined filaments that form three-dimensional open cells, with an average size of about 150 micrometers. This particular cellular morphology, combined with the material's high porosity (greater than 95%), plays a fundamental role in its acoustic performance.

Figure 2: Basotect sample (diameter 4.5cm, height 5cm)

The open-cell structure allows sound waves to penetrate deeply into the material, where acoustic energy is dissipated through multiple mechanisms: viscous friction of air moving through the pores, thermal losses due to heat exchange between air and material skeleton, and structural dissipation caused by filament vibrations. The combination of these phenomena makes Basotect particularly effective in acoustic absorption, especially at medium and high frequencies.

The trend of Basotect's acoustic absorption coefficient as a function of frequency shows a characteristic behavior: it starts from relatively low values at low frequencies (below 250 Hz), then grows rapidly in the medium frequency region (500-2000 Hz) where it reaches very high values, above 0.8. At high frequencies (above 2000 Hz) it maintains excellent performance with absorption coefficients approaching unity. This behavior makes it particularly suitable for applications where effective control of the sound field in medium-high frequencies is required, such as in the acoustic treatment of conference rooms, recording studios or industrial environments.

EPS, commonly known as expanded polystyrene or polystyrene, is a cellular plastic material with peculiar characteristics. Its structure is composed of a multitude of small closed cells, obtained through a process of expansion and subsequent sintering of polystyrene beads containing an expanding agent. Unlike

Basotect, EPS's closed-cell morphology, combined with its high structural rigidity, gives the material completely different acoustic properties.

Figure 3: EPS sample (diameter 4.5cm, height 6cm)

From the point of view of interaction with sound waves, EPS behaves predominantly as a reflective surface. The closed-cell structure indeed prevents sound wave penetration into the material, drastically reducing the capacity for energy dissipation within the material. The acoustic absorption coefficient of EPS presents very low values across the entire frequency spectrum. Precisely because of these characteristics, EPS finds its main use not in acoustic absorption, but in thermal insulation and, in some specific cases, in acoustic insulation through air transmission through reflection phenomena. Its predominantly reflective nature makes it an ideal material for verifying the correct functioning of acoustic absorption measurement techniques: an accurate measurement system should clearly detect this characteristic of poor absorption, thus providing a sort of "calibration" of the measurement method itself.

2.1.2 Mixed Materials Present in the Car Seat

The research on the acoustic properties of the analyzed materials is set in a specific application context: high-end car seats, with particular reference to the Hyundai Genesis EQ900 seat. This seat represents an excellent example of how different material solutions are integrated to satisfy multiple functional requirements, including thermal comfort, ergonomics, aesthetics, and, not least, acoustic comfort. The seat presents a complex and functional stratification:

- Central Areas (seat and backrest): perforated leather to allow the operation of air conditioning systems and acoustic absorption, coupled with expanded polyurethane to optimize air diffusion.
- Side Areas (armrests, headrest): smooth leather for greater wear resistance, coupled with TNT (non-woven fabric) to ensure structural stability and acoustic contribution.
- Internal Layers: the leather system described above actually serves to cover the expanded polyurethane layer found throughout the seat to ensure ergonomic support. Below this is a metal mesh that acts as structural support both for the seat and for all those mechanisms and channels necessary for seat movement and adjustment, safety systems (side airbags), cooling, heating, comfort offered by springs and shock absorbers, presence and weight sensors.
- Lower Coating: composed of technical fabrics for mechanism protection, waterproof membranes, and floor mounting systems.

The main elements needed to understand the study in question are:

- expanded polyurethane;
- non-woven fabric;
- smooth leather;
- perforated leather.

Figure 4: Sample of expanded polyurethane (diameter 4.5cm, height 4.5cm)

The analyzed expanded polyurethane in this study, with a density of 30-40 kg/m³ and a thickness of 4.5 cm, shows particularly interesting acoustic absorption characteristics. To fully understand its behavior, it is essential to analyze both its physical structure and the mechanisms through which it interacts with sound waves. Our sample presents a highly porous cellular structure, characterized by interconnected cells (open cells) that form a continuous network through which sound waves can propagate. With a density of 30-40 kg/m³, typical cell dimensions fall within the range of 0.1-0.5 mm, creating a structure that effectively balances rigidity and damping capacity. The different color does not seem to cause significant structural changes; however, in respect of repeatability, it was subsequently measured always in the same direction.

Acoustic absorption in expanded polyurethane occurs mainly through two mechanisms:

- Viscous Dissipation: this is the dominant mechanism, where sound energy is converted into heat through friction generated by air movement in the material's pores. The density of 30-40 kg/m³ creates optimal air flow resistance: sufficiently high to allow energy dissipation, but not so high as to cause excessive sound wave reflection on the surface.
- Structural Dissipation: the elastic structure of polyurethane vibrates in response to sound waves. With this density, the material is flexible enough to vibrate but rigid enough to provide good

structural damping, converting part of the mechanical energy into heat through internal friction of the material.

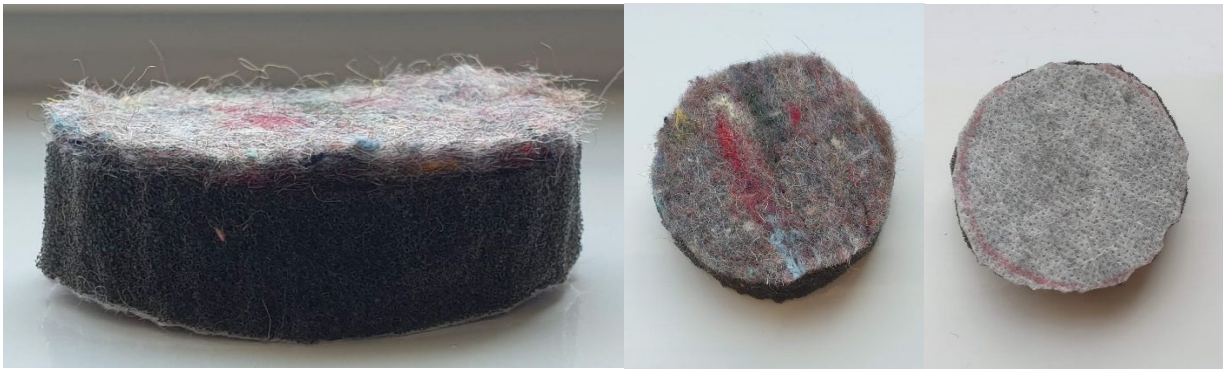

Figure 5: Sample of non-woven fabric (diameter 4.5cm, height 1.4cm), with focus on the right on the two different bases of the same non-woven cylinder.

The non-woven fabric (TNT) sample analyzed has a thickness of 1.4 cm and presents a white face and a colored one. Measurements were taken on both sides to evaluate possible differences due to material stratification and potential asymmetries in its structure.

TNT is a material made up of synthetic or natural fibers, consolidated mechanically, thermally, or chemically, without being woven. This structure creates a fiber network with:

- high porosity;
- random fiber orientation;
- many contact points between fibers;
- interstitial channels of variable dimensions.

In TNT, acoustic absorption occurs mainly through:

- Friction Dissipation: in this material too, viscous dissipation occurs when sound waves cause air to vibrate between the fibers. This process is particularly effective because the fibers create numerous tortuous paths for air in the air-fiber interaction, given also the random orientation of the fibers.
- Structural Dissipation: the fibers can vibrate in response to the sound wave, although this contribution is generally smaller compared to friction dissipation.

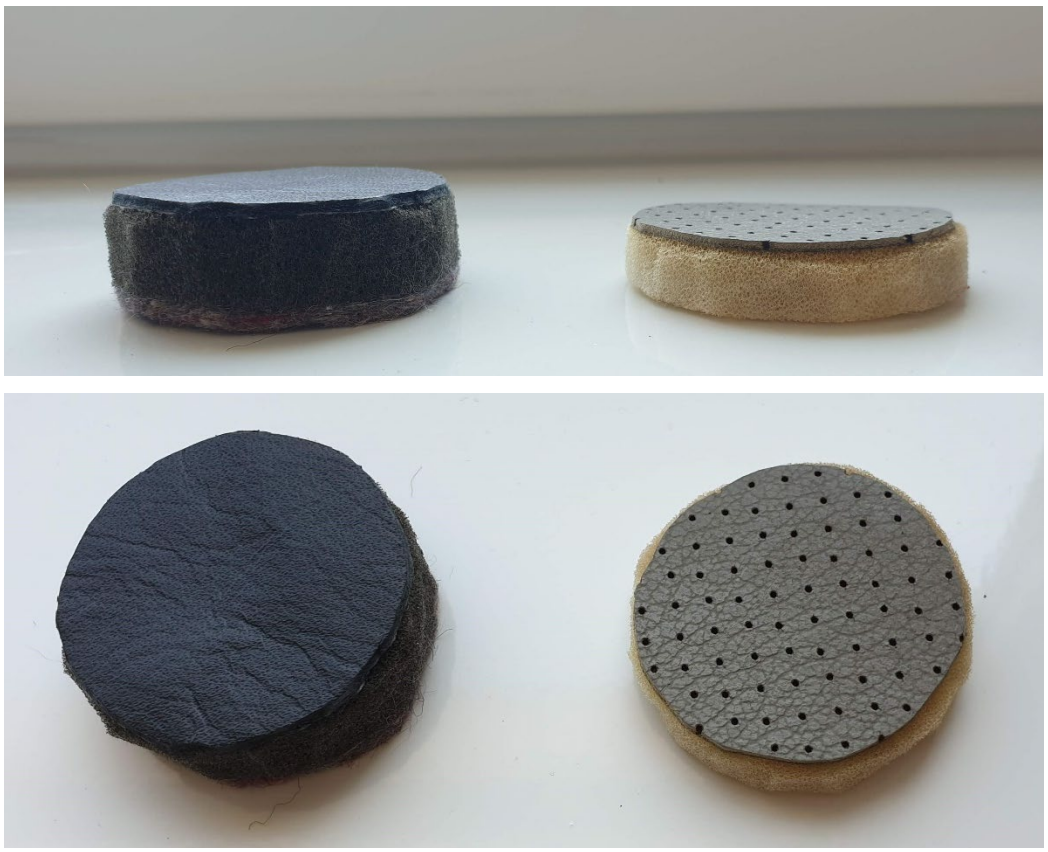

Figure 6: Smooth leather sample (left) and perforated leather (right), both with 4.5cm diameter. For Kundt tube measurements, the leathers were self-supported: the perforated one by PU and the smooth one by TNT (as in production).

The leather sample comes in two versions, perforated and smooth, as the studied seat has some areas (central seat and backrest) covered with perforated leather and others with smooth leather (armrests in both the seat and backrest). The seat is actually covered, in the perimeter areas, also with alcantara-type fabric that was not analyzed because it was not possible to record a significant measurement in those points with the probes used. Leather is a complex natural material, composed mainly of collagen fibers interwoven in a dense three-dimensional structure. From a composition perspective, it presents different layers with different mechanical properties: the surface layer is more compact and less porous, while the underlying layers present a more open fibrous structure. In our case, with a thickness of 1 mm, the leather maintains this stratification albeit on a reduced scale. When used as an acoustic material, leather presents different behaviors. These behaviors depending on whether it is smooth or perforated, while maintaining

the same basic composition. This structural difference determines two completely different absorption mechanisms.

In the case of smooth leather, the compact and non-porous surface creates an almost impermeable barrier to sound waves. In this configuration, when coupled with a TNT layer and PU in production, the system works according to the mass-spring principle. The leather acts as a mass element, moving like a piston in response to incident sound waves, while the underlying TNT provides the elastic (spring) element of the system. The situation changes completely when the leather is perforated. The introduction of holes transforms the material into an array of Helmholtz resonators, where each hole, in combination with the air volume in the underlying polyurethane, creates an acoustic resonator. The fundamental difference between the two systems lies in how sound energy is dissipated. In the smooth leather system, absorption occurs mainly through the conversion of sound energy into mechanical energy (leather movement) which is then dissipated in the TNT layer. In the perforated system, instead, energy is dissipated through air oscillations in the holes (Helmholtz effect) and subsequently in the underlying porous material.

Another interesting aspect is how the leather surface interacts with sound waves in both cases. In smooth leather, the compact surface favors the reflection of high frequencies, limiting absorption. In perforated leather, instead, the holes create entry points for sound waves, reducing surface reflection and allowing greater interaction with the underlying absorbent material. Therefore, the simple addition of perforations to the leather could modify not only the efficiency of acoustic absorption but also the physical mechanisms through which this occurs. This transformation from a mass-spring system to a system of Helmholtz resonators represents an excellent example of how relatively simple structural modifications can produce substantial changes in the acoustic properties of a material.

Based on all these materials, according to the concept of porosity and lambda/4, the frequencies below represent the theoretical point of maximum absorption based on the thickness of each sample.

Material	Thickness [cm]	Thickness [m]	Density [Kg/m3]	Theoretical ideal frequency [Hz]
Basotect	5	0.050	≈ 9	≈ 1700
EPS	6	0.060	≈ 15-30	≈ 1417
PU	4.5	0.045	≈ 30-40	≈ 1889
TNT	1.4	0.014	≈ 20-40	≈ 6071

PU+TNT (sample placed under smooth leather)	6.5	0.065	≈ 45	≈ 1308
PU+TNT (sample placed under perforated leather)	5.5	0.055	≈ 43	≈ 1545

Table 1: Physical data of known materials and seat components, important for acoustic absorption evaluations.

The densities have been estimated based on literature data or obtained when possible from the supplier for all materials except the composites, which were calculated based on the thicknesses of the individual materials that compose them.

Below such identified frequencies, we expect to have less effective absorption that can be partially improved with greater thicknesses than those examined.

2.2 Instrumentation

The acoustic characterization of materials requires the use of specific measurement instrumentation and dedicated software for data processing. In this study, several complementary instruments were employed: the Kundt's tube as a standardized reference for acoustic absorption measurements in laboratory, the Microflown probe and the Sonocat system for in-situ measurements, while for data acquisition and processing, the Zoom recorder and Adobe Audition, MATLAB and Excel software were used, thus creating a complete and reliable measurement and analysis chain.

2.2.1 Kundt's Tube as Reference

The Kundt's tube, being a Chung & Blaser method standardized according to ISO 10534-2 standard as seen in previous chapters, was used in this study as a reference system for acoustic characterization of materials.

Figure 7: Diagram of the four-microphone Kundt's tube used at the UNITS laboratory (using only 2 microphones).

It uses two fixed microphones and is based on the calculation of the transfer function between them. The tube configuration used in this study presents a modular structure with different blocks. The first block, located at the left end of the tube, acts as a cap that can be mounted or removed: it remains mounted during acoustic absorption measurements, while it is manipulated during sound transmission loss (STL) measurements. In this study, we mainly used the microphones (¼ inch size) in positions mic1 and mic2, contained in a block whose length equals three times the tube diameter (which in this case is 4.5 cm). The second block, equipped with mic3 and mic4 positions, was not used for absorption measurements, but only in STL measurements, where mic2 was subsequently repositioned in these locations. There is also a 20 cm spacer which, although not explicitly required by the standard (except for measurements with fluids), was maintained in all measurements to prevent any turbulence in the sound field. In the same block as microphones 1 and 2, there is a speaker with a diaphragm diameter equal to that of the tube, connected in turn to a digital signal processing system that allows direct extraction of the acoustic absorption coefficient and STL. The tube also includes a sample holder that ensures airtight sealing during measurement (if the sample is actually well cut).

The total pressure at any point in the tube is the sum of incident and reflected sound waves. At the positions of the two microphones (mic1 and mic2), the total pressure can be expressed as:

$$P(mic1, t) = p_i(mic1, t) + p_r(mic1, t)$$

$$P(mic2, t) = p_i(mic2, t) + p_r(mic2, t)$$

Using the incident and reflected components of sound pressure at points mic1 and mic2, the auto and cross spectral densities (S11, S22 and S12) can be estimated at these points:

$$S11 = \frac{1}{[p1(f,T) * p1^{*}(f,T)]}$$

$$S22 = \frac{1}{[p2(f,T) * p2^{*}(f,T)]}$$

$$S12 = \frac{1}{[p1(f,T) * p2^{*}(f,T)]}$$

where:

- f is the pressure wave frequency;
- T is the length of the time series recording;
- $p1(f,T)$ and $p2(f,T)$ are the finite Fourier transforms of the pressure time series at points mic1 and mic2, and the asterisk denotes the complex conjugate.

The frequency response function (transfer function) H_{12} can be calculated as:

$$H_{12} = \frac{S_{12}(f)}{S_{11}(f)}$$

Similarly, it is possible to obtain the transfer functions associated with the reflected component H_r(f) and the incident component H_i(f).

The expression of the complex reflection coefficient R(f) is given by:

$$R(f) = \frac{H_{12} - H_i}{H_r - H_{12}} * e^{2jkx^1}$$

The term e^{2jkx^1} in the reflection coefficient formula is fundamental for a correct interpretation of measurements in the Kundt's tube, since measurements are made at a certain distance from it. Without this term, we would obtain the reflection coefficient in the microphones' reference plane, not on the sample surface. Recalling that:

- j is the imaginary unit and indicates the complex nature of the correction;
- k is the wave number ($k = 2\pi/\lambda$, where λ is the wavelength);
- x_1: distance between the sample surface and the first microphone;
- the factor 2 indicates that we are considering the round-trip path of the wave (first time from speaker to sample, second time when reflected from the sample. During this path, the wave accumulates a phase shift proportional to the distance traveled).

The microphones in the Kundt's tube are not positioned directly on the material surface, but must be located at a certain distance from it. This creates the need for a mathematical correction that allows us to "transport" the measurements made at the microphone positions to the sample surface. This is why the formula is multiplied by the exponential described above. Moreover, through a rotation in the complex plane, this mathematical term also adapts the signal amplitude to account for wave propagation in space and compensates for the phase shift that the sound wave accumulates in its round trip between the microphones and the sample. It is interesting to note how the effect of this correction varies with frequency. At high frequencies, where the wave number k is larger, the correction becomes particularly significant. This is because high-frequency sound waves complete more cycles in the path between the microphones and the sample, accumulating a greater phase shift that must be compensated. Conversely, at low frequencies, where k is smaller, the effect of the correction is less pronounced, since the accumulated phase shift is smaller.

From this, we can now obtain the absorption coefficient (α):

$$\alpha = 1 - |R|^2 = 1 - \left|\left[\frac{H_{12} - H_i}{H_r - H_{12}} * e^{2jkx^1}\right]\right|^2$$

And also the complex normalized acoustic impedance:

$$Zo = \frac{(1 + |R|)}{(1 - |R|)}$$

Therefore, although the tube works by acquiring sound pressures, it allows characterization of the material both from an energetic point of view (absorption, i.e., how much energy is absorbed) and from the impedance point of view (how the material "reacts" to the incident sound wave) [3].

2.2.2 PU Probe System (Microflown)

In the PU probe system (Pressure-Velocity), the characterization of materials through the acoustic absorption coefficient requires knowledge of two fundamental physical quantities: sound pressure (p) and particle velocity (u). The Microflown probe used in this study consists of a probe, a spherical speaker, and a structure (impedance gun) that allows keeping the probe aligned with the speaker at a fixed distance. This structure is also equipped with a practical handle for measurements made holding the Microflown by hand and a convenient hook for measurements with the Microflown mounted on photographic tripods (or even for microphone stands). The probe capsule contains two elements: a condenser microphone and a hot-wire anemometer. The anemometer is used to measure particle velocity, measured in meters per second (m/s), which represents the velocity at which medium particles, typically air, oscillate around their equilibrium position during the passage of the sound wave. The anemometer's operation is based on two very thin platinum wires heated electrically: when the sound wave passes through the wires, the movement of air particles modifies their temperature asymmetrically. The temperature difference between the two wires is proportional to particle velocity, thus allowing a direct measurement of this vector quantity. Regarding sound pressure measurement, this is performed through a traditional condenser microphone, which measures local air pressure variations caused by the passage of the sound wave and is measured in Pascal (Pa). Sound pressure, being a scalar quantity, provides information about the total energy present in the sound field, including both incident and reflected energy [8].

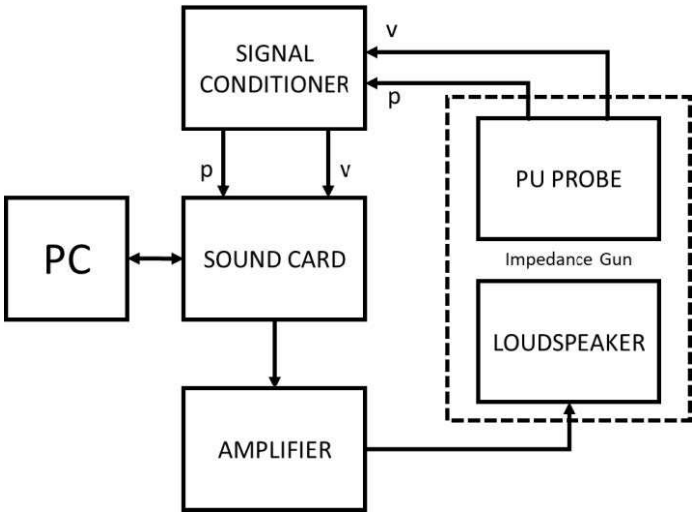

Figure 8: Operating scheme of the Microflown Probe (image from citation [1]).

The measurement system can be configured in two different modes:

1. Native Microflown System:

   In this configuration, the three devices (signal conditioner, audio card, and amplifier) are replaced by only two components provided by the manufacturer: a signal conditioner and a dedicated data acquisition system to be connected to your laptop.

2. Non-native Microflown Configuration:

   When using only the Impedance Gun, this is connected to the original Microflown signal conditioner and subsequently to the Zoom F8 audio card. The acoustic speaker is connected through a dedicated amplifier to the same Zoom F8 from which the signal necessary to excite the material to be characterized will be sent through a Matlab script. The system simultaneously manages signal playback and recording, thus ensuring correct signal synchronization and preserving phase relationships between excitation and material response, similarly to what happens in the native Microflown system. [9]

The combination of pressure and velocity allows determination of fundamental acoustic parameters such as impedance, energy density and sound intensity. Specific acoustic impedance (Z) is defined as the complex ratio between sound pressure and particle velocity at a specific point in the medium. This parameter is fundamental for understanding how sound energy interacts with materials. Sound intensity,

which quantifies the flow of acoustic energy in the sound field, is instead a vector quantity characterized by both magnitude and direction and is expressed as the product of sound pressure and particle velocity. The acoustic absorption coefficient (α) is closely related to the acoustic impedance of the material:

- Materials with acoustic impedance very different from that of air tend to reflect sound energy more, showing low absorption coefficients.
- Materials with acoustic impedance similar to that of air tend to absorb sound energy more, showing higher absorption coefficients. [10] [11]

The acoustic absorption coefficient is calculated by the native Microflown software through three main methodologies: the Mirror Source Model method, the Plane Wave Method, and the Sound Intensity Method. The mirror source model method is based on a representation of the reflected sound wave as if it came from a "mirror" source positioned symmetrically with respect to the material surface. This approach takes into account near-field effects between the incident and reflected waves, making it particularly suitable for measurements in non-anechoic environments, such as car interiors or concert halls. The sound intensity method is instead based on direct measurement of incident and reflected sound intensity from the material surface. The absorption coefficient is calculated as the ratio between absorbed sound intensity (difference between incident and reflected intensity) and incident sound intensity. This method requires measurements at two distinct points and can be influenced by sample geometry, but offers good resistance to background noise. The plane wave method, which is the one used in the study, is based on the assumption that the sound field incident on the material surface is a plane wave [3]. Using the native Microflown software for calculating the acoustic absorption coefficient can generate problematic results, particularly negative peaks in the absorption coefficient α. These negative values are physically impossible from an energetic point of view, thus indicating an error in the native software processing. To overcome this limitation, an alternative approach was chosen: the Microflown hardware (complete Impedance Gun with probe, speaker, and support structure) is used, but the proprietary software is excluded. The system is instead interfaced with an external audio card and a PC, thus allowing more accurate and physically coherent data processing. However, when measuring the acoustic absorption coefficient using the plane wave method, we face a particular challenge in the near field. The method is theoretically based on the assumption that sound waves incident on the material surface are plane waves. In the near field, waves are spherical, not plane. To overcome this limitation, a calibration technique based on the matching filter is used [9]. The matching filter is created through a free-field

calibration measurement, where the probe is pointed away from reflecting surfaces (typically at the center of the room). From this measurement, the H1 transfer function is obtained as:

$$H1 = \frac{Gxy}{Gxx}$$

where:

- Gxy is the cross-spectrum between pressure and velocity;
- Gxx is the pressure autospectrum.

This transfer function, converted into a filter in the time domain (matching filter), implicitly contains:

- the ideal ratio between pressure and velocity in free field;
- the instrumentation frequency response;
- the acoustic characteristics of the measurement environment.

The matching filter is applied through a convolution with the measurements made on the material:

$$ir_{pressure_{cal}} = ir_{pressure} \otimes matching_{filter_{pressure}}$$

$$ir_{velocity_{cal}} = ir_{velocity} \otimes matching_{filter_{velocity}}$$

where $\otimes$ represents the convolution operation.

This operation allows:

- Normalizing measurements with respect to the reference condition.
- Eliminating near-field effects.
- Correcting wave non-planarity.

Once these corrections are applied, the absorption coefficient can be calculated through two main methods using a Matlab script created by the previous PhD student Leonardo Saccenti [9] or through an Aurora plugin in Audition [9]:

a. Farina-Fausti Formula [12]:

$$\alpha_{FF} = \frac{4|Re(Gxy)|}{(Gxx + Gyy + 2|Re(Gxy)|)}$$

where:

- Gxy is the cross-spectrum between velocity and pressure;
- Gxx is the pressure autospectrum;
- Gyy is the velocity autospectrum.

b. Chung and Blaser Formula:

First, the reflection coefficient R is calculated:

$$R = \frac{|Z| - 1}{|Z| + 1}$$

Where Z is the normalized acoustic impedance calculated as:

$$Z = \frac{p}{v}$$

Then the absorption coefficient is calculated:

$$\alpha_{CB} = 1 - |R|^2$$

The measurement process therefore occurs:

1. Acquisition of calibration measurement in free field: the probe is oriented not toward the sample to be measured, but toward the center of the environment where the tests will be conducted (for example, at the center of the laboratory for measurements conducted in laboratory environment).
2. The calibration is processed differently depending on the system used. In the case of native software, it is loaded as the first measurement and the software automatically provides its control and validation. If instead the alternative system is used, the calibration is processed through the H1 transfer function, from which the matching filter is obtained.
3. Measurements are performed on the material to be characterized.
4. Calibration is applied to the measurements. With native software this process is automatic. In the alternative system, instead, measurements are acquired via audio card and the matching filter is applied through convolution, an operation that can be performed either through a MATLAB script or through the Aurora plugin of Adobe Audition.
5. The absorption coefficient is then calculated. The native software exclusively uses the Chung-Blaser formula, while with MATLAB or Audition it is possible to employ both formulas previously described.

Traditional methods, like the Kundt's tube and reverberation chamber, present several limitations that the PU probe technique manages to effectively overcome, such as its ability to be used directly in situ, eliminating the need for these specialized environments. This advantage translates into greater practicality and a significant reduction in measurement costs. The Kundt's tube requires samples of specific and standardized dimensions, often involving sampling and cutting of the material to be analyzed. This operation can alter the acoustic properties of the material and does not allow evaluation of its behavior in actual installation conditions. The PU probe, instead, can be used on surfaces of any size, preserving the material's integrity and allowing measurements in real usage conditions. The frequency response represents another advantage of the PU probe. While traditional methods often present limitations in the analyzable frequency range, particularly at low frequencies, the PU probe offers accurate results over a wide frequency band. This aspect is particularly relevant when characterizing materials with complex behaviors or when studying acoustic phenomena that involve different frequency components [13]. The extremely small dimensions of the Microflown, besides making it easily usable for in-situ measurements, make it a point sensor for most frequencies of interest, a characteristic that ensures high

spatial resolution in measurements. Its "figure-8" directivity makes it particularly resistant to background noise compared to traditional microphones, thus offering greater immunity to environmental interference [14].

However, the signal-to-noise ratio (SNR) emerges as one of the most critical parameters at low frequencies. A low SNR can introduce significant distortions in measurements, compromising accuracy in acoustic impedance estimation and making model calculation application more complex. High background noise presence, structural vibrations, and low source efficiency at low frequencies are all factors that can contribute to inadequate SNR. In non-anechoic environments, reflections from walls, floors, and other objects can interfere with the sound field and further reduce SNR [15].

Setup conditions also play a fundamental role. The receiver height, that is, the distance between the PU probe and the material surface under examination, represents a critical factor. Excessive height can cause interference between incident sound waves and those reflected from the material surface, creating zones of anomalous sound pressure. On the other hand, too small a height can amplify source near-field effects, increasing sound field reactivity and introducing errors in intensity measurements [16]. Sample dimensions must be sufficient to avoid edge effects that could alter the material's acoustic behavior. The presence of surface irregularities and the material's intrinsic properties can influence measurement accuracy. Structural vibrations, particularly critical at low frequencies, can be transmitted through the support system and interfere with measurements.

The reactivity of the sound field, especially when taking measurements near highly reflective surfaces or at low frequencies, is a critical element because the sound field can become highly reactive, compromising the accuracy of intensity measurements.

The need for accurate calibration represents another significant challenge. The calibration process must be executed with extreme attention to ensure reliable results [8] [17] [18].

The Microflown probe stands out as an extremely versatile and valuable instrument thanks to its ability to simultaneously measure sound pressure and particle velocity, as well as perform non-destructive measurements directly in situ. However, to fully exploit its potential and ensure reliable results, a deep understanding of the factors that influence its accuracy, such as receiver height and signal-to-noise ratio, is fundamental. Only through accurate management of these parameters, combined with precise calibration and implementation of appropriate operating procedures, is it possible to obtain maximum performance from this measurement instrument.

Looking to the future, a further expansion of PU probe applications is foreseeable, particularly in the field of real-time quality control and characterization of innovative materials. The development of new data processing algorithms and improvement of calibration techniques could lead to even greater measurement precision, especially at low frequencies and in complex environmental conditions [8].

2.2.3 Zoom F8 Audio Card

In this research, the acquisition of data related to the acoustic absorption coefficient required the use of specific, high-quality instrumentation. In particular, a central role in the research was the Zoom F8 multitrack audio card, chosen for its technical characteristics and versatility. The Zoom F8 audio card, belonging to the F series, is equipped with 8 inputs and 2 main outputs, ensuring operational flexibility in line with experimental requirements. The configuration was simplified thanks to the dedicated "ZOOM H and F-Series Multi Track Driver", which allowed recognition of the device as a standard audio peripheral and seamless integration into the workflow. Channel setup was optimized using the "trimmer link" function, which allows simultaneous gain adjustment on all channels, ensuring uniformity in response. The ability to activate phantom power greatly expanded microphone options, an aspect that would prove crucial in the measurements discussed in Chapter 4.

The control of acquisitions and subsequent data processing required the integration of the Zoom F8 in a working environment consisting of MATLAB and Audition software, as will be detailed in section 2.2.4. MATLAB enabled the automation of many procedures, while Audition provided the necessary tools for detailed analysis of acquired audio signals, particularly important for the elaborations that will be presented in Chapter 4. The choice of the Zoom F8 proved strategic also in terms of audio quality. The card provides adequate resolution and signal-to-noise ratio for acoustic measurements, ensuring the data precision necessary for the subsequent comparative analyses that will be discussed in section 5.1. This configuration allowed overcoming some of the limitations highlighted in the previous section regarding native Microflown software, creating a more flexible and controllable acquisition chain. The results obtained with this instrumentation will be compared with those of the Sonocat system in section 5.2, highlighting the strengths of each approach.

2.2.4 Audition Software

The analysis of data acquired with the Zoom F8 was based on the combined use of Adobe Audition 1.5 software and the Aurora plugin suite. The choice of Audition as the main platform was motivated by its intuitive interface and wide range of editing tools, which proved particularly useful for the type of analysis required in this study. The integration of Aurora plugins represented a key element in the processing workflow, providing specific tools for professional audio analysis. These plugins allowed:

- Performing signal cleaning through dedicated filters.
- Applying calibration files necessary to ensure measurement accuracy.
- Conducting in-depth spectral analysis to understand the energy distribution of sound across different frequency bands.

This last aspect proved fundamental for identifying the most significant frequencies for our study and evaluating the effectiveness of absorbent materials in different bands, as will be detailed in Chapter 4. The Aurora plugins also provided essential tools for calculating a series of fundamental acoustic parameters, including the acoustic absorption coefficient. These parameters, as will be discussed in section 5.1, were decisive for:

- Accurately quantifying the absorbing properties of tested materials.
- Validating theoretical models developed.
- Enabling direct comparison with measurements made through the Kundt's tube (section 2.2.1).

The combination of Audition and Aurora made it possible to extract detailed information from the acquired data and accurately quantify the acoustic properties of tested materials. The results of these analyses will be compared with those obtained through numerical simulations presented in Chapter 3, providing cross-validation of different methodological approaches used in this study. The effectiveness of this processing chain proved particularly evident in the analysis of composite materials and complex structures like car seats, where precision in acoustic characterization is fundamental for correct modeling of system behavior, an aspect that will be explored in sections 4.2.2 and 4.2.3.

2.2.5 Spherical Microphone Array (Sonocat)

In the landscape of modern acoustic technologies, microphone arrays have introduced a true revolution in how we study and analyze sound. These systems, consisting of groups of microphones organized

according to precise geometric patterns, capture and analyze the sound field with a level of detail previously unimaginable through a sophisticated technique called beamforming. This technique works like an acoustic zoom system: just as a camera can focus on a specific subject, a microphone array can electronically "point" in a precise direction, amplifying sounds coming from that direction and attenuating those coming from others [19] [20]. Beamforming is based on the principle that signals captured by different microphones are processed taking into account the time sound takes to reach each microphone [21] [22] [23]. Beamforming implementation can follow different strategies, each with its own peculiarities. The simplest version, known as Delay-and-Sum [24], works so that each microphone receives a precisely calculated "delay", so that signals coming from the direction of interest sum constructively, while those coming from other directions tend to cancel each other out. For a sound wave arriving at an angle θ relative to the array axis, the delay τ_i for each microphone can be calculated as:

$$\tau_{\mathrm{i}} = \frac{(d_{\mathrm{i}} \cdot r)}{c}$$

Where:

- d_{i} is the position vector of microphone i;
- r is the unit vector in the direction of interest;
- c is the speed of sound in air.

There are then more sophisticated versions, such as MVDR (Minimum Variance Distortionless Response) adaptive beamforming, [25], which can dynamically adapt to sound field conditions, with optimal weights calculated as:

$$w = \frac{[R^{-1}a]}{[a^{\mathrm{H}}R^{-1}a]}$$

Where:

- R is the spatial correlation matrix of the signals;
- a is the steering vector in the desired direction;

- a^{H} is the conjugate transpose of a.

In the time domain, beamforming is expressed as [26]:

$$y(x,t) = \Sigma_{\mathrm{n}}{}^{=1\,\mathrm{m}}\, s_{\mathrm{n}}\left(\frac{x}{c} - \left(t + \Delta_{\mathrm{n}}(\theta^{0})\right)\right)$$

This formulation describes how the output signal y(x,t) is the sum of signals from each microphone (s_n), appropriately delayed. The delay $\Delta_n(\theta^o)$ for each microphone is calculated as:

$$\Delta_{\mathrm{n}}(\theta^{0}) = \left(d \cdot \frac{\sin(\theta^{0})}{c}\right) \cdot n$$

where d is the spacing between microphones, θ^o is the desired steering angle, c is the speed of sound and n is the microphone index.

In the frequency domain, the same operation is expressed as:

$$Y(x,\omega) = \Sigma_{\mathrm{n}}{}^{=1\,\mathrm{m}}\, R_{\mathrm{n}}(x,\omega) \cdot e^{j\omega\Delta_{\mathrm{n}}(\theta^{0})}$$

Here, instead of applying time delays, phase shifts are applied through complex multiplications. This formulation proves particularly advantageous for digital implementation and offers greater flexibility in controlling the frequency response.

It is precisely in the frequency domain implementation that the Kirkeby filter comes into play, performing a crucial role in the beamforming process. The Kirkeby filter is used for regularized inversion of array response matrices, a necessary step to obtain optimal beamforming coefficients. Its mathematical formulation [1] becomes:

$$H[k]M \times VM \;=\; C[\vartheta, \varphi, k]M \times D' \cdot\; A[\vartheta, \varphi]D \times V \;\cdot\; e^{-j\pi k}$$
$$\cdot\; [C[\vartheta, \varphi, k]M \times D' \cdot\; C[\vartheta, \varphi, k]D \times M \;+\; \beta[k] \cdot\; IM \times M]^{-1}$$

where H[k] is the beamforming filters matrix; C is the array response matrix; A is the target directivity matrix; β[k] is the regularization parameter, I is the identity matrix. This technique has proven effective both with linear and planar arrays, where microphones are arranged along a straight line or on a plane [27] and with spherical configurations where microphones are distributed on a sphere [1]. Linear and planar arrays find their natural application in scenarios where the sound source is approximately coplanar with the array itself [28]. heir constructive simplicity and contained costs make them particularly suitable for applications requiring mono or two-dimensional beamforming [28] [19].

The SonoCat, specifically, represents a significant evolution of this technology.

Figure 9: Sonocat probe showing measurement axes. Image from provided manual.

The system is composed of eight digital MEMS microphones, strategically arranged inside an aluminum sphere of only 15 millimeters radius [29]. This geometric configuration is not random: the spherical arrangement of microphones allows capturing the three-dimensional sound field completely and efficiently. The system operates in a frequency range between 50 Hz and 6.3 kHz, with a sampling frequency of 48 kHz and 24-bit quantization, characteristics that will be compared with those of the Microflown probe in section 5.2. The peculiarity of the SonoCat lies in the implementation of two distinct models for sound field processing. [21] [30]. The first approach is based on the decomposition of the sound field into spherical harmonics, while the second uses the local plane wave method. These models

are not alternative but complementary, and are used synergistically to obtain a complete characterization of the acoustic field, an aspect that will prove particularly important in the in-situ measurements discussed in section 4.3.2. The decision to use microphone arrays, and particularly the SonoCat, stems from a careful evaluation of their advantages over traditional methods. Where the Kundt's tube is confined to analyzing small samples in the laboratory, and pressure-velocity probes offer only point measurements, microphone arrays allow studying extended surfaces in their actual conditions of use.

The versatility of microphone arrays manifests in several aspects:

- Analysis of large surfaces.
- Study of acoustic behavior from different angles.
- Adaptability to different measurement conditions.
- Complete view of the sound field.

The spherical harmonics decomposition offers significant advantages:

- Mathematical "elimination" of the instrument's influence on the sound field.
- Characterization of directional absorption behavior.
- Precise determination of incident and reflected sound energy.
- Optimization of acoustic material placement.

However, the system also presents some limitations:

- The spherical harmonics model works better in the absence of rigid objects nearby.
- Ideal free field conditions are rarely available in real situations.
- Multiple reflections in closed environments complicate the analysis.
- Low-frequency limitations due to the relationship between wavelength and array dimensions (particularly evident below 300 Hz).
- System complexity requiring specific expertise.
- Considerable implementation costs.

To overcome these limitations, the SonoCat implements the local plane wave method, which:

- Models the acoustic field as a superposition of incident and reflected waves.
- Takes into account the physical presence of the sphere in the sound field.
- Provides reliable results in close-range measurements.
- Works effectively even in the presence of environmental reflections.

The practical implementation of these models in the SonoCat is based on the use of eight digital MEMS microphones, strategically arranged inside an aluminum sphere with a 15-millimeter radius [29]. The system operates in a frequency range between 50 Hz and 6.3 kHz, with a 48 kHz sampling frequency and 24-bit quantization.

For spherical harmonics decomposition, the SonoCat uses zero and first-order modes of the expansion [30, 26]. This apparent simplification proves sufficient to accurately characterize the sound field for absorption measurement purposes, allowing precise determination of both incident and reflected sound energy.

The local plane wave method focuses on a more immediate representation of the acoustic field, mathematically modeling the sphere's scattering effect on plane waves. This approach:

- Proves particularly effective in close-range measurements (3 cm from the surface).
- Allows obtaining wave amplitudes as if the instrument were not present.
- Maintains its effectiveness even in the presence of environmental reflections.
- Overcomes the limitations of the spherical harmonics model in non-ideal conditions.

This dual implementation allows the SonoCat to adapt to different measurement conditions, offering a flexible solution for acoustic characterization of materials both in laboratory and in situ. The combination of the two approaches allows obtaining a complete characterization of the material's acoustic properties, taking into account both the directional behavior of absorption and the effects of environmental reflections.

This unification represents an important advancement in acoustic characterization of car seats, offering a more efficient approach that combines scientific accuracy and practical applicability.

2.3 Setup used

The experimental analysis of the acoustic absorption coefficient required the implementation of different experimental configurations, each with specific characteristics and suitable for particular types of materials or measurement conditions. In particular, as anticipated in previous sections, three main experimental setups were used: the Kundt's tube, the Microflown pressure-velocity probe, and the Sonocat spherical array.

2.3.1 Kundt's Tube Setup

The Kundt's tube, being a standardized method according to ISO 10534-2 standard as seen in previous chapters, was used in this study as a reference system for acoustic characterization of materials.

Figure 10: Kundt's tube set up for absorption study with two microphones.

Sample preparation represented a critical phase of the measurement process: the specimens were cut manually trying to obtain maximum precision possible in the circular shape required by the tube.

Figure 11: detail of the Kundt's tube in which the calibration sample is placed on the left (melamine) and one of the measured samples on the right (in this case the perforated leather).

However, this manual procedure highlights the need to develop a standardized method for sample preparation in the future, as will be discussed in the conclusions (Chapter 6). The absence of a uniform and repeatable cutting process can lead to imperfections that are recorded during measurement, potentially introducing errors in the acoustic characterization of the sample. As will be highlighted in the comparison with in-situ techniques (section 5.1), when the sample diameter is slightly smaller than that of the tube, gaps are created between the material and the walls. These spaces allow air passage, generating acoustic losses that can lead to an overestimation of the absorption coefficient, as the system records as material absorption also the dissipation due to these air passages. On the other hand, a sample with diameter larger than that of the tube requires forced compression during installation. This compression alters the physical properties of the material, introducing internal stresses that can generate spurious resonances, thus compromising the accuracy of measuring the real acoustic characteristics of the material.

The measurement procedure was performed using the properly assembled Kundt's tube, ensuring acoustic sealing between the various tubular sections. The system was excited with a sine sweep signal from 5 to 5000 Hz lasting 10 seconds. Before proceeding with measurements of the samples under examination, a system calibration was performed using a reference melamine sample of 5 cm thickness, characterized by a known acoustic absorption coefficient equal to 1. This calibration phase is fundamental to ensure the accuracy of subsequent measurements. The various samples were then tested paying particular attention to correct installation in the sample holder.

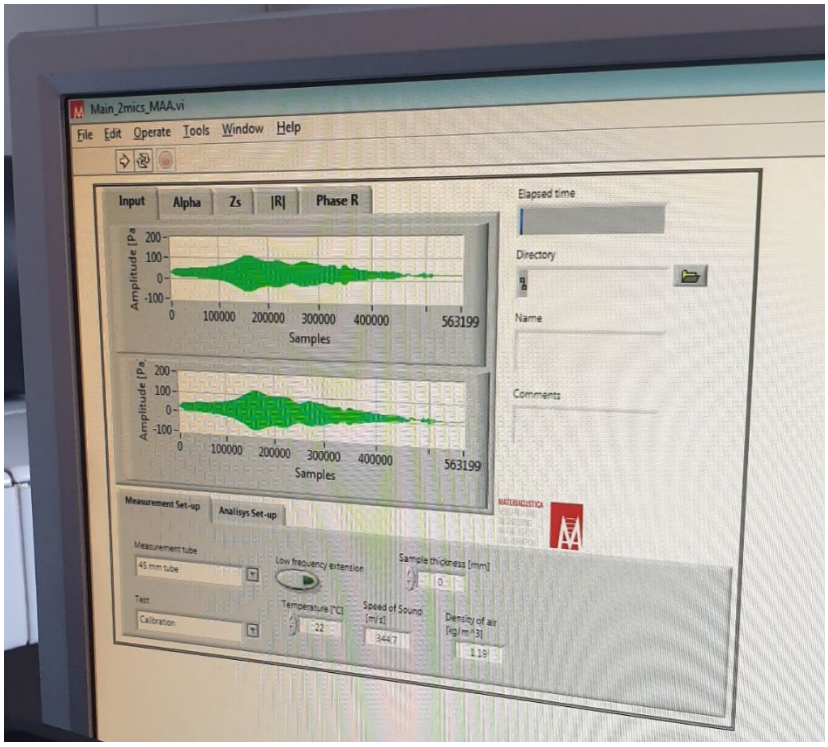

Figure 12: Software used for recording measurements and related processing.

Data processing was carried out through the system's dedicated software, which applied the initial calibration to derive the acoustic absorption coefficients. Although the system is designed to operate reliably in the frequency range between 125 Hz and 4000 Hz, some anomalies were observed, such as unexpected peaks at 3150 Hz found in the EPS sample, suggesting the presence of intrinsic physical limitations of the measurement system. The results of these measurements, which will be presented in detail in section 4.1, will allow validation of the in-situ methods developed in this study, providing a reference basis for evaluating the accuracy of the new proposed methodologies.

2.3.2 Optimal Microflown Setup

The complete Microflown system includes, in addition to the probe (microphone + anemometer), a spherical speaker that plays a crucial role in measurements. This speaker, with a diameter of 10.1 cm, is housed in a rigid plastic structure and can be modeled as a sphere with a moving piston. More specifically, it presents a sphere radius (a) of 50.5 mm and a piston radius (b) of 37.5 mm. This configuration was

designed to generate a sound field with known radiation impedance and ensures high broadband radiation efficiency compared to traditional omnidirectional sources. At low frequencies, its directivity is comparable to that of a point source, without the presence of significant side lobes. [8] This detailed characterization of the probe's behavior will provide essential parameters for subsequent numerical modeling of the spherical speaker through Comsol software, as will be discussed in Chapter 3.

In measurements with the Microflown probe, two different excitation signals were used: white noise and sine sweep, both with a duration of 10 seconds. White noise is a random signal that contains all frequencies with equal energy, simulating uniform noise across the spectrum. Sine sweep, instead, is a sinusoidal signal that varies its frequency continuously over time, in this case covering the range from 20 Hz to 20000 Hz. Comparative analysis of the results, which will be presented in detail in section 4.2.1, shows substantial equivalence in the frequency range between 600 Hz and 10000 Hz. However, below 600 Hz significant differences emerge, where sine sweep demonstrates greater accuracy and reliability. This superiority of sine sweep can be attributed to several intrinsic characteristics of the signal. First, the information in the time domain is concentrated in a very short impulse response (IR), allowing better temporal resolution. Additionally, sine sweep offers the possibility to isolate and exclude system non-linearities, ensuring a cleaner measurement. A particularly relevant advantage is the ability to exclude unwanted reflections, creating virtually anechoic measurement conditions. Finally, at low frequencies, sine sweep ensures a better signal-to-noise ratio (SNR), a crucial aspect for measurement accuracy in this critical band.

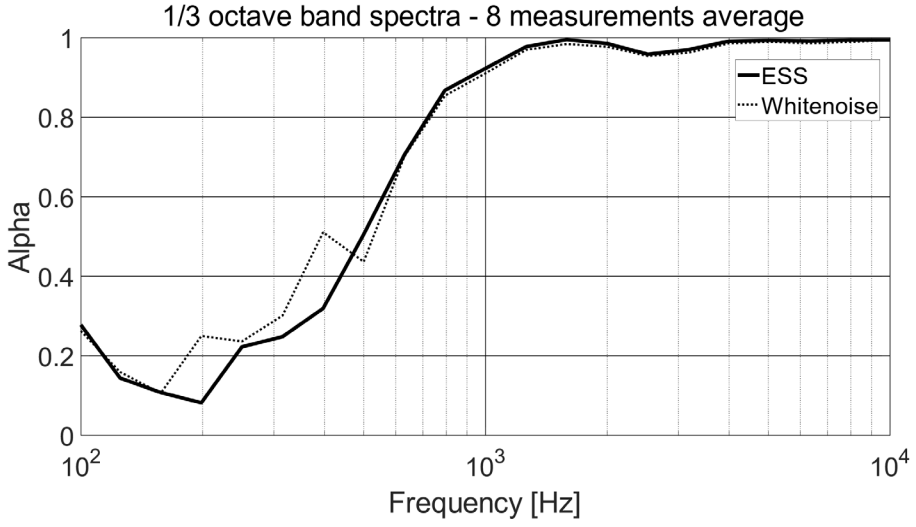

Figure 13: Comparison between white noise and sine sweep during measurement of Basotect with Microflown probe.

This superiority of sine sweep was initially verified using a Basotect sample, a material with well-known acoustic properties that allowed reliable validation of results. Subsequently, the same trend was confirmed in numerous other measurements on different materials, consolidating the choice of sine sweep as the preferential excitation signal for this type of study.

Regarding operating distances, the system provides specific configurations: the speaker is positioned 27 cm from the probe through a manual support (impedance gun) that maintains this constant distance. The distance between the probe and the sample to be measured can be variable: typically 3.5 mm is used for acoustic impedance measurements in the near field [9] [8] [11]. While for applications requiring greater spatial precision, the distance can be reduced from about 10 mm to 0.5 mm (an aspect that will be explored in section 4.2.2 where results of measurements on automotive seats will be discussed).

The system's operative frequency range is between 200 Hz and 10 kHz. The lower limit is mainly determined by the reduced dimensions of the speaker, which do not allow extending the measurement to lower frequencies. The upper limit of 10 kHz is instead related to the difficulty of accurately calculating impedance phase beyond this frequency [31]. The results of these limitations and their impact on measurements will be discussed in depth in Chapter 5.

In implementing the Microflown measurement system, particular attention must be dedicated to the geometric configuration of the setup. The distance between the acoustic speaker and the probe is kept fixed by the instrument's design itself, thus eliminating a potential variable. The distance between the probe and the sample is instead a critical parameter that must be accurately controlled: technical literature recommends maintaining it in a range between 5 mm and 1 cm to obtain optimal measurements and for now we will apply this requirement.

A fundamental aspect of the setup concerns sample positioning. The probe's operating principle is based on measuring the sound wave that, after passing through the sample, returns to the probe itself carrying information about the material's acoustic characteristics. This process necessarily requires that the sound wave, after passing through the material, is reflected back towards the probe. To ensure this reflection, as will be demonstrated through the results presented in section 4.3, the use of a reflective plate positioned behind the sample becomes necessary. This element serves multiple functions in the measurement setup: it helps create a more controlled sound field similar to a plane wave, reduces unwanted diffusion and reflections from other surfaces in the environment, and acts as a barrier against

reflections coming from surrounding objects. These characteristics ensure that the measurement is mainly influenced by the interaction between the sound wave and the sample under examination.

However, as will emerge from comparison with other methods discussed in section 5.2, the reflective plate is not an indispensable element for the measurement method to function. The Microflown probe is indeed designed to measure the acoustic impedance of the material and derive the absorption coefficient even in the absence of a dedicated reflective surface. As an alternative to using the reflective plate, there are several strategies to ensure accurate measurements. One can operate in anechoic environments, designed to minimize reflections, apply mathematical models like the mirror source model or Q-term model to correct near-field effects, or perform measurements at different distances from the sample to extrapolate the absorption coefficient value for an incident plane wave [8] [32]. In measurements of the automotive seat, presented in section 4.3.2, a specific configuration will be implemented that involves positioning the sample in an elevated position relative to the reflective surface, a solution that will prove fundamental for obtaining accurate results in characterizing its acoustic absorption properties.

To validate the Microflown probe measurement setup, a series of comparative tests were conducted using a Basotect sample positioned on two different rigid and reflective surfaces: a marble slab and a wooden slab. The following graph shows data obtained from the two measurements with the Microflown system and its native Velo5 software, compared with data obtained from the Kundt tube (Basotect_Kundt) and data from the Basotect sample supplier (G+). Measurements of just the wooden panel (Wood), just the marble panel (Marble) along with those of Basotect with wooden backing (Wood+Bas) and with marble backing (Marble+Bas) were measured multiple times. The graph shows the two most significant measurements of each to show the trend obtained.

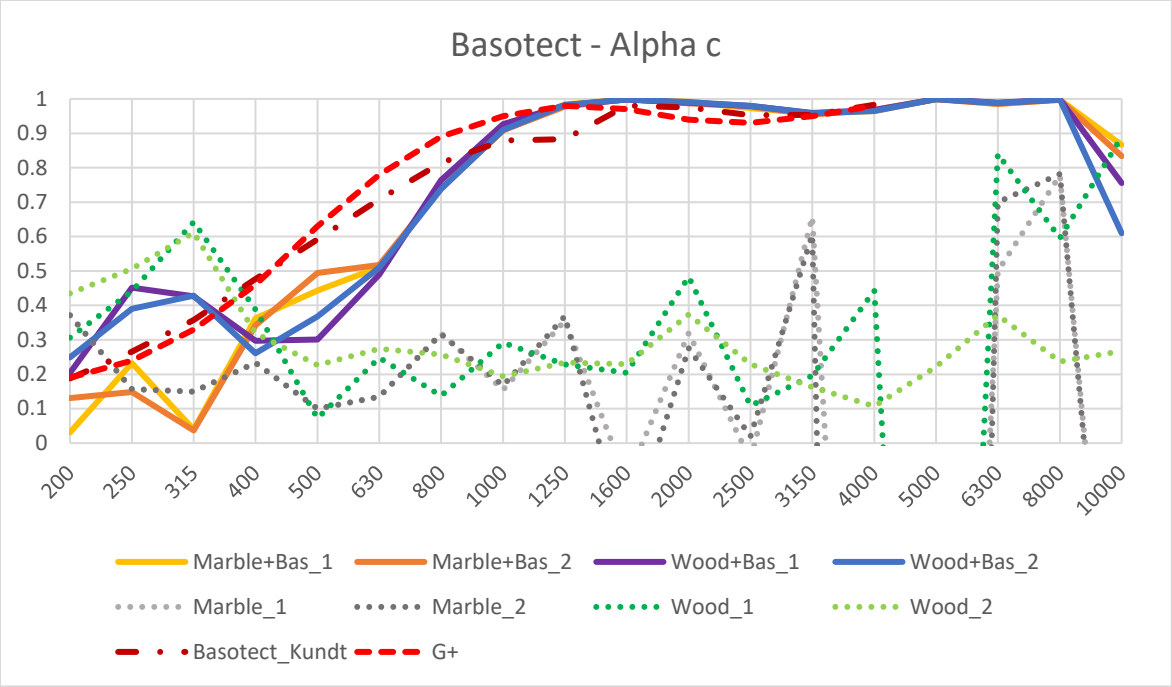

Figure 14: Basotect behavior in two different situations: the first two measurements with a marble panel underneath, the subsequent two with a wooden panel.

From the data obtained, it emerges that both surfaces, being rigid and non-porous materials, show very low absorption coefficients as expected (between 0.1 and 0.3 for marble and between 0.2 and 0.4 for wood in most mid frequencies), confirming their highly reflective nature. When measuring Basotect positioned on these surfaces, the results show absorption coefficients consistent with the material's characteristics, particularly in the mid-high frequency region (between 1000 and 8000 Hz), where the coefficient remains stable and close to expected values for this type of sound-absorbing material. The graph shows remarkable consistency in results between measurements made with Basotect positioned on wood and on marble in the frequency range between 630 Hz and 8000 Hz. However, below 630 Hz, significant differences are observed between the two configurations, with some peaks showing even opposite behaviors. Comparing these results with reference values - both those obtained through the Kundt tube and those provided by the Basotect manufacturer - it emerges that measurements made with marble as support surface offer greater accuracy. This suggests a direct correlation between the reflective properties of the support surface and measurement precision: the more reflective the surface, the lower the measurement error. Furthermore, although the manufacturer states that the Microflown probe is operational up to 10000 Hz, experimental results suggest that the effective reliability limit of the

instrument settles around 8000 Hz. Beyond this frequency, the appearance of irregular peaks in the data clearly indicates a physical limit of the instrument in its ability to make accurate measurements.

In light of the results obtained that confirm the importance of a reflective surface, it was decided to directly exploit the laboratory's tiled floor as a support surface for the samples, given its reflective nature. The next phase of experimentation focuses on optimizing two critical setup parameters. First, verifying the optimal distance between the microphone and sample, which according to specifications should be maintained between 5 mm and 1 cm. Second, evaluating the most effective positioning mode of the probe, comparing manual use through the appropriate grip with mounting on tripod using the provided mounting hole.

Experimental analysis focused on evaluating two fundamental parameters for optimizing measurements with the Microflown probe: the optimal distance between probe and sample and the instrument positioning mode.

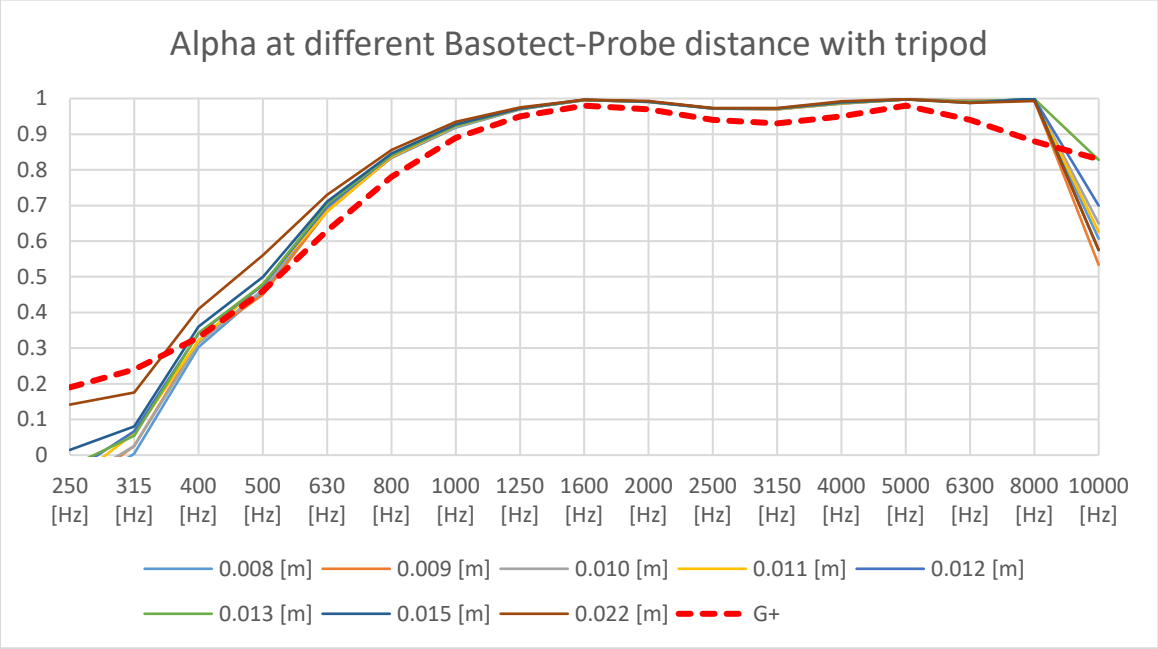

Figure 15: Comparison of acoustic absorption coefficient at various distances between sample and probe, with Microflown fixed to a tripod.

Regarding distance, systematic measurements were performed using a tripod support, varying the distance from 8 mm to 22 mm (in 8 steps). Results show remarkable consistency in absorption coefficient values for medium and high frequencies (800 Hz to 8000 Hz), where variations in distance minimally influence results. In this frequency range, absorption coefficients remain substantially stable, with values varying from about 0.83 to 1.00, regardless of measurement distance. At low frequencies (250-630 Hz), greater sensitivity to measurement distance is observed. In particular, increasing the distance from 8 mm to 22 mm, a progressive increase in absorption coefficient values is noted. For example, at 250 Hz, the coefficient changes from -0.11 to 0.19, suggesting that measurements at greater distances tend to overestimate absorption at low frequencies. The optimal distance for measurements therefore falls in the 8-13 mm range, where the best compromise between stability at high frequencies and accuracy at low frequencies is obtained.

Figure 16: Measurement distance of Microflown probe from sample (in this case the seat backrest).

Regarding comparison between measurements made with probe mounted on tripod and those performed manually, data shows significant differences.

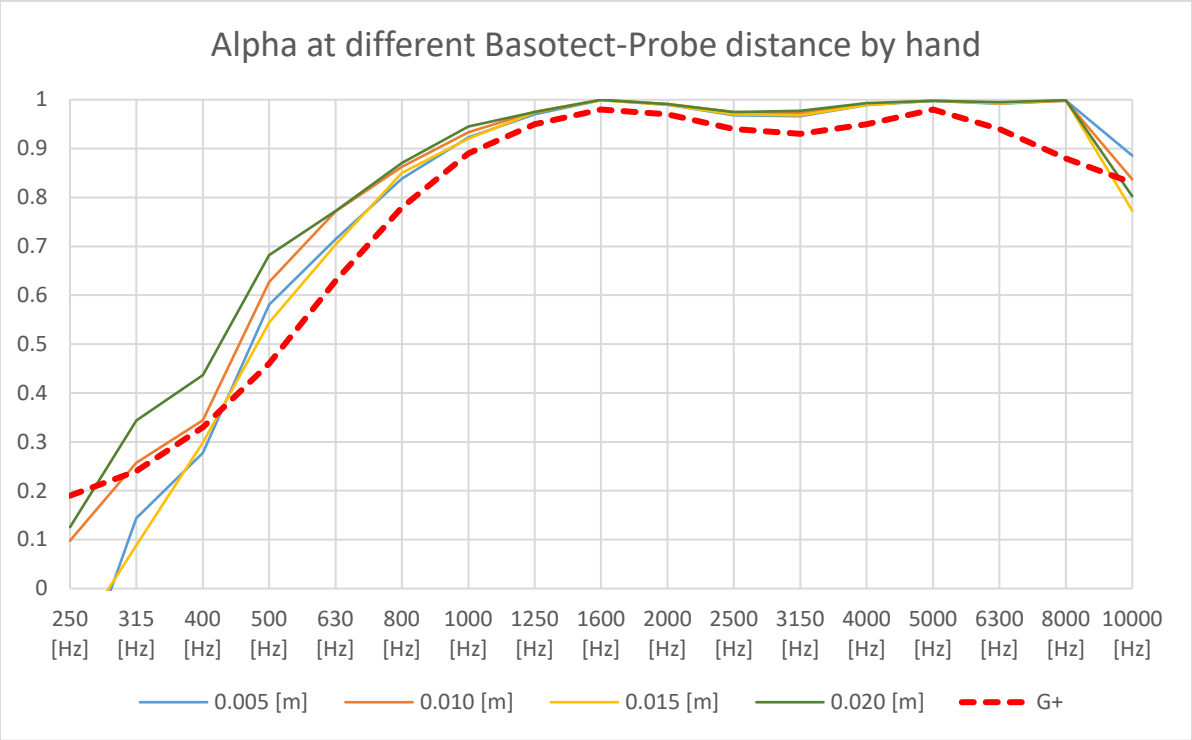

Figure 17: Comparison of acoustic absorption coefficient at various distances between sample and probe, with Microflown held by hand.

Manual measurements, performed at distances of 5, 10, 15 and 20 mm, show greater variability compared to tripod measurements, especially at low frequencies. This variability can be attributed to the lower stability of manual position compared to tripod mounting. Considering that the Microflown anemometer measures particle displacement in air, tripod mounting offers greater repeatability and stability of measurements compared to manual positioning. Nevertheless, measurements taken while holding the probe by hand also seem to give good results (an important condition given its in situ use). It is interesting to note that both measurement modes show optimal measurement reliability in the frequency band between 800 Hz and 8000 Hz, since in this range results are less sensitive to setup variations.

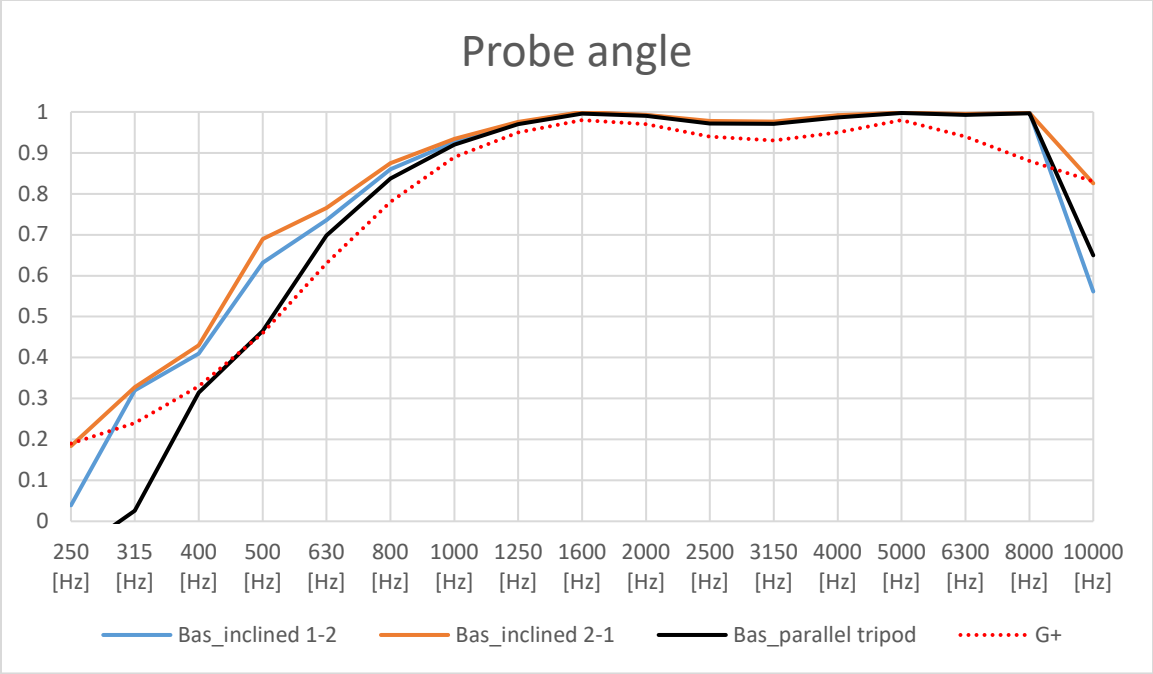

Figure 18: Different angle of the probe relative to the sample to be measured.

An important phase of experimentation concerned analysis of the influence of Microflown probe orientation relative to the sample surface. While the manufacturer recommends positioning parallel to the surface, tests were conducted with different angles to empirically validate this indication. Two inclined configurations were tested: in the first, called "Bas_inclined 1-2" [fig.18], the probe tip (where microphone and anemometer are housed) was maintained at the standard distance of about 1 cm from the sample, while the opposite end was raised by an additional centimeter. In the second configuration, "Bas_inclined 2-1", the opposite inclination was applied, with the tip more distant from the sample and the posterior end closer. Results from these tests, compared both with measurements taken with the probe in parallel position and with reference data provided by the Basotect manufacturer, revealed an important criticality: probe inclination introduces significant errors at frequencies below 800 Hz, with a tendency to overestimate the absorption coefficient in this frequency band. This evidence was further confirmed by a series of additional measurements that showed the same behavior. Based on these results, the need to maintain the probe in a position parallel to the sample surface during all measurements was confirmed, thus validating the technical specifications provided by the manufacturer and ensuring greater accuracy of results, particularly critical at low frequencies.

The Microflown manufacturer recommends using samples with minimum dimensions of 30 x 30 cm to obtain accurate measurements of acoustic absorption coefficient. This indication is primarily based on considerations related to edge effects and sample representativeness, particularly critical for porous materials where the amount of contained air significantly influences acoustic properties. [8] [9] [18]

However, our experimental investigations have confirmed what had already been observed [9]. The probe is capable of providing reliable measurements on an effective area of 20 x 20 cm. Beyond this dimension, data shows that the sample begins to be affected by edge effects, even when tested on larger surfaces (as verified on a 50 x 50 cm sample).

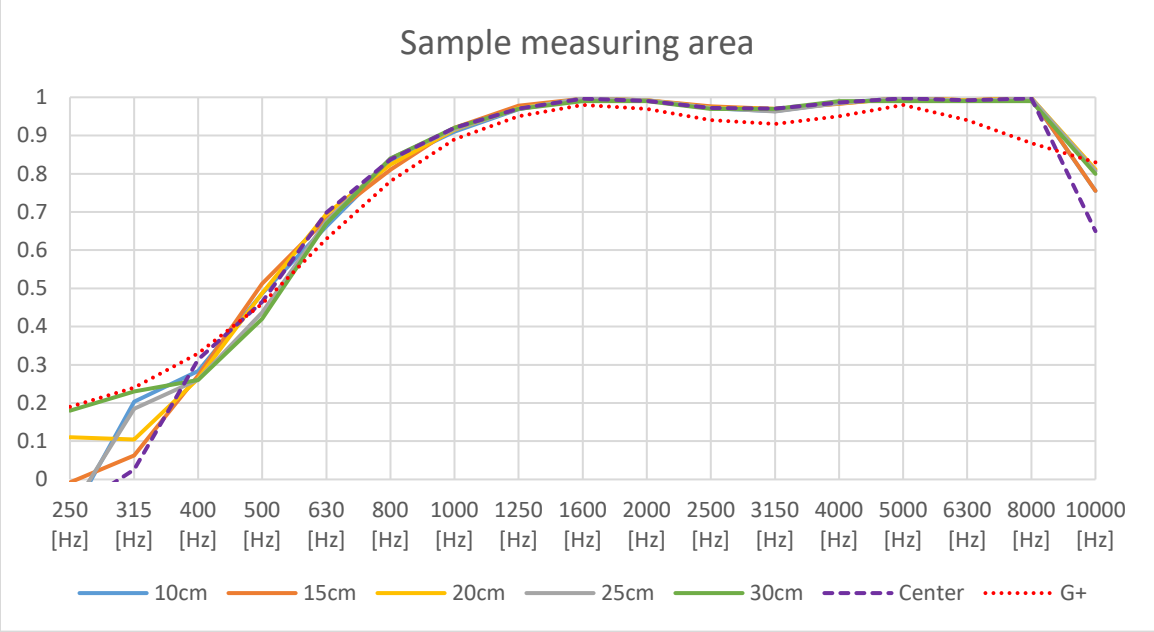

Figure 19: Study of how well the probe can optimally measure the sample in terms of surface area.

This discrepancy from manufacturer specifications represents an important optimization of the measurement process. It is essential to keep this limit in mind during planning and execution of tests, ensuring that the sample's area of interest falls within these dimensions to guarantee reliability of results. In the case of larger samples, it is advisable to divide the area into 20 x 20 cm portions when characterizing the entire sample or specific regions of it.

The acquisition software provides an initial screen dedicated to entering environmental parameters and measurement settings. Environmental parameters include temperature, atmospheric pressure, and relative humidity, which influence the calculation of air density (rho) and sound speed. Technical settings include:

Ambience Data	Temperature	20°
	Atmospheric pressure	101325 Pa
	Relative humidity	0.5 %
	Rho	1.2047 kg*m^-3
	Sound velocity	343.149 m/s
Analog input	Sample rate	48000
FFT settings	Amplitude Mode	RMS
	Window	Hanning
	FFT points	16384
	Window overlap	75
Distances	Probe-Sample	0.01 cm
Measurement time		10 sec
Signal	Sine sweep	20 Hz-20 kHz

Table 1: Typical data used during measurement with the complete Microflown system.

In parallel, an in-depth analysis of optimal signal conditioner settings was conducted. After several comparative tests between fixed gain configurations and different voltage settings, the best results were obtained by positioning the gain knob in the central position (12 o'clock), with voltage set to 4.38V. This configuration allowed obtaining a sound pressure level (SPL) of 88.4 dB, a value that coincides with the SPL produced by the laboratory's Genelec speaker when emitting the same sine sweep signal. This SPL correspondence is not coincidental: it derives from a previous comparative study between the Microflown system and an alternative setup composed of Genelec speaker, laser and microphone. Although the latter system was subject to in-depth analysis, its accuracy proved inferior to that of the Microflown system, motivating the choice not to include it in the present study. [1]

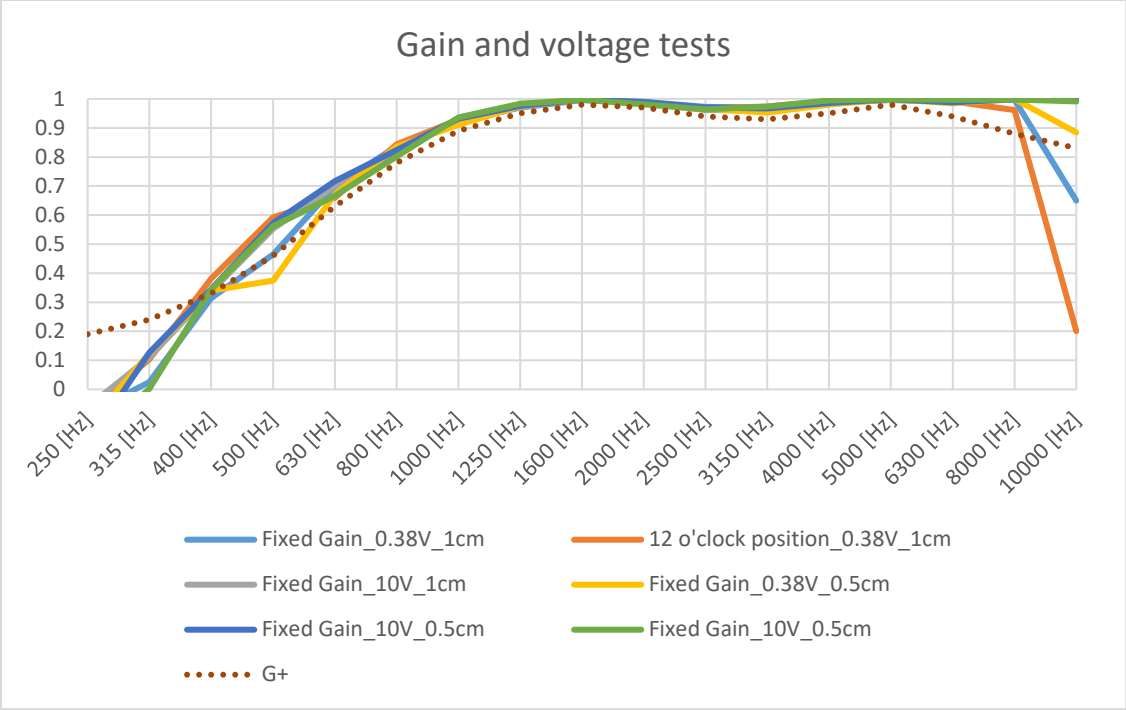

Figure 20: Comparison of tests for gain and voltage setting in microflown system.

The established measurement configurations therefore provide:

- Volume knob positioned at 12 o'clock;
- DAQ sensitivity output: 4.38V;
- DAQ sensitivity input (0 and 1): 1V;
- Probe-object distance: 0.01m;
- Use of tripod;
- Sine sweep: 100Hz-10000Hz, duration 10 seconds;
- Probe parallel to surface;
- Sample centering relative to probe (surface coverage of 20 cm x 20 cm) to avoid edge effects.

This systematic methodology allows complete acoustic characterization, taking into account peculiarities of different components and potential measurement criticalities. The application of measurement methodologies developed on materials can be extended to studying a more complex composite system: the automotive seat. Recalling that the automotive seat presents a complex layered structure. Starting from the surface we find three types of covering (perforated leather, smooth leather in lateral areas, the latter not measurable due to insufficient dimensions), followed by a TNT layer in the case of smooth

leather, a common polyurethane foam layer and a rigid blue composite material layer in compressed TNT. The structure is completed by specific metallic elements: a non-removable steel cage in the seat that contains car systems, a metal structure covered by rigid plastic in the backrest, and a metal frame covered in smooth leather in the headrest.

The seat's complex multilayer structure made it necessary to systematically subdivide it into zones characterized by homogeneous acoustic properties. After several optimization attempts, a mapping was defined that identifies the following characteristic areas:

- For the seat:
  - Front part: two distinct lateral zones, a central zone characterized by presence of stitching and a front central zone without stitching;
  - Rear part: two lateral zones and five central zones differentiated based on varying polyurethane thickness.
- For the backrest:
  - Front part: two lateral zones, a central zone with stitching and an upper central zone without stitching;
  - Rear part: a storage compartment in lower part, a smooth zone in central part and a leather band in upper part.

The headrest was subdivided into front and rear part, excluding from measurements the integrated screen that could not be removed.

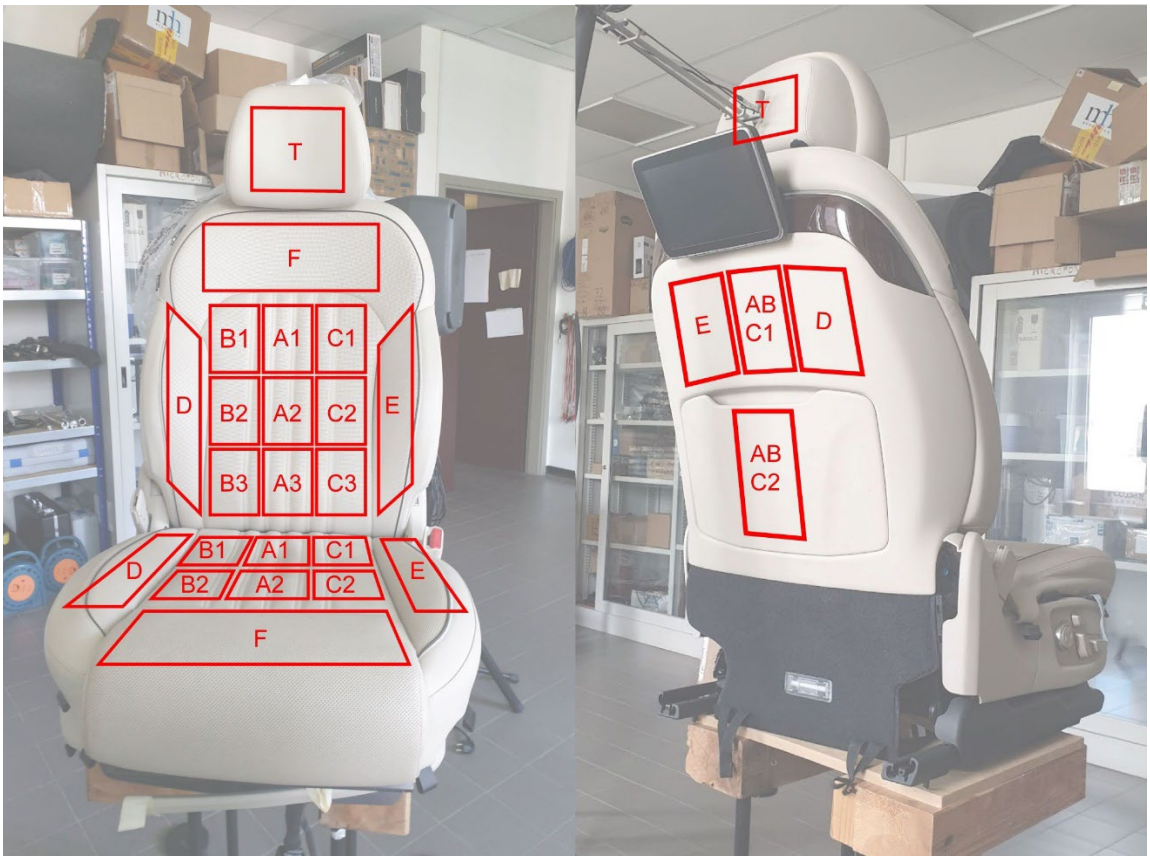

Figure 21: Initial mapping area of front and back of the seat.

Although numerous measurement points were initially identified, these were subsequently optimized and reduced, having found non-significant variations between adjacent points. It is important to note that, due to the intrinsic non-homogeneity of the material (due to both slight variations in layer height and presence of underlying mechanical structure), it was not possible to identify points with perfectly identical acoustic characteristics.

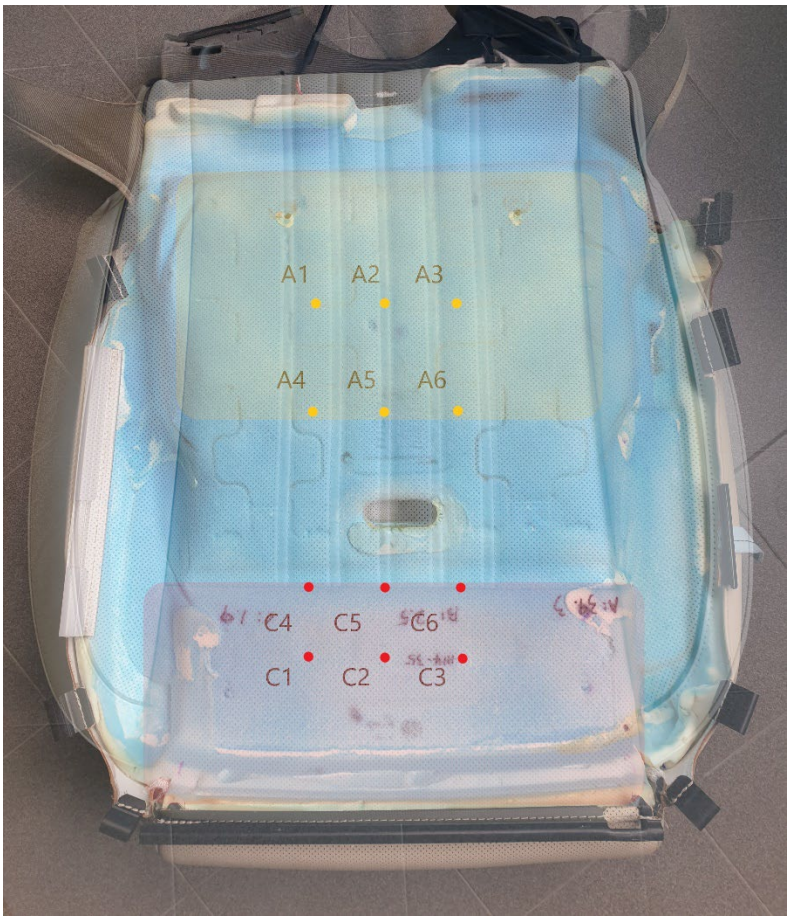

Figure 22: Mapping of area under the cuscion of the seat.

The blue/light blue material present between the polyurethane foam and the seat's metal structure is a support element, probably a compressed non-woven fabric, that serves multiple functions: it reinforces the foam increasing its strength and durability, maintains the seat's shape and prevents deterioration of the expanded polyurethane. During measurements of the lower part of the seat, this layer showed significant acoustic variability due to its non-planar geometry, characterized by different heights that follow the ergonomic profile of the seat. However, results of these measurements will not be presented as subsequent tests showed that for more accurate acoustic characterization, it is preferable to take measurements with the seat raised rather than directly placed on the ground.

Even in the alternative implementation without the native Velo5 software, the measurement setup maintained its basic configuration. The Microflown signal conditioner remained an integral part of the system, processing probe signals which are then sent to the Zoom F8 audio card: channel 1 records the

microphone signal (sound pressure) while channel 2 acquires the anemometer signal (particle velocity). These two signals are saved in a single two-channel ".wav" file. Regarding acoustic excitation, the Microflown speaker was directly connected to the Zoom F8, through which a sine sweep signal with a duration of 10 seconds is generated, covering the frequency range from 20 to 20000 Hz. The acquisition process is managed by a MATLAB script. That script ensures synchronization between signal emission and response recording, eliminating phase shift problems between signals. This synchronization can also be done through the use of Plogue Bidule software as can be seen in the image below.

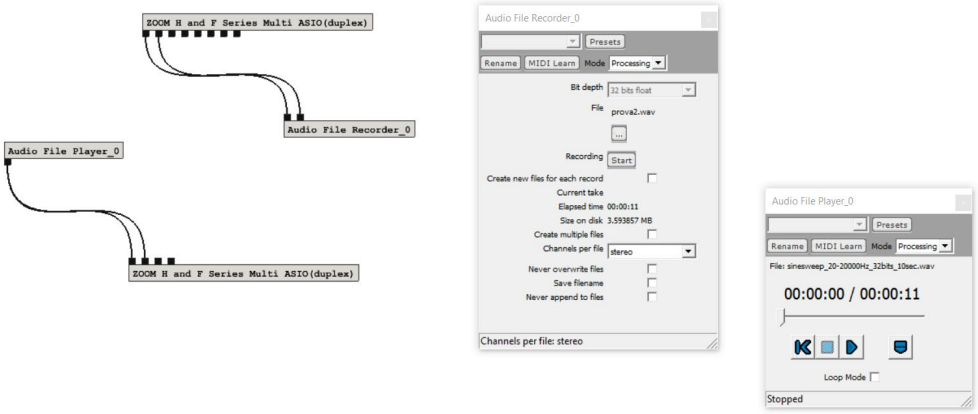

Figure 23: Bidule setup as an alternative to Matlab script for starting the acoustic signal simultaneously with measurement recording.

This synchronization is crucial not only to avoid phase errors but also to minimize any latency effects in the acquisition system. The post-processing phase involves applying the matching filter to each measurement through a convolution process (as already described in previous chapters). The matching filter is derived from a calibration measurement made in free field: the calibration signal is processed through an H1 transfer function using Adobe Audition's Aurora plugin, thus generating the matching filter needed for calibration. Once calibrated measurements are obtained, the acoustic absorption coefficient (α) is calculated through two complementary methodologies: the Farina-Fausti formula and the Chung-Blaser method.

Farina-Fausti Formula: $\alpha = 2 * \frac{I}{Dc+I}$

Chung-Blaser Formula: $\alpha = 1 - \left(\frac{|Z|-1}{|Z|+1}\right)^2$

The Farina-Fausti formula seen previously is in this case represented in energetic terms. The term I represents acoustic intensity and Dc is the product between energy density D (J/m³) and sound speed *c*, resulting dimensionally in an intensity (W/m²). The ratio I/Dc, known as energy ratio r_E (defined by Gerzon), is a fundamental parameter in Ambisonics theory that characterizes the nature of the sound field:

- r_E = 0: purely reactive field, without net energy propagation (incident energy equals reflected energy). In this case the sound field near the material surface is dominated by reactive phenomena, typical of low frequencies or highly reflective materials.
- r_E = 1: totally propagative field, with energy propagating without reflections. In this case there is an effective absorption condition, where sound energy is effectively dissipated by the material [33].

This energetic interpretation provides a deeper understanding of the physical meaning of measurements and helps validate results obtained in different sound field conditions.

In the Chung-Blaser formula, which calculates the absorption coefficient from normalized acoustic impedance |Z|, the term ((|Z|-1)/(|Z|+1)) represents the reflection coefficient R, so the formula can also be written as $\alpha = 1-R^2$. As will emerge from results analysis, a hybrid approach combining the two formulas will become necessary. The combined use of the two methods (Farina-Fausti and Chung-Blaser) indeed provides a more complete characterization of material acoustic behavior. While the Chung-Blaser method is based on acoustic impedance and offers a direct measurement of material's intrinsic properties, the Farina-Fausti formula, through interpretation of energy ratio r_E, allows better understanding of how the material interacts with the sound field. The practical implications of using both methods combined proved significant during in situ measurements. Analysis of the energy ratio r_E in the Farina-Fausti formula allowed identification of potentially problematic measurement conditions:

- In the case of highly reflective materials:
  - r_E is very low (close to 0).
  - Indicates a predominantly reactive field.

    - Suggests need for particular attention in interpreting results at low frequencies.
    - May require longer measurement times to obtain stable results.
- For highly absorptive materials:
    - r_E is close to 1.
    - Indicates a predominantly propagative field.
    - Confirms measurement reliability.
    - Allows shorter acquisition times.
- In intermediate cases:
    - r_E value provides information about measurement quality.
    - Helps identify possible environmental interferences.
    - Guides choice of optimal acquisition parameters.

The Chung-Blaser method has instead provided direct information about material properties and greater robustness to environmental conditions.

2.3.3 Sonocat Optimal Setup

The measurement methodology with SonoCat was optimized through a series of systematic tests. The probe features an ergonomic functional design: the handle is equipped with a structure that, when the instrument is positioned in contact with the surface, automatically maintains the sphere at a distance of 1 cm from the sample surface with the z-axis perpendicular to the surface itself. While technical specifications suggest an optimal distance of 3 centimeters from the surface, our measurements have demonstrated the possibility of operating effectively even at shorter distances, down to 1 centimeter from the sphere's outer edge (corresponding to 2 centimeters from its center).

Figure 24: Detail of the Sonocat probe showing how the body of the structure itself maintains a fixed distance between probe and sample.

This constructive feature has proven particularly advantageous from a practical standpoint. Contrary to what might initially be feared, direct contact of the probe with the surface has not generated problems of undesired mechanical coupling. No phenomena of vibration conduction between sample and probe or vibrational feedback loops that could compromise measurement accuracy were observed. This robustness of the system with respect to direct contact is a particularly relevant characteristic that expands the operational possibilities of the instrument. In the absence of a stable support like a tripod, direct contact with the surface offers greater stability during measurement, eliminating undesired perturbations caused by the natural movement of the operator's hand when the instrument is held in suspension. This experimental evidence, combined with the absence of mechanical coupling issues, guided the methodological choice to conduct measurements with the instrument directly resting on the surfaces under examination, thus ensuring greater repeatability and reliability of acquired data.

However, SonoCat's performance presents some characteristic limitations at low frequencies, a phenomenon that deserves in-depth analysis to understand its causes and possible mitigation strategies. This limitation manifests mainly below 300 Hz, despite technical specifications indicating an operating range extending between 50 Hz and 6300 Hz [30] [23]. The reasons for this limitation are rooted in both the physical structure of the instrument and the implemented theoretical models. From a hardware perspective, the distance between microphones, constrained by sphere dimensions of 30 mm diameter, becomes a critical factor at low frequencies. When sound wavelength becomes significantly larger than

the distance between microphones, the instrument's ability to accurately discriminate sound field components is significantly reduced [27] [34]. Added to this is a theoretical limitation: the implemented mathematical models, both spherical harmonics decomposition and local plane wave method, assume conditions that become less valid at low frequencies. In particular, the assumption of stationary sound field and the hypothesis that the instrument's sphere does not significantly influence the sound field show their limits when wavelength increases. Under these conditions, the sound field tends to be more dynamic and the sphere's influence on measurement becomes more pronounced. Moreover, a crucial factor that influences measurement precision, particularly at low frequencies, is the signal-to-noise ratio (SNR). This parameter becomes particularly critical at low frequencies, where the acoustic signal is intrinsically weaker and thus more susceptible to background noise interference [26]. In real environments, where measurements are inevitably influenced by reflections and unwanted sound sources, maintaining adequate SNR becomes fundamental for obtaining reliable measurements. Considering these evidences, we can therefore define the frequency range of effective interest for reliable measurements between 300 Hz and 6300 Hz. This interval represents the operational window in which the instrument guarantees maximum accuracy and repeatability of measurements, allowing reliable characterization of the acoustic properties of materials under examination.

In this case too, the samples of materials were placed on the laboratory's tiled floor to simulate a reflective plane and exclude it from absorption measurements. While for the seat, measurements were acquired directly inside the vehicle to validate the in-situ measurement of the Sonocat probe. The Sonocat probe, consisting of a spherical array of 8 MEMS microphones with a total diameter of 30 mm, was then positioned on various samples maintaining the same distance from each different sample.

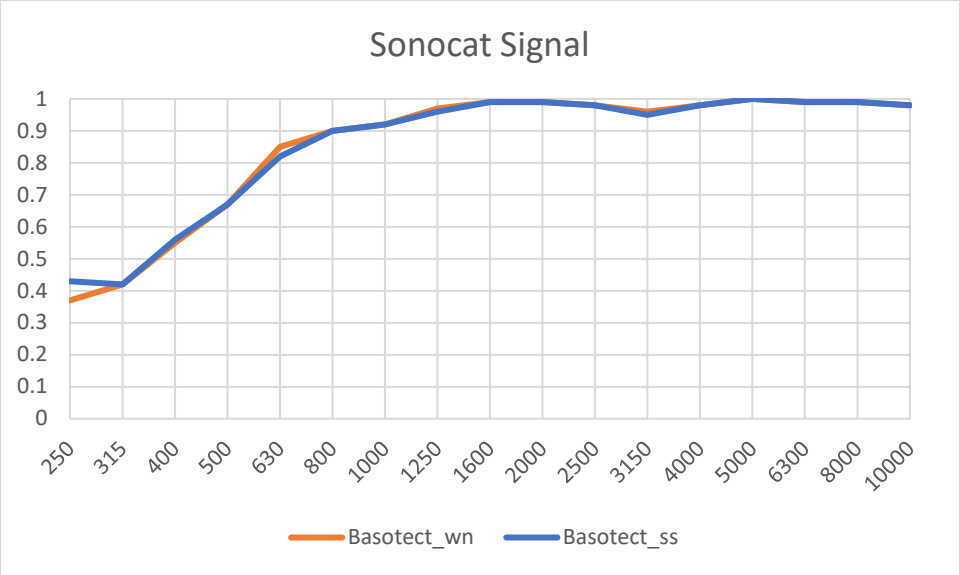

Figure 25: Comparison between use of white noise signal and sine sweep during Basotect measurement with Sonocat probe.

Each sample was excited by a sine sweep signal lasting 10 seconds, covering the frequency range from 20 Hz to 20 kHz. The difference between using white noise doesn't seem to significantly affect Basotect measurements, but for the reasons already listed, sine sweep was preferred to maintain as the signal.

Figure 26: Instrumentation obtained from renting the Sonocat probe, including probe, connection cable, laptop with native software.

The SonoCat, connected via USB to the computer with pre-installed dedicated software, represents an integrated measurement and analysis system that is particularly sophisticated. The software not only performs simple data acquisition but implements a complete process of processing and validation of acoustic absorption coefficient measurements, providing results in third-octave bands through easily consultable Excel tables. What makes this system particularly interesting is its self-validation capability. The software incorporates a series of automatic checks that ensure measurement reliability. Among these, a fundamental check verifies that incident power is always greater than reflected power for each analyzed frequency. When this condition is not met, the software intelligently interprets the situation by calculating an emission coefficient, displayed as a negative value, instead of an absorption coefficient [30]. The validation system goes beyond these basic checks, including verifications of sound field stability, signal-to-noise ratio, and correctness of measurement geometry. This comprehensive approach to data validation, combined with real-time visualization of results, is particularly important in in-situ measurements, where conditions are not controlled as in the laboratory.

The Sonocat's method for calculating the acoustic absorption coefficient of a material in a stationary sound field is based on the ratio between two fundamental quantities:

$$\alpha = \frac{W_{ac}}{W_{in}}$$

Where W_ac is the active sound power, averaged over time, representing the acoustic energy actually absorbed by the sample, and W_in is the incident sound power, representing the total acoustic energy reaching the sample surface [30]. Both these powers are calculated by integrating their respective sound intensities over the sample surface. The absorption coefficient is thus obtained from the ratio between these two quantities, providing a specific value for each analyzed third-octave frequency band.

The SonoCat software offers two possible measurement approaches: point or scanning. For this study, the point method was chosen, a methodological choice motivated by two main reasons. First, this mode allows a more direct comparison with measurements made with the Microflown probe, enabling a more accurate comparative evaluation between the two instruments. Second, the point method allowed thorough evaluation of the instrument's ability to provide repeatable measurements both in the same point and in adjacent points, thus providing validation of the spatial stability of measurements.

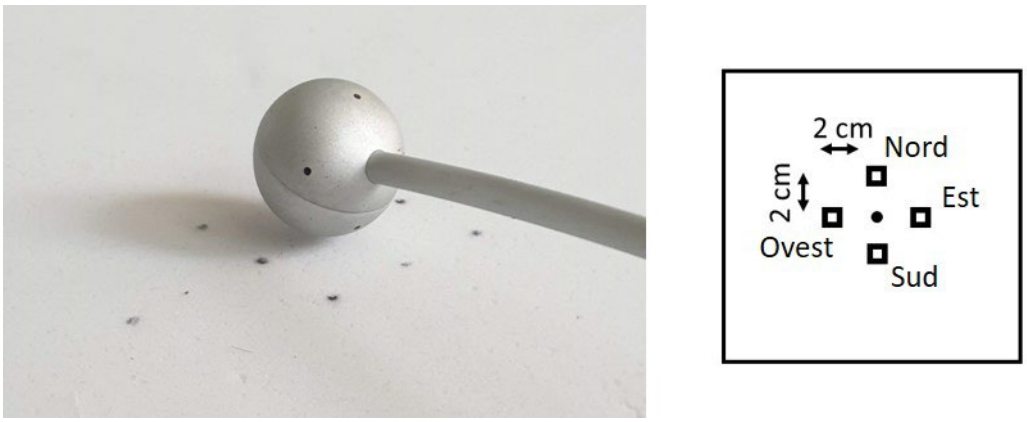

Figure 27: Detail of the probe during measurement of localized points on the sample (schematized on the right) where the double point in the left photo is taken as a reference for mapping point positions relative to the sample.

To obtain a representative characterization of the entire sample, a geometrically balanced measurement scheme was adopted: four measurement points (A, B, C, and D) were arranged to form a diamond, with a fifth point in the center. This arrangement was designed to ensure that each measurement point was equidistant from both the center and the edges of the sample, thus ensuring uniform surface coverage and a balanced evaluation of its absorption properties. Particular attention was dedicated to each point, where repeated measurements were taken whose results were subsequently arithmetically averaged, in order to obtain a more representative and statistically robust value for this crucial position. The acquired data were processed by the dedicated SonoCat software, which provided acoustic absorption coefficients in third-octave bands for each measurement point, allowing a detailed analysis of the spatial variability of the material's acoustic properties. In all these cases, the Sonocat probe was used with its native software with the following settings:

Signal	Sine Sweep
FFT length [-]	8192
Frequency resolution [Hz]	5.859375
Number of averages [-]	150
Overlap percentage [%]	50
Recording time [s]	12.88533
Window type [-]	Hann
Temperature [°C]	20°C
Relative humidity [%]	50
Atmospheric pressure [Pa]	101325
Scan area [m²]	0.05

Table 2: Data entered in native Sonocat software for measurement recording.

To ensure proper comparison with measurements made using the Microflown probe, particular attention was paid to the choice of scanning area. The selected values were maintained similar between the two instruments, a choice motivated not only by the need for direct comparison of results but also by the necessity to avoid unwanted edge effects, particularly critical in measurements taken on seats. Regarding recording times, a peculiarity of the SonoCat software emerged that deserves thorough discussion. The recording time turns out to be slightly longer than the actual duration of the sine sweep signal used, including silence margins both at the beginning and end of the measurement. This characteristic is not directly modifiable by the user, as the recording time is automatically determined by the software through a specific formula [30]:

$$\text{Recording Time} = \left(\left(1 - \frac{overlap\ percentage}{100}\right) \times number\ of\ averages + \frac{overlap\ percentage}{100}\right) \times \frac{FFT\ length}{sampling\ frequency}$$

The total recording duration is indeed calculated as the product between the FFT length and the effective number of analysis windows (determined by the number of averages and overlap percentage), all normalized with respect to the sampling frequency.

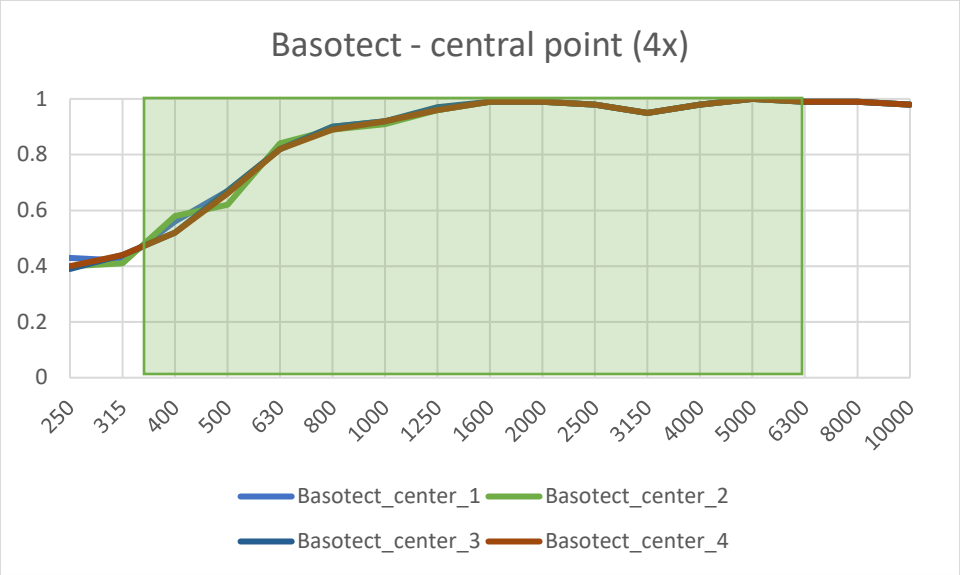

Figure 28: Four measurements taken at the same central point of the Basotect sample with the Sonocat probe.

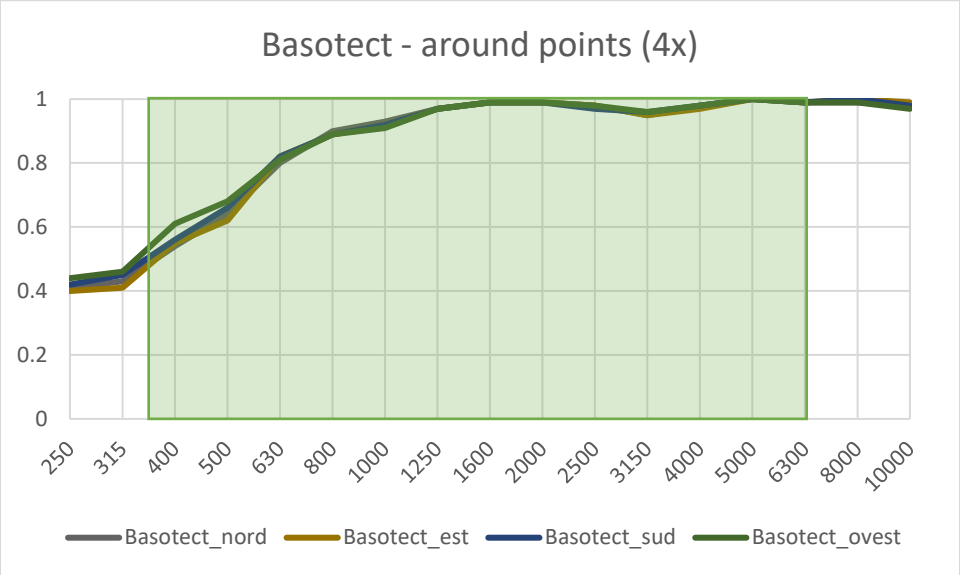

Figure 29: Four measurements taken at the cardinal points around the central one, of the Basotect sample with the Sonocat probe.

It is evident how also in this case (like the Microflown) the robustness and repeatability of measurements in a controlled environment, like the laboratory, on a known material, like Basotect, prove appreciable.

The sound source configuration for measurements was subject to careful evaluation both in terms of positioning and speaker choice. Initially, following standard acoustic measurement practices, the LG speaker (dimensions 10x10x14 cm) was positioned one meter from the sample. This distance indeed

represents a typical configuration in the relationship between source and receiver in acoustic measurements. Subsequently, with the acquisition of more experience in using the SonoCat and with a view to making a direct comparison with the Microflown probe, the distance was reduced to 26 centimeters. This modification was not casual, but aimed at exactly replicating the measurement conditions used with the Microflown probe, thus allowing a precise and methodologically rigorous comparison between the two instruments.

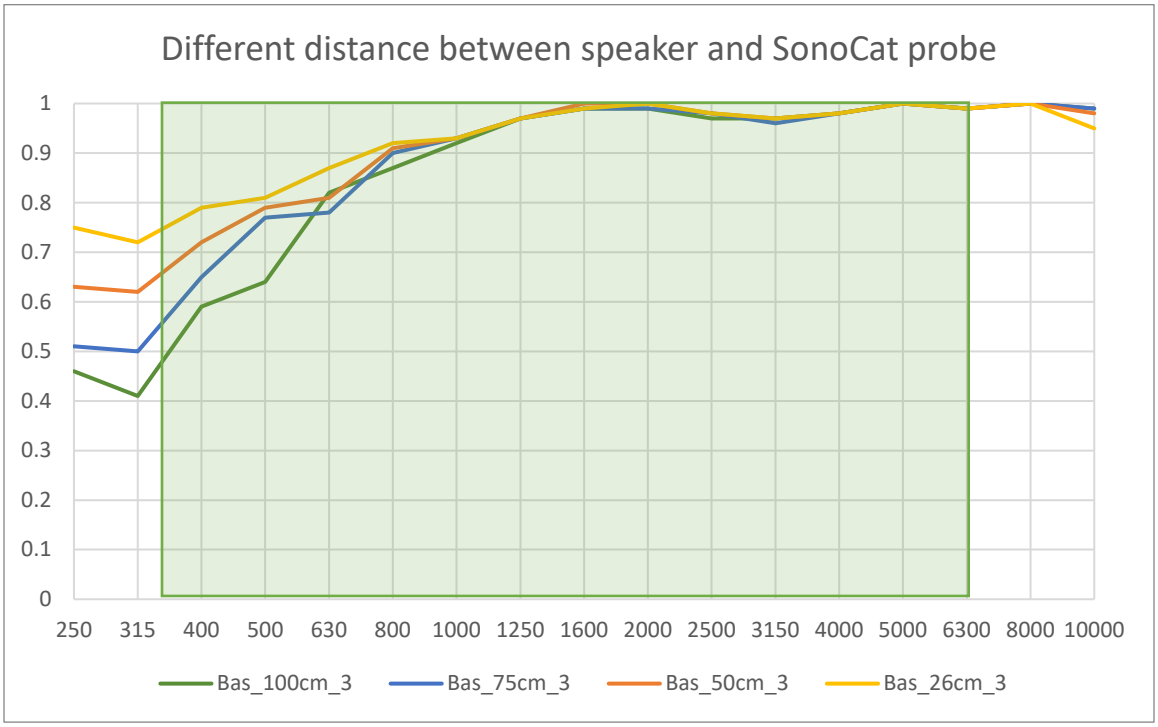

Figure 30: Behavior of the basotect at different distances between the speaker and the SonoCat probe.

The analysis of data collected at three different measurement distances (100 cm, 50 cm, and 26 cm) reveals interesting patterns that deserve careful discussion. The variation in distance between the sound source and the measurement system (probe + sample) shows a significant influence on the measured absorption coefficients, particularly evident in specific frequency bands. At low frequencies (330-500 Hz), a clear trend emerges: absorption coefficients increase significantly as the source distance decreases. This increase is particularly relevant and suggests better material characterization capability at low frequencies when the source is closer. In the middle frequencies (630-2000 Hz), differences between various distances become less pronounced, but a slightly higher value is still maintained for the 26 cm configuration. In this

region, absorption coefficients are generally very high (0.85-1.00) for all distances. At high frequencies (2500-6300 Hz), results tend to converge, showing minimal differences between different configurations. This suggests that in this range, source distance has less significant influence on measurement.

A particularly notable aspect is the excellent repeatability of measurements for each configuration. The three repeated measurements at the central point show minimal variations, in the order of 0.01-0.02, regardless of the distance used. This indicates good stability of the measurement system in all tested configurations. The overall data analysis suggests that the configuration similar to the Microflown probe, with source at 26 cm, represents the optimal choice from 800-1000Hz upward:

- It seems to overestimate at low frequencies.
- Maintains excellent measurement repeatability.
- Shows good coherence between measurements at different points of the sample.
- Allows direct comparison with measurements made with the PU probe (Microflown).

This distance choice will however be necessary during measurements inside the car. The reduced dimensions of the interior space would not allow typical distances of 1m (or at most 60cm). While closer distances like those similar to the Microflown probe are better manageable in limited environments. The ideal compromise between metrological and practical needs will be to measure at 26 cm, with damping calculated based on results obtained from Basotect measurements at various distances. From these, a correction factor was extracted given by the ratio between α(100cm) and α(26cm) of the known Basotect material. Here are the correction factors for each band:

Frequency [Hz]	Correction Factor
250	0.613
315	0.569
400	0.747
500	0.790
630	0.943
800	0.946
1000	0.989

1250	1.000
1600	1.000
2000	0.990
2500	0.990
3150	1.000
4000	1.000
5000	1.000
6300	1.000
8000	1.000
10000	1.042

Table 3: Correction factor identified for measurements at 26cm inside the car cabin.

The correction factor is more significant at mid-low frequencies (250-500 Hz), where values at 26 cm overestimate absorption and the correction factor would lower this overestimation. While at other frequencies, the modification is minimal. This method assumes that the ratio between measurements at the two distances is a stable characteristic of the measurement system and not of the specific material, therefore presupposes some limitations. However, since the most significant modification proved to be limited to low frequencies and with not excessively different levels, measurement at 26cm in particular cases seems to be acceptable even for the Sonocat probe.

The speaker choice required particular attention, considering the peculiar measurement geometry that required positioning the speaker facing downward. In this context, speakers of contained dimensions were chosen, accepting as a compromise lower performance at low frequencies. Two models were tested: an LG speaker, which proved to be the most effective choice, and an Anker (Bluetooth) speaker of smaller dimensions (6 cm diameter and 6 cm height). The latter, however, showed some criticalities, mainly due to its narrower sound cone which, directly centering the probe, created non-uniform excitation of the sample compared to the larger LG speaker.

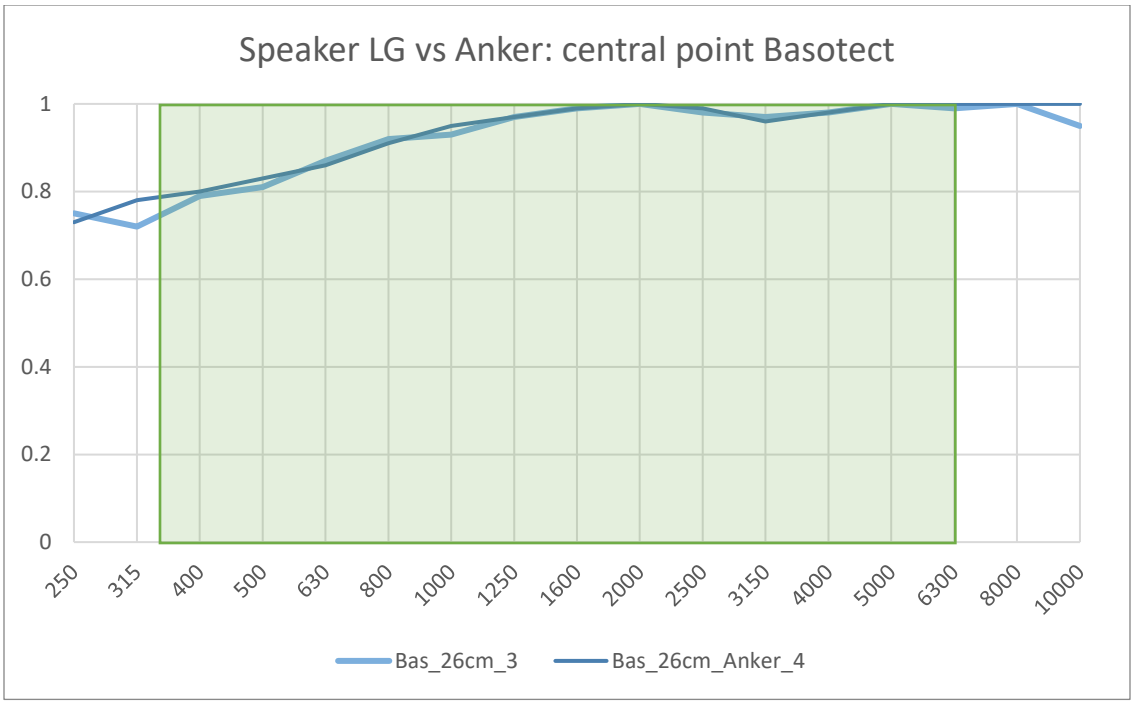

Figure 31: Use of two different speakers with different dimensions to evaluate the influence of the speaker on measurements.

Observing the trend of absorption coefficients across the frequency spectrum, a substantial homogeneity emerges in the results between the two sources. The differences found are generally contained, with variations in the order of a few hundredths in the absorption coefficient. This suggests good robustness of the measurement method with respect to source choice. At low frequencies, between 250 Hz and 500 Hz, some more marked differences are observed between the two sources. This difference could be attributed to the different directivity of the two sources at low frequencies, where the more contained dimensions of the Anker speaker could influence the radiation pattern. In the middle frequency region, between 630 Hz and 2000 Hz, the two sources provide practically identical results, with negligible differences. This indicates that in this frequency band, crucial for many acoustic applications, the choice of source is not particularly critical. At high frequencies, above 2000 Hz, a slight tendency of the Anker speaker to provide marginally higher absorption coefficients is noted, with the most significant difference at 10000 Hz where the Anker speaker records a coefficient of 1.00 versus 0.95 for the LG speaker. This difference actually shows once again a physical limitation of the smaller speaker, measuring a value too theoretical to be true.

Even observing a more extensive series of measurements, the data confirm the same trend.

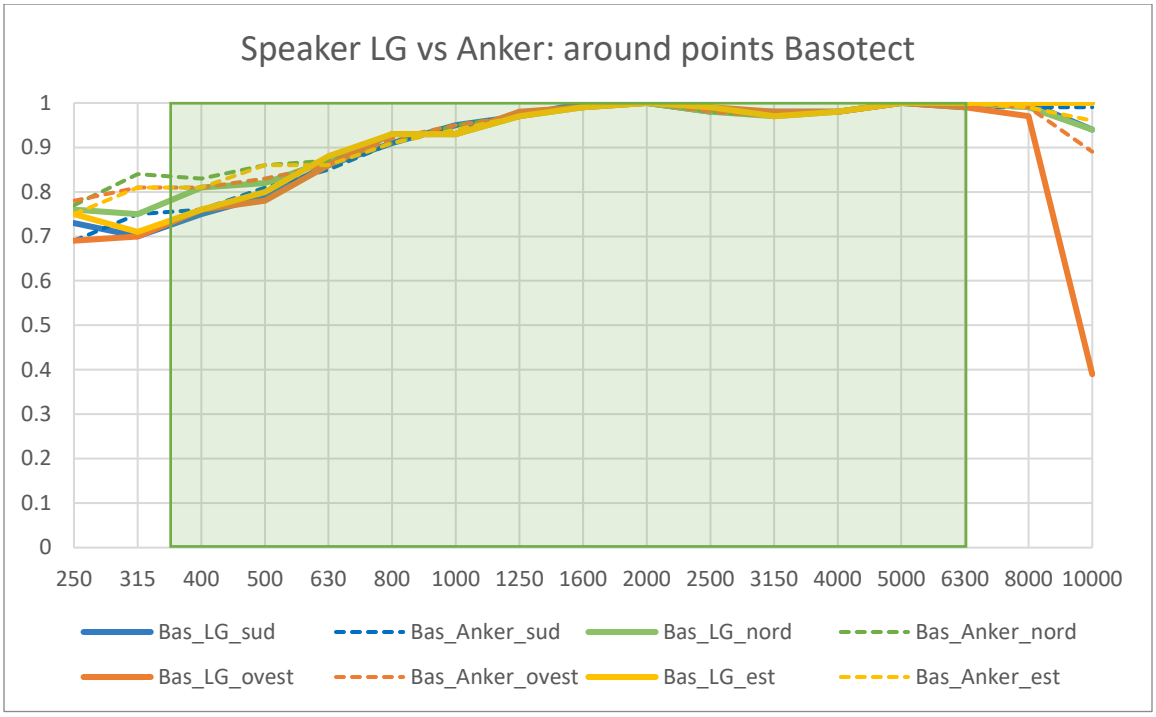

Figure 32: Further analysis of the difference in the use of the two speakers in the points measured around the central one.

The Anker speaker shows greater spatial variability compared to the LG speaker at low frequencies. This greater spatial variability with the Anker speaker suggests a less uniform sound field, probably due to its smaller dimensions and consequent lower directivity. Indeed, at low frequencies, a smaller speaker tends to behave like an omnidirectional source, with less controlled directivity that can lead to a less uniform distribution of sound energy in the measurement area. In contrast, the LG speaker, with its larger dimensions, maintains better directivity even at low frequencies, ensuring a more uniform sound field and more coherent measurements. At medium and low frequencies, the data confirm a certain concordance between the two sources observed previously. The observed spatial variability suggests the importance of taking measurements at multiple points and considering the average of results, regardless of the source used. At medium and low frequencies, the data confirm the excellent concordance between the two sources observed previously. The observed spatial variability suggests the importance of taking measurements at multiple points and considering the average of results, regardless of the source used. This approach helps compensate for sound field inhomogeneities and provides a more representative characterization of the material as a whole. Overall, both sources provide comparable and reliable results.

However, the LG speaker confirms itself as the preferable choice for several reasons. Its larger size ensures better response at low frequencies and a more uniform sound field in the measurement area. Moreover, the greater stability of results across the entire frequency spectrum suggests better overall reliability in measurements. This setup optimization phase has highlighted how the choice and positioning of the sound source are critical elements for ensuring the accuracy and repeatability of acoustic measurements.

3. Simulation with Comsol Multiphysics

3.1 Acoustic Simulation

Numerical simulation today represents a fundamental tool for the analysis and optimization of complex acoustic systems. In this study, COMSOL Multiphysics was chosen for its ability to handle multiphysical problems through different numerical approaches: from the Finite Element Method (FEM) to the Boundary Element Method (BEM), up to Ray Tracing [35]. In the specific field of acoustics, COMSOL offers a complete suite of tools for modeling and simulation of sound propagation in fluids and solids [36]. Of particular interest for this study is its ability to simulate acoustic measurements such as those described in UNI EN 1793-5 standard, which defines procedures for determining acoustic characteristics of noise reduction devices. The results of these simulations will be compared with experimental measurements in section 5.3.

3.1.1 Creation of the Geometric Model of the Seat

Geometry represents the fundamental domain on which the equations governing acoustic phenomena are solved [37] [38]. In the specific case of this study, the first significant obstacle concerned the geometric modeling of the seat and its import into COMSOL. The intrinsic complexity of the seat, characterized by curved shapes, padding, and structural details, posed significant challenges both in terms of modeling and file format compatibility. The first attempts with software like Blender, FreeCAD, Fusion 360, and SolidWorks highlighted fundamental issues related to the interoperability of export formats. The initial attempts involved using various commonly supported file formats such as .stl, .step, and SolidWorks native files. However, these formats systematically generated problems with internal nodes in the structure, compromising the model's integrity once imported into COMSOL. An alternative approach was to simplify the problem by initially modeling only half of the seat in SolidWorks, with the intention of using mirroring operations to complete the geometry. This strategy was explored in two modes: the first involved mirroring in SolidWorks before exporting in .stl and .step format, but showed criticalities in the junction between the two halves during Comsol processing; the second consisted of importing only half of the seat into COMSOL and using the software's native mirroring functionality. This latter approach, which involved creating two separate files - one for geometry and one for simulation - initially seemed promising, but showed significant limitations when trying to subdivide the geometry into sections for assigning different acoustic absorption coefficients.

A breakthrough came when we obtained access to the original 3D model provided by the car manufacturer for the passenger seat. However, even this geometry required a "cleaning" and optimization process suggested by the same company that supported me in studying the seat (ASK, Reggio headquarters). In this specific case, the complex geometry of the seat was simplified by joining appropriate faces with the "Form Composite Faces" function. While superfluous and problematic details that could compromise mesh quality were removed using the "Remove Details" function. The file was exported in ".mphbin" a native COMSOL format. Subsequently it is imported to proceed with the elimination of superfluous details, problematic nodes, and anomalous geometries generated during the import process. The use of the "Convert to Solid" function proved crucial in transforming what was essentially a set of surfaces into a coherent solid, necessary for subsequent acoustic analyses.

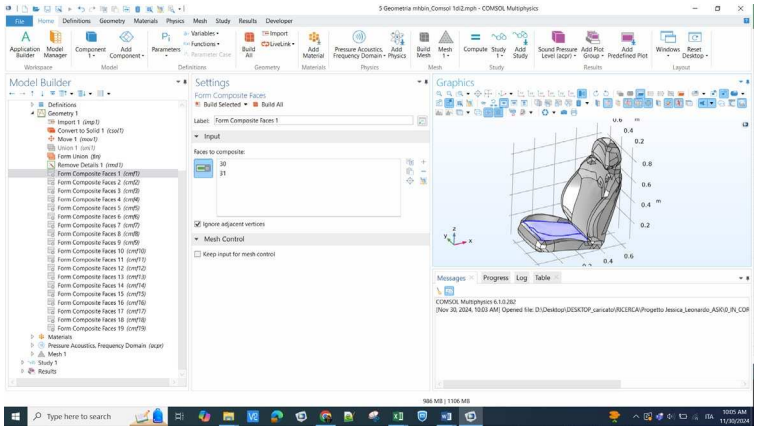

Figure 33: Comsol interface and related seat geometry during the area creation phase.

This process of geometric optimization highlights how critical model preparation is for acoustic simulations, especially when dealing with complex geometries like that of a car seat, which requires not only accurate shape representation but also the possibility of defining differentiated acoustic properties for different surfaces. As can be observed from the previous image, the seat was divided into the same zones identified during the measurement of the real seat surfaces with the Microflown probe..

3.1.2 Acoustic Simulation Strategy and Assignment of Measured Alpha Values

The crucial next step is represented by the choice of acoustic simulation strategy: the Finite Element Method (FEM), which discretizes the entire calculation domain into finite elements, and the Boundary

Element Method (BEM), which discretizes only the boundary of the calculation domain. In the specific case of the seat study, the choice fell on FEM for several fundamental reasons:

1. Geometric Complexity: FEM proves particularly suitable for problems with complex geometries and non-homogeneous materials, as in the case of the car seat. While BEM requires only boundary discretization, FEM, by discretizing the entire calculation domain, allows a more accurate representation of acoustic property variations within the seat volume.
2. Material Properties: The need to model different seat zones with different acoustic absorption coefficients makes FEM more appropriate, as it allows more direct and precise management of material properties within the calculation domain.
3. Acoustic-Structural Interaction: FEM offers greater capabilities in managing multiphysical problems, such as the interaction between the acoustic field and the seat structure.

Once the FEM methodology was chosen, the need to implement a Perfectly Matched Layer (PML) emerged. The PML is a fundamental tool for this type of acoustic simulations for several reasons:

1. Simulation of Open Domains: The PML acts as an artificial layer that absorbs acoustic waves passing through it, allowing simulation of an open domain (like the environment around the seat) within a finite computational domain. This is crucial for reproducing the test conditions of EN 1793-5 standard, where measurements take place in free field.
2. Prevention of Reflections: The PML minimizes unwanted reflections from the computational domain boundaries, ensuring that acoustic waves are absorbed rather than reflected. This is particularly important for obtaining accurate results in absorption measurements.
3. Computational Efficiency: Compared to other techniques for simulating open domains, the PML offers a good compromise between accuracy and computational cost. To implement it effectively, it was necessary to create a rectangular domain around the seat, where the PML layer could be properly defined and optimized.

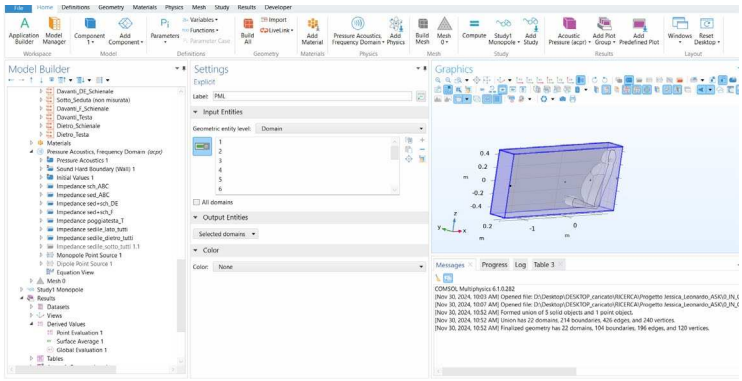

Figure 34: FEM simulation in Comsol of the measured seat.

The combination of FEM and PML required particular attention in mesh definition, especially in the PML layer, where a swept mesh with at least 6 elements is recommended to ensure optimal absorption of acoustic waves. This configuration, although more complex to implement compared to BEM, offers the flexibility and accuracy necessary to correctly simulate the seat's acoustic behavior under the conditions specified by the standard.

After defining the FEM methodology and the need for PML, the next phase involved detailed construction of the simulation domain. This required several critical steps:

- Construction of the Computational Domain:
  - Creation of an external parallelepiped that delimits the total simulation space.
  - Definition of the PML layer within this volume.
  - Precise positioning of elements according to EN 1793-5 standard: two front microphones at distances of 25 cm and 100 cm respectively. A third microphone placed behind the seat at a distance of 25 cm. The speaker at a distance of 165 cm from the seat always in line with the three previous microphones.
- Definition of Physical Domains: the model was divided into distinct domains. Thus, the PML domain, the internal domain (excluding seat, microphones, and speaker) representing the air volume, specific domains for seat, microphones, and speaker were created.
- Implementation of "Pressure Acoustics, Frequency Domain" (acpr) Physics: this physical interface was chosen for its specific characteristics including the ability to calculate pressure variations for acoustic wave propagation in fluids under quiescent background conditions and adaptability to frequency domain simulations with harmonic variations of the pressure field.

In particular, the acpr physics allowed adding suitable elements for carrying out the simulation in question. The addition of the "impedance" function allowed the association between the various identified seat zones with the acoustic absorption coefficient obtained from Microflown measurements. Special attention was devoted to defining boundary conditions, with specific implementation of Sound Hard Boundary (SHB) for the internal part of the PML domain, excluding the seat domain, allowing correct modeling of the interaction between acoustic waves and rigid surfaces and appropriate management of interfaces between different acoustic domains.

A crucial aspect of the simulation concerned sound source modeling. Initially, the choice was to opt for a faithful representation of the Microflown probe's speaker, accurately reproducing its physical dimensions. This approach was chosen to rigorously adhere to UNI CEN/TS 1793-5:2006 standard, which prescribes a series of measurements at different speaker incidence angles. The standard specifically requires rotation of the speaker-microphone assembly in nine different positions, with 10° increments. This procedure is designed to:

- Sample reflections from different surface areas.
- Consider the effect of complex surface structures.
- Calculate spatial averages of the "reflection index" (RI) for each third-octave band.
- Simulate different traffic noise arrival directions in real conditions.

Following these requirements, complete simulations were conducted with the speaker modeled in its real dimensions, rotated according to the standard specifications. However, analysis of the simulation results revealed that variations in acoustic response with varying incidence angle were negligible. This discovery led to reconsidering the modeling approach. Given the limited influence of angularity on acoustic response, a significant simplification was opted for, implementing a Monopole Point Source. This choice was motivated by several factors:

- The uniformity of response observed in multi-angle simulations.
- Significant reduction in computational complexity.
- The Monopole Point Source's ability to provide uniform radiation.
- Greater efficiency in simulation management.

This simplification differs from microphone modeling, which was maintained as cylindrical elements with their own surface, since their position and physical geometry are crucial for correct detection of sound pressure levels at specific points required by the standard. A Monopole Point Source represents an

idealized sound source that radiates energy uniformly in all directions and behaves like a pulsating sphere whose radius tends to zero. Initially, the source's sound power was mathematically calculated in third-octave bands and then replaced with power values measured during actual simulation measurement.

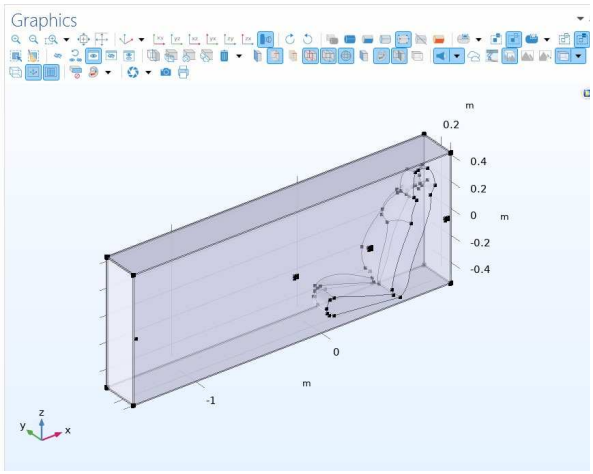

Figure 35: Detail of geometries used within the FEM simulation..

Another fundamental element in carrying out the simulation was mesh sizing, which required particular attention to ensure accurate results. The mesh strategy was based on the fundamental principle that correlates element size to sound wavelength (λ), with particular reference to the λ/4 criterion [37]. The maximum element size must be less than a quarter of the wavelength (λ/4): this ensures sufficiently fine discretization to accurately capture acoustic wave behavior. Furthermore, sizing varies with frequency, since wavelength is inversely proportional to it: for higher frequencies (shorter wavelengths), a finer mesh is needed; while for lower frequencies (longer wavelengths), larger elements can be used.

The choice of mesh type was differentiated based on the nature of objects and domains to be discretized. Free Triangular mesh for microphones and seat, characterized by unstructured triangular elements and accurate representation of geometric details. Free Tetrahedral mesh for the internal volume part of the parallelepiped, characterized by three-dimensional tetrahedral elements and the ability to efficiently fill complex three-dimensional spaces. The simulation was performed using frequency domain analysis, also implementing a Parametric Sweep to investigate the system's response at frequencies of interest in third-octave bands. The implementation of the Parametric Sweep has indeed allowed automatic execution of successive simulations for each third-octave frequency. This overall configuration has allowed creation of

a simulation environment that faithfully reproduces the test conditions specified by EN 1793-5 standard, enabling accurate analysis of the seat's acoustic behavior. After completing the simulation with FEM method, a comparative analysis was conducted using Ray Tracing, to verify at the same time which simulation method would be more suitable for such a study. This alternative approach involved some significant differences in modeling.

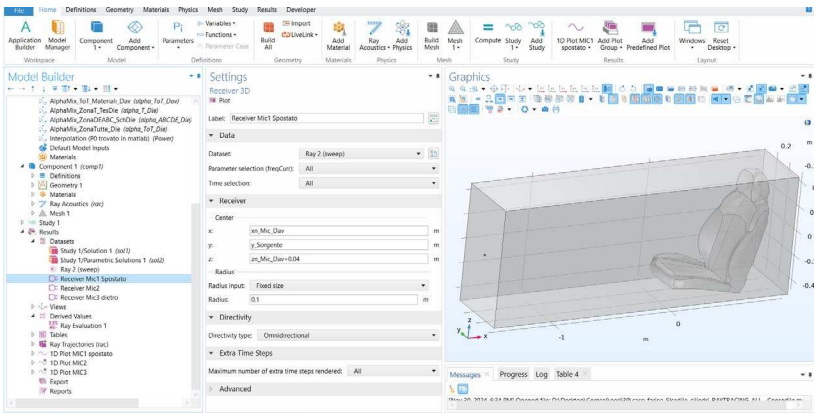

Figure 36: Ray Tracing simulation in Comsol of the measured seat.

FEM has as its operating principle the resolution of acoustic equations in each element of the discretized domain. Instead, Ray Tracing is based on tracing acoustic rays that propagate like beams of light. These sound rays propagate in straight lines and interact with surfaces through reflection, absorption, or transmission. The advantage of Ray Tracing lies in lower computational cost for high frequencies and greater attention to sound propagation. However, it presents lower accuracy at low frequencies and certain sensitivity to surface mesh quality [31]. Both simulations were executed without seat both in FEM and Ray Tracing to validate the base behavior of the model and verify correct implementation of boundary conditions.

3.2 Validation of the Simulation with Real Measurements

Subsequently, a real case of what was represented inside Comsol was simulated. The seat was positioned 1 meter from the floor to replicate the free field conditions of the simulations. Speaker and microphones were arranged according to standards, as in the simulations. Acquisition of microphone signals and generation of the sweep signal (20Hz-20KHz) for the speaker (passing through an amplifier) were

implemented using the Zoom audio card, already described in section 2.2.3. The speaker at the same height as the microphones was placed both in the configuration in front of the seat and behind it, to verify the presence of interesting interactions. Calibration was done by recording the environment at the same measurements but in the absence of the seat and was used in post-processing through a specially created Matlab script. In particular, the analysis process is articulated in several phases: initially, the audio signals recorded by the two microphones are converted from time domain to frequency domain through the application of Fourier transform. This transformation allows obtaining a detailed spectral representation of the signals, highlighting the energy distribution across different frequency bands. For each analyzed frequency band, the difference between the transmitted pressure signal (recorded by the front microphone) and the received signal (recorded by the rear microphone) is calculated. This difference represents the attenuation introduced by the seat to the passage of the sound wave. The absorption coefficient α is then calculated for each frequency using the formula:

$$\alpha = 1 - \left(\frac{Preceived}{Ptransmitted}\right)$$

where $Preceived$ represents the sound pressure measured by the receiving microphone positioned behind the seat, while $Ptransmitted$ is the sound pressure recorded by the transmission microphone placed in front of the seat. This experimental methodology will allow verification in section 5.3 of the correspondence between numerical predictions and real behavior of the seat, providing complete validation of the simulation approach developed.

Figure 37: Setup of real measurements (EN-1793-5).

4. Analysis of Obtained Experimental Measurements

4.1 Kundt's Tube

4.1.1 Measurements of Known Materials

Comparative analysis between Basotect and EPS revealed substantial differences in their acoustic performance, despite their comparable thicknesses (5 cm for Basotect and 6 cm for EPS). This diversity is mainly attributable to their fundamentally different cellular structure: Basotect presents an open-cell structure, while EPS is characterized by closed cells, as discussed in section 2.1.1. Applying the lambda/4 principle presented in Chapter 1, theoretical predictions suggest optimal absorption around 1700 Hz for Basotect and 1417 Hz for EPS. The measurements confirm this prediction for Basotect, which indeed shows a significant absorption peak around 1600 Hz. EPS, however, behaves notably differently: it maintains a low absorption coefficient for most of the spectrum, showing only a slight increase beyond 1250 Hz, with a peak at 1600 Hz that appears in some measurements but is absent in others.

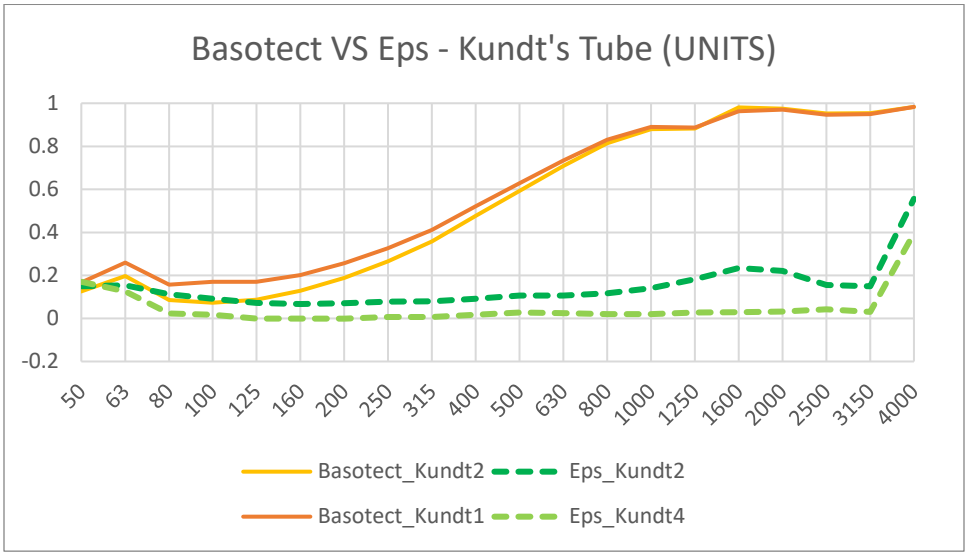

Figure 38: Comparison of alpha values of known materials measured with the Kundt's Tube.

The analysis of measurement quality reveals significant differences between the two materials. Basotect demonstrates excellent reliability in repeated measurements: even considering the two tests that present the greatest discrepancy between them, variations are minimal, confirming the method's robustness for this type of material. This aspect will be further confirmed by comparison with in-situ measurements presented in section 5.1. EPS, on the contrary, presents considerable variability: comparison between

different measurements shows substantial differences both in general trend and in the presence or absence of specific absorption peaks. This marked variability in measurements suggests possible limitations of the Kundt's tube in characterizing highly reflective materials like EPS, indicating that the peak observed at 1600 Hz might be the result not only of material properties but also of external factors such as errors in sample mounting or unintentional system resonances. The precision of measurements in the Kundt's tube is closely correlated to sample preparation and installation and represents a challenge of the method. When the sample diameter is slightly smaller than that of the tube, gaps are created between the material and the walls that generate unwanted acoustic losses. These losses can lead to an overestimation of the absorption coefficient, as the system records as material absorption also the dissipation due to air leaks. On the other hand, a sample with diameter larger than that of the tube requires forced compression during installation, which can introduce mechanical stresses in the material. These stresses can generate spurious resonances that artificially alter the measurement of acoustic absorption, compromising the accuracy of characterizing the material's real properties. Therefore, the uncertainty of the EPS data, beyond it being a reflective material, may be caused by these two issues [39] [40].

Experimental observations find correspondence in the structural characteristics of the two materials. Basotect, characterized by an open-cell structure and a low density of 9 kg/m³, offers ideal conditions for sound energy dissipation: its structure allows sound waves to effectively penetrate the material, where energy is dissipated through friction with the internal structure. EPS, instead, with its closed-cell structure and higher density (15-30 kg/m³), behaves substantially differently: its structural configuration creates a barrier to sound wave penetration, significantly reducing the capacity for energy dissipation within the material.

4.1.2 Measurements of Car Seat Samples

It is important to specify that the samples analyzed in the Kundt's tube do not come directly from the Hyundai Genesis EQ900 seat used for in-situ measurements. For laboratory tests, samples of materials with characteristics equivalent to those observed in the original seat were instead used, carefully selecting components that reproduced the same structural and acoustic properties of the reference seat.

The analysis of measurements made with the Kundt's tube on expanded polyurethane and non-woven fabric reveals distinctive and complementary acoustic behaviors.

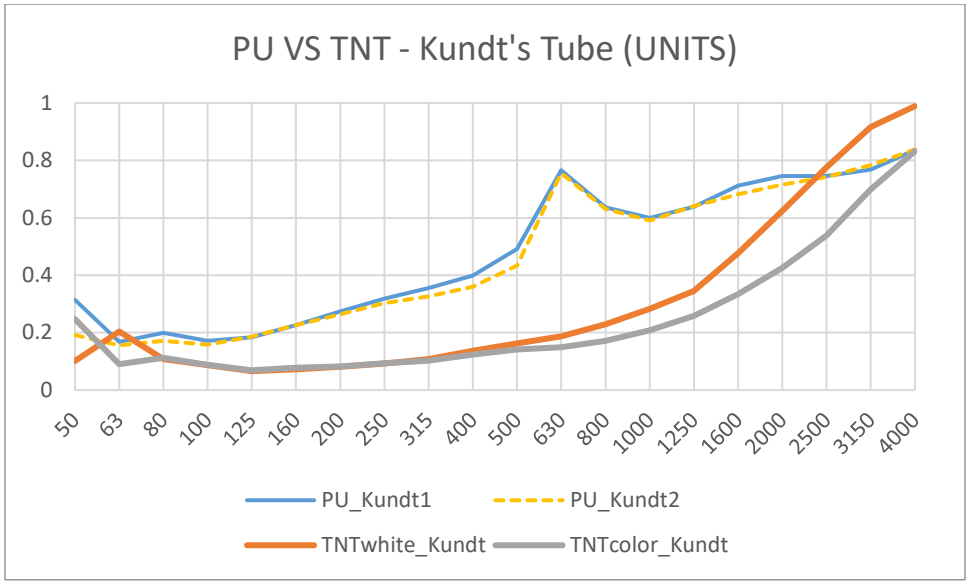

Figure 39: Comparison of alpha values of Expanded Polyurethane and Non-Woven Fabric materials present in a car seat and measured with the Kundt's Tube.

Expanded polyurethane, with a thickness of 4.5 cm and a density of 30-40 kg/m³, shows significant absorption already at low frequencies ($\alpha > 0.15$) with a marked peak around 630 Hz ($\alpha \approx 0.76$) and maintains good absorption at high frequencies ($\alpha \approx 0.84$ at 4000 Hz). This behavior can be attributed to its open-cell structure that favors viscous dissipation.

A particularly interesting aspect concerns precisely the position of its absorption peak. According to the lambda/4 principle, considering the 4.5 cm thickness of the material, we would have expected a maximum absorption around 1889 Hz. However, measurements show a pronounced peak at 630 Hz, a frequency significantly lower than theoretically predicted. It is important to note that, although the material still shows an increase in absorption around the theoretical frequency of 1889 Hz, confirming the validity of the lambda/4 principle, the presence of this anticipated peak at 630 Hz suggests the existence of additional absorption mechanisms.

The non-woven fabric, with thickness of 1.4 cm, shows instead a very different behavior, with excellent performance primarily at high frequencies. The absorption coefficient increases progressively with frequency, reaching very high values above 2000 Hz. This characteristic relates to its fibrous structure: the thin and densely interwoven fibers create numerous interaction points with the sound wave, particularly

effective when the wavelength becomes comparable with the characteristic dimensions of the fibrous structure. It is interesting to note how the TNT, despite its reduced thickness, manages to provide exceptional absorption at high frequencies, demonstrating high efficiency per unit thickness. This complementarity between polyurethane (effective at low and medium frequencies) and TNT (effective at high frequencies) suggests potential advantages in combining them use in multilayer systems, where each material can contribute optimally in its preferential frequency band.

The analysis of leather-TNT composite systems offers interesting insights for understanding how leather, both smooth and perforated, modifies the acoustic behavior of TNT (remembering that both leather samples are self-supported by TNT).

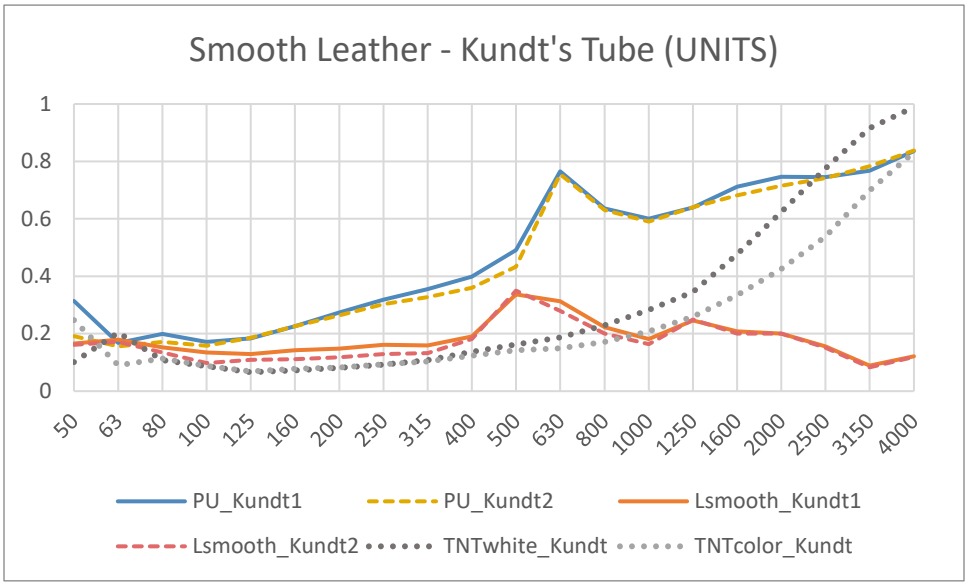

Figure 40: Comparison of alpha values to identify the behavior of the sample with smooth leather, comparing it with the trend of PU and TNT alone (measured with the Kundt's Tube).

Remember that TNT alone shows increasing absorption with frequency. However, this characteristic is radically modified when TNT is coupled with the two types of leather.

In the case of the sample formed by smooth leather and TNT with PU (called Lsmooth), a characteristic absorption peak is observed at 500 Hz ($\alpha \approx 0.35$) followed by a decrease in absorption at high frequencies. The smooth leather, acting as a reflective barrier, dominates the surface acoustic behavior of the system. The peak at 500 Hz is attributable to the functioning of the system as a mass-spring resonator, where the

leather acts as mass while the PU+TNT system underneath provides the spring effect. The presence of the PU layer between the leather and TNT significantly modifies the overall rigidity of the system compared to what was previously hypothesized, thus influencing the resonance frequency of the system. The Lsmooth trend is very similar to that of PU but lower (less absorbent) and shifted to the left. The frequency shift could be caused by:

- The presence of smooth leather that adds reflective mass to the system.
- Adding mass to a resonant system typically lowers the resonance frequency, so the complete system becomes a "slower" mass-spring oscillator.

While the amplitude reduction could be due to:

- The non-porous surface of smooth leather reflects part of the sound energy.
- The sound wave must pass through this reflective layer before reaching the PU and TNT, so less energy is available to be dissipated by PU and TNT.

This behavior confirms that, while polyurethane remains the main responsible for the absorption mechanism, smooth leather significantly modifies the system's performance, acting both on the resonance frequency through its inertial contribution, and on absorption efficiency through its reflective properties.

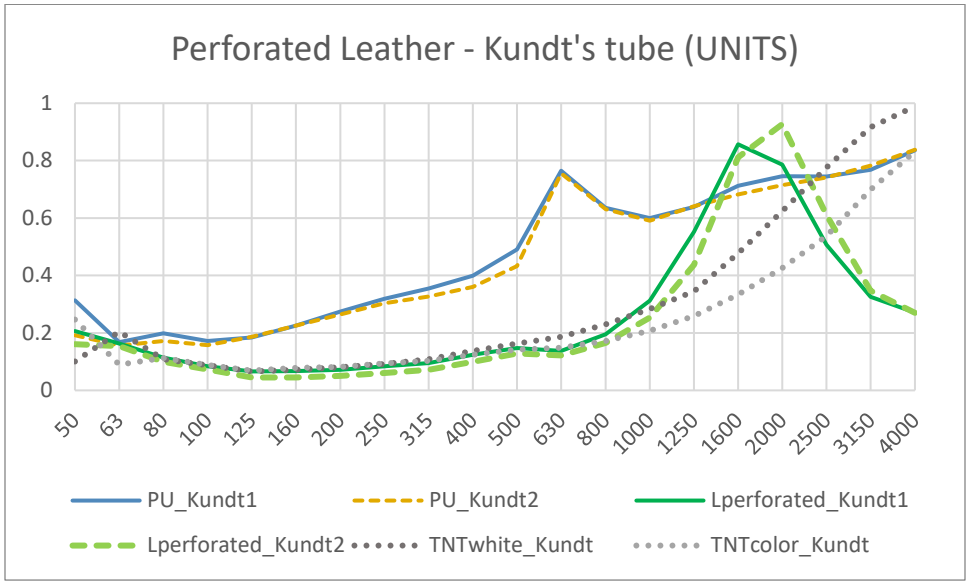

Figure 41: Comparison of alpha values to identify the behavior of the perforated leather sample, comparing it with the trend of PU and TNT alone (measured with the Kundt's Tube).

The situation changes considerably with perforated leather (self-supported by PU alone). The peak this time is even increased and shifted towards high frequencies (between 1600-2000 Hz with $\alpha \approx 0.81$-0.93). The frequency shift could be caused by:

- The perforations in the leather create an array of Helmholtz resonators.
- Each hole, together with the air volume in the underlying PU, forms a resonator.
- The reduced dimensions of the holes (1 mm diameter and 2 mm apart) and air cavities determine higher resonance frequencies.

While the amplitude increase could be due to:

- A synergy occurs between two mechanisms: the Helmholtz resonators created by the perforations and viscous dissipation in the underlying PU which is reached more easily in this case compared to smooth leather, thanks to direct passage of sound energy through the holes.
- The PU provides optimal damping for the resonators resulting in an improvement over the previous case of PU's dissipative mechanism.

In practice, perforated leather does not act as a barrier (as in the case of smooth leather) but as a system of tuned resonators that, working in synergy with the underlying PU, optimizes acoustic absorption. It's as if the perforations created "preferential channels" through which sound energy is first concentrated (resonator effect) and then effectively dissipated in the underlying PU.

This comparative analysis demonstrates how leather, depending on its surface structure, can radically modify the acoustic behavior of the underlying material: smooth leather tends to hide the properties of TNT, while the perforated version allows partial expression of its absorbent characteristics, while still dominating the overall system behavior with its resonance mechanisms.

The combination of:

- Very small holes (1 mm);
- Regularity of hole distribution with close spacing (2 mm);
- Thin leather thickness (≈ 1 mm);
- Controlled volume of air in the underlying PU;
- Creates ideal conditions for creating a regular pattern of resonators that can interact with each other optimizing absorption at medium-high frequencies.

To verify this statement, we can calculate the theoretical resonance frequency of the Helmholtz resonators formed by the holes.

The resonance frequency for a Helmholtz resonator is given by:

$$f = \left(\frac{c}{2\pi}\right) * \sqrt{\frac{A}{V * L}}$$

where:

- c is the speed of sound (≈ 340 m/s);
- A is the hole area (π * (0.0005 m)² = 7.85 * 10^{-7} m² for 1 mm diameter holes);
- L is the neck length (leather thickness, about 1 mm = 0.001 m);
- V is the air cavity volume in the PU (which we can approximate considering the "air cell" associated with each hole).

For volume V, considering the 2 mm spacing between holes, each hole has an influence area of about 4 mm² on the surface. Considering a depth in PU of 45 mm (0.045m), we obtain V ≈ 4 mm² × 45 mm = 180 mm³ = 1.8 * 10^{-7} m³.

Inserting these values:

$$f = \left(\frac{340}{2\pi}\right) * \sqrt{\frac{7.85 * 10^{-7}}{1.8 * 10^{-7} * 0.001}} \approx 1720\ Hz$$

The result gives us a resonance frequency in the order of 1500-2000 Hz, which effectively corresponds to the peak observed experimentally.

We can affirm that the Kundt's tube is providing reliable measurements as a starting point. Let's see if even with multi-layer material samples, similar results are obtained.

To more faithfully reproduce the composition of the Hyundai Genesis EQ900 seat, two multilayer samples were created by combining the previously analyzed materials. These composite systems replicate the layering present in the original seat, allowing laboratory study of configurations representative of the real structure, although not coming from direct coring of the seat.

Figure 42: Representative sample of the seat (smooth leather with PU and TNT and yellow PU) with final height of 6.5cm.

Analysis of the combined system data of smooth leather with PU and TNT and the addition of the yellow PU layer (called PULsmooth) reveals interesting acoustic behavior that reflects the interaction between the different layers.

By arithmetically averaging the measured values of PULsmooth (red dashed line in figure 16), it is evident how the system maintains moderate absorption ($\alpha \approx 0.2$-0.3) at low and medium frequencies, while decreasing significantly at high frequencies (>2500 Hz). A slight peak occurs around 630 Hz ($\alpha \approx 0.256$). The four measurements of the PULsmooth system show some variations among themselves, while maintaining a coherent general trend. This variability, although contained, highlights the importance of performing multiple measurements of the same sample to obtain a more robust and reliable characterization of acoustic behavior. Once again, the observed differences can be attributed mainly to the intrinsic criticalities in the preparation and positioning of samples in the Kundt's tube, confirming the need for a statistical approach based on repeated measurements to minimize the effects of these experimental variables.

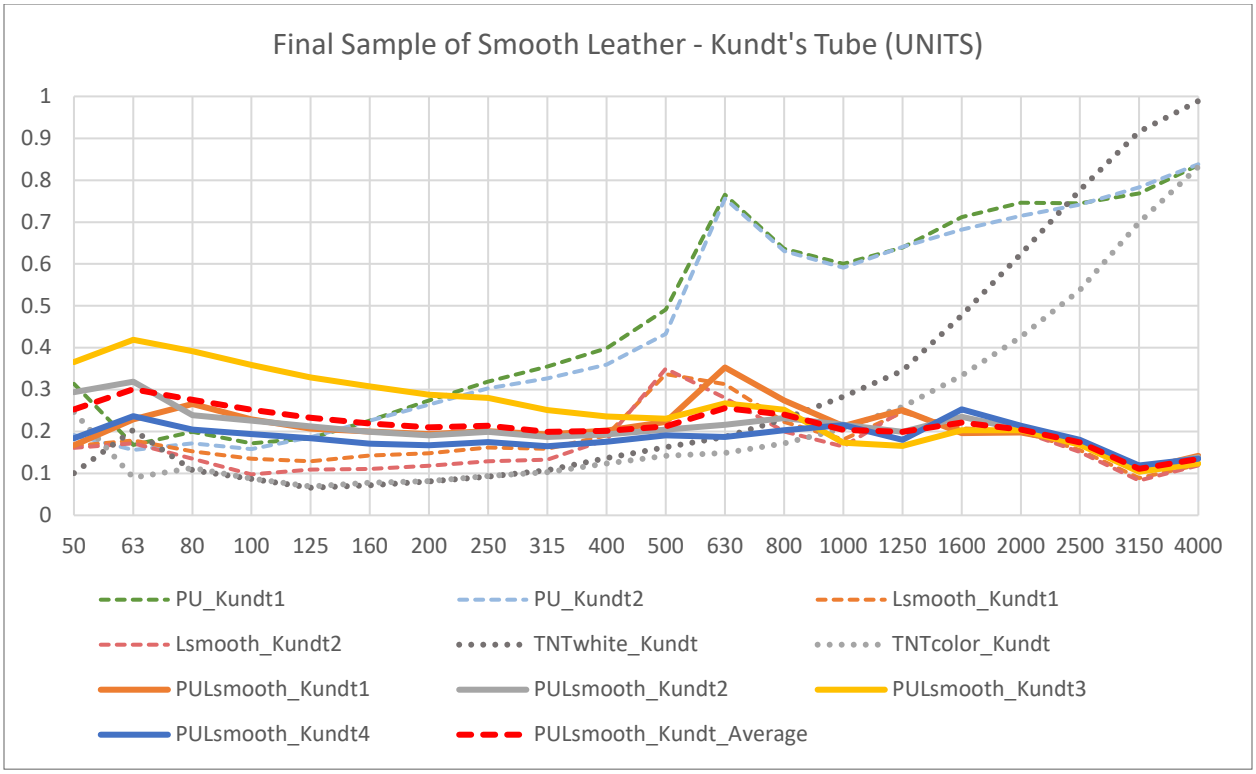

Figure 43: Comparison of previous trends with the sample composed of smooth leather, PU, TNT, PU.

Comparing these results with previous measurements of individual components, it can be observed that:

1. Comparison with single PU (which showed peak at 630 Hz, $\alpha \approx 0.76$):
   - The characteristic PU peak at 630 Hz is still visible but strongly attenuated ($\alpha \approx 0.35$).
   - The presence of surface smooth leather significantly reduces the overall absorption effectiveness.
   - The increase in total thickness (6.5 cm) does not improve absorption as might be expected.
2. Comparison with smooth leather + PU + TNT system (which showed peak at 500 Hz):
   - The characteristic peak at 500 Hz is less pronounced.
   - The general trend shows more uniform but reduced absorption.
   - High frequencies show a decrease in absorption similar to the original system.

Therefore, smooth leather continues to dominate surface behavior, limiting sound wave access to underlying layers. Despite the addition of supplementary PU, this cannot compensate for the barrier effect of leather but the system still maintains a memory of PU's resonant behavior (peak at 630 Hz) in attenuated form.

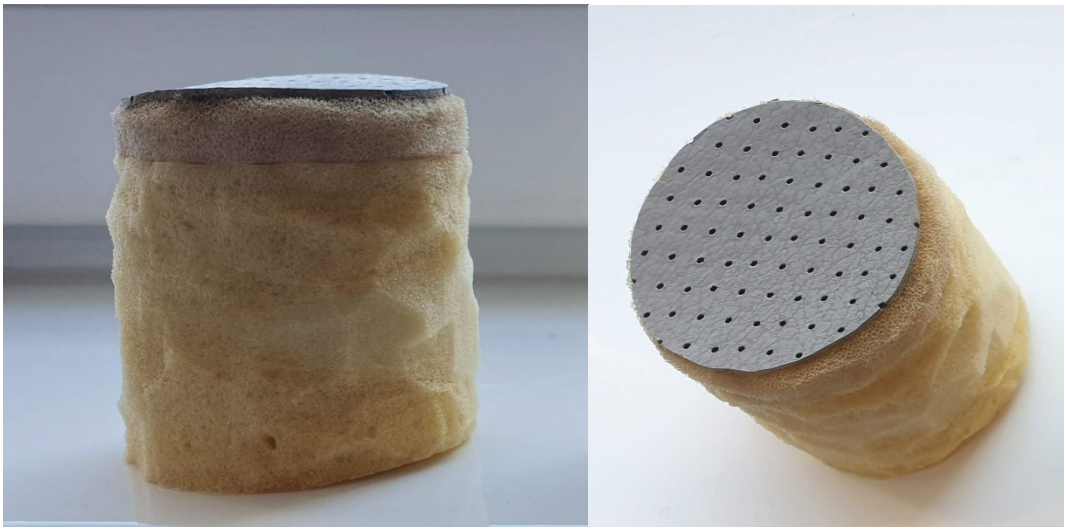

Figure 44: Representative sample of the seat (perforated leather with PU and yellow PU) with final height of 5.5 cm.

Observing instead the combined system of perforated leather with its underlying PU and the addition of yellow PU layer (called PULperf) shows interesting behavior that reflects the interaction between components.

In this case too, one can average the four measurements to obtain a single value, however in this case an interesting diversity occurred between the first two measurements and the last two. The issue of mounting and cutting the sample inserted in the Kundt's tube occurs once again:

- The first two measurements might present a slightly different mounting that modified the effective distance between layers.
- A small variation in coupling between layers could have altered the resonant behavior of the system.
- Different pressure in mounting could have modified the effective thickness of PU. This would change both the air volume available for Helmholtz resonators and the elastic properties of PU.
- In the first two measurements, the leather holes might have been partially obstructed or deformed.
- A different alignment of holes with respect to the PU structure could modify resonator effectiveness.
- The first two measurements show an anticipated peak (800 Hz) that could indicate a smaller resonant cavity.

- The last two measurements show behavior more similar to the original PU, suggesting better coupling between layers.

The overall average shows that the system still maintains significant absorption between 500 and 1250 Hz, but the observed variability once again underlines the critical importance of mounting in these multilayer systems, especially when resonant elements like holes in the leather are present.

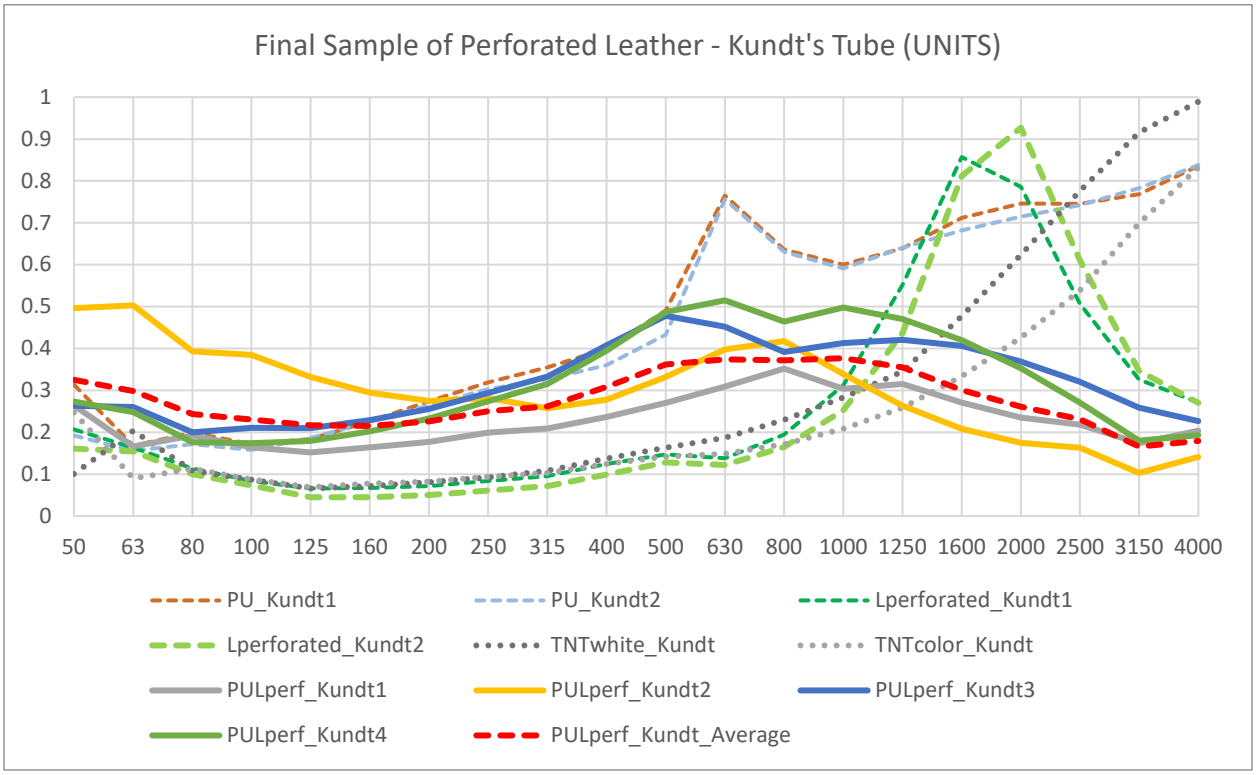

Figure 45: Comparison of previous trends with the sample composed of perforated leather, PU, PU.

Comparing these results with previous measurements of individual components, it can be observed that:

1. Comparison with single PU (peak at 630 Hz, $\alpha \approx 0.76$):
   - The characteristic PU peak at 630 Hz is still visible ($\alpha \approx 0.42$-0.52).
   - The peak intensity is reduced but less drastically compared to the case with smooth leather.
   - PU maintains a greater influence on overall behavior.
2. Comparison with perforated leather + PU system (peak 1600-2000 Hz):
   - The high-frequency peak typical of perforated leather is significantly attenuated

- The effect of Helmholtz resonators seems to be less dominant
- The presence of additional PU seems to "dampen" the resonant behavior of the holes.

Therefore, leather perforation allows better interaction with underlying layers: the system indeed maintains characteristics of both PU (peak at 630 Hz) and perforated leather. Moreover, the addition of supplementary PU seems to favor absorption mechanisms typical of polyurethane over those of Helmholtz resonators. Unlike the system with smooth leather, in this case the coupling of materials produces a more balanced behavior, where both absorption mechanisms (viscous dissipation of PU and hole resonance) contribute to overall behavior, albeit with a prevalence of PU effect.

4.2 Microflown

4.2.1 Measurements of Known Materials

A fundamental aspect for validating an in-situ measurement instrument is its ability to provide consistent and reliable results in real operating conditions. The analysis of repeatability and robustness of the Microflown probe was conducted through two complementary series of tests: repeated measurements at the same point and measurements around the reference point.

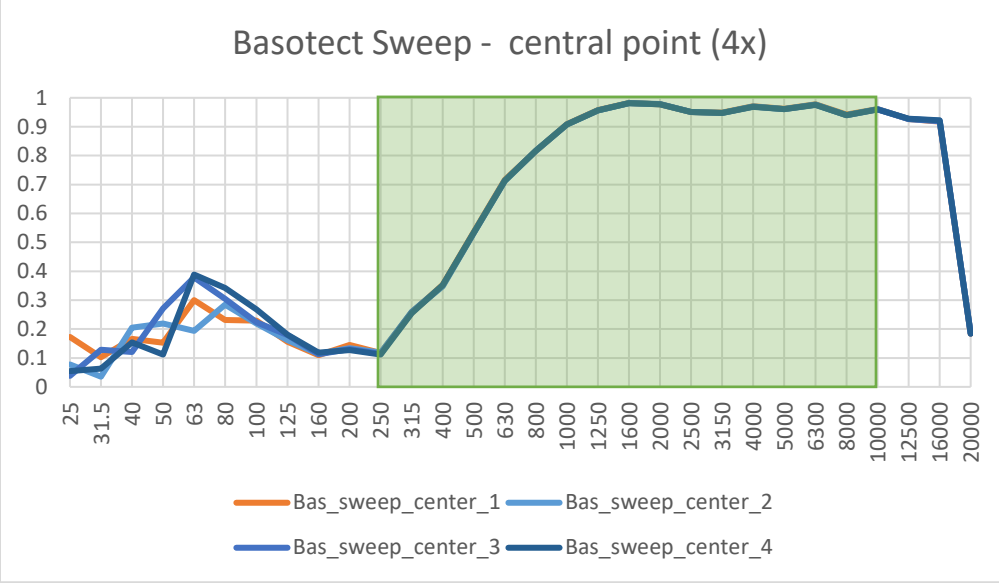

Figure 46: Measurement of Basotect absorption (100 cm x 50 cm) with the Microflown probe at the same point 4 times.

The first series of tests, consisting of four successive measurements in the same position, demonstrated excellent repeatability of the instrument, with practically overlapping absorption curves, confirming what was anticipated in section 2.2.2.

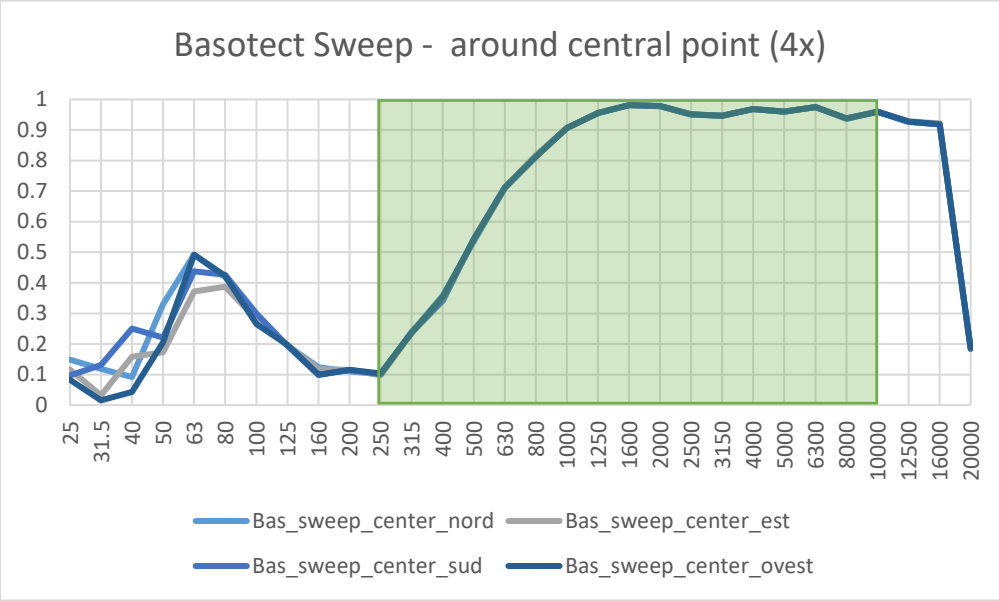

Figure 47: Measurement of Basotect absorption (100 cm x 50 cm), with the Microflown probe at 4 points around the center at a distance of 2 cm from it.

The second series, performed by moving the measurement point by 2 cm in the four cardinal directions, confirmed the system's robustness, showing substantial invariance of results with respect to small variations in measurement position. The almost perfect overlap of results obtained in these two test series is particularly significant in the probe's operating range (250-8000 Hz). Although some discrepancies are observed at very low frequencies, these fall outside the instrument's declared operating range (250-10000 Hz) and therefore do not affect measurement validity. This dual verification of repeatability (same point) and robustness (adjacent points) is crucial for in-situ applications, where measurement conditions are not always ideal. The instrument's ability to provide consistent results, both in repeated measurements and in slightly different positions, confirms the reliability of the measurement method and its applicability in practical acoustic characterization contexts.

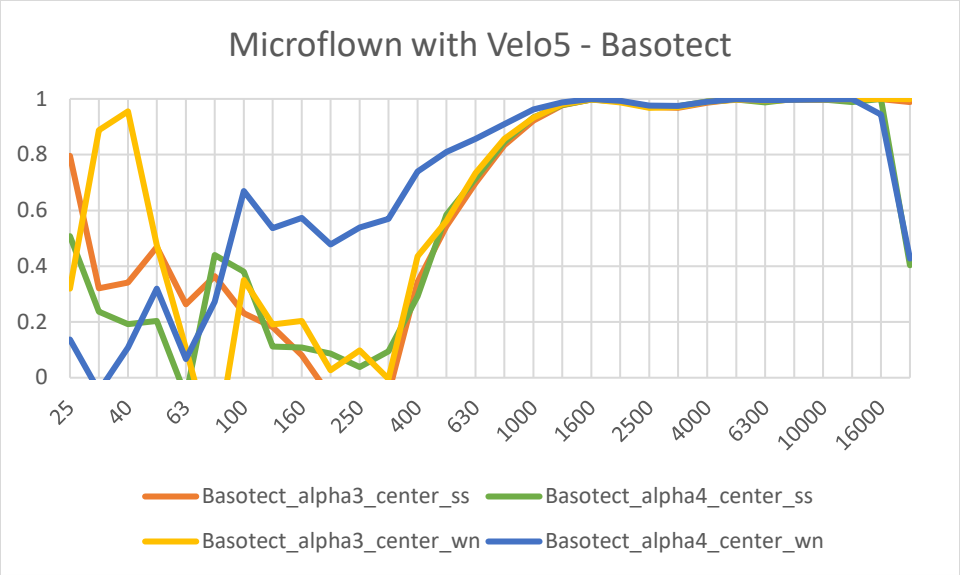

Figure 48: Comparison of measurements with the complete Microflown system and its native Velo5 software on the Basotect sample.

During the study, numerous comparative measurements were conducted to evaluate the performance of the complete Microflown system with native Velo5 software in the two identified optimal configurations:

- Fixed gain activated with 10V output (alpha3);
- Fixed gain deactivated, with gain set at 12 o'clock and voltage 4.38V (alpha4), calibrated to obtain 88dB equivalent to the reference laser system.

The results of these configurations will be compared with numerical simulations presented in chapter 3 and with Sonocat measurements in section 5.2. For each configuration, two excitation signals were used: sine sweep and white noise. Comparison of results shows that:

- In the medium and high frequency region (800-8000 Hz), both configurations show coherent and reliable results, with very similar absorption coefficients regardless of the type of gain used.
- At low frequencies (<800 Hz), the configuration with deactivated fixed gain (Alpha 4) combined with white noise signal showed a very different trend (almost opposite) to those of the other three.
- The sine sweep signal produces more stable and repeatable results compared to white noise in both configurations, particularly evident at low frequencies where white noise shows greater variability and some physically implausible values.

These results suggest preferring the configuration related to alpha4 to maintain consistency with the study conducted with the laser (same settings): fixed gain disabled with gain at 4.38V. For sample excitation, sine sweep has proven to be the optimal choice, as confirmed by an in-depth study published during the doctoral course [1]. This type of signal, compared to alternatives like white noise, enabled us to obtain more accurate and repeatable measurements thanks to its ability to optimally concentrate energy at different frequencies. Particularly at low frequencies, there is greater variability in results with white noise that can be attributed to three main factors:

- White noise has a uniform energy distribution across all frequencies, while sine sweep concentrates energy at each frequency at specific moments, proving more effective especially at low frequencies where more energy is required to obtain a good signal-to-noise ratio.
- The absence of fixed gain (Alpha 4) makes the system more sensitive to signal variations. When this combines with a less structured signal like white noise, it can lead to less stable measurements at low frequencies, where the system is intrinsically more sensitive.
- The signal-to-noise ratio (SNR) at low frequencies is generally more critical. White noise, having energy distributed across the entire spectrum, provides less useful energy per frequency compared to sine sweep, a situation that becomes particularly problematic when fixed gain is disabled.

These aspects are validated through comparison with numerical simulations presented in Chapter 3.

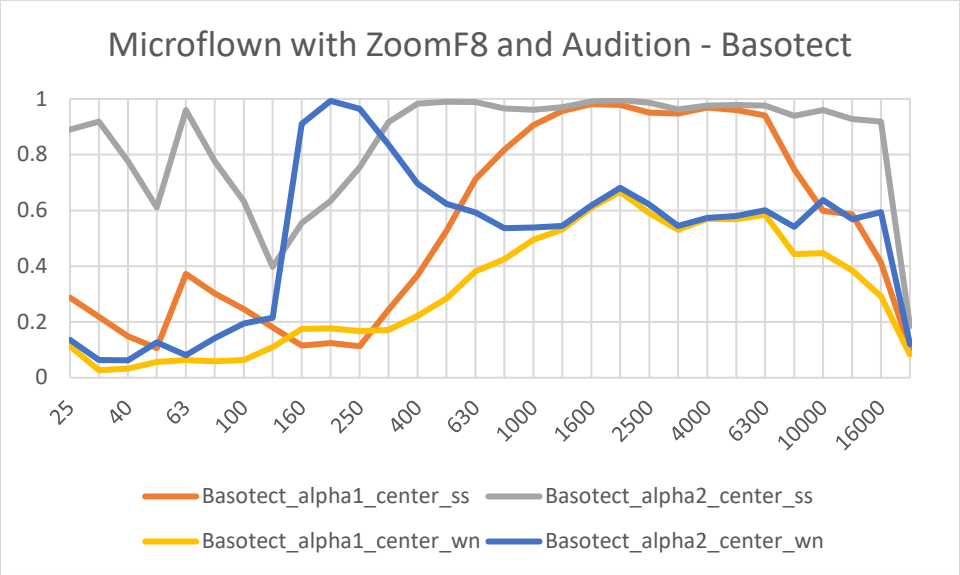

Figure 49: Comparison of measurements with Microflown system connected to ZoomF8 audio card and post-processing use of Audition on Basotect sample.

During measurements with the complete Microflown system including native Velo5 software, the recurring presence of negative absorption coefficients was encountered, particularly evident at low frequencies. Since negative absorption values are physically impossible (negative energy not being conceivable) the alternative system configuration described in section 2.2.2 was chosen. This configuration involves excluding the Velo5 software in favor of an acquisition chain based on ZoomF8 audio card and Adobe Audition for post-processing, thus allowing physically coherent results to be obtained. With Audition, two formulas were applied: Farina-Fausti for alpha 1 and Chung-Blaser for alpha2. From comparative analysis of the two formulas with the two excitation signals (sine sweep and white noise) several observations emerge:

- With sine sweep signal, the Farina-Fausti formula (alpha1) shows a more gradual and physically plausible trend, particularly effective in medium and high frequencies (500-8000 Hz).
- With sine sweep signal, the Chung-Blaser formula (alpha2) tends to overestimate absorption, especially at low frequencies, with values exceeding 0.9 below 400 Hz, but performing better at high frequencies.
- With white noise signal, both formulas show less reliable results compared to sine sweep.
- With white noise signal, absorption values are generally lower and less stable.

The comparative analysis of the two formulas has highlighted the need for a hybrid approach to obtain optimal results in acoustic characterization. The Farina-Fausti formula shows best reliability in the range 250-5000 Hz. For frequencies above, between 5000 and 10000 Hz, the Chung-Blaser formula provides more accurate results. This complementarity suggests adopting a combined method that exploits the strengths of both formulas in their respective optimal frequency bands. The sine sweep signal confirms itself again as the most appropriate choice for system excitation, ensuring greater stability and repeatability of results compared to white noise in both formulations.

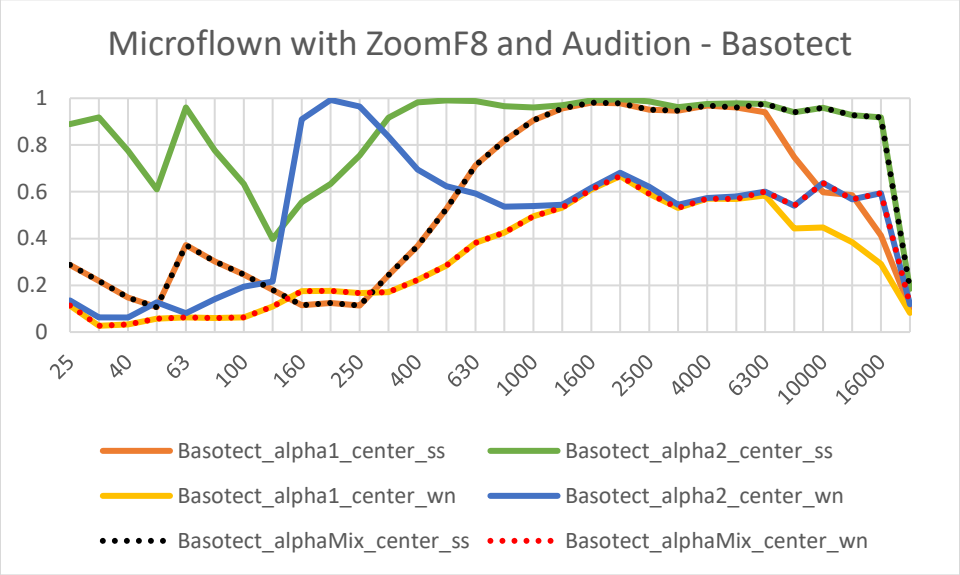

Figure 50: The combination of Farina-Fausti formula with Chung-Blaser allows obtaining an alphaMix more suitable for describing Basotect behavior.

The same study was executed on the EPS sample as counter verification.

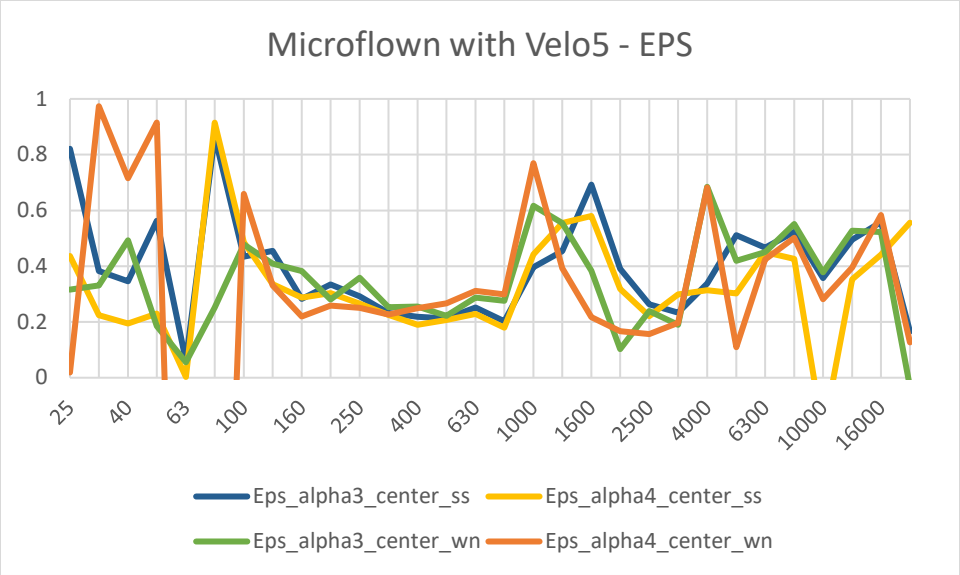

Figure 51: Comparison of measurements with complete Microflown system and its native Velo5 software on EPS sample.

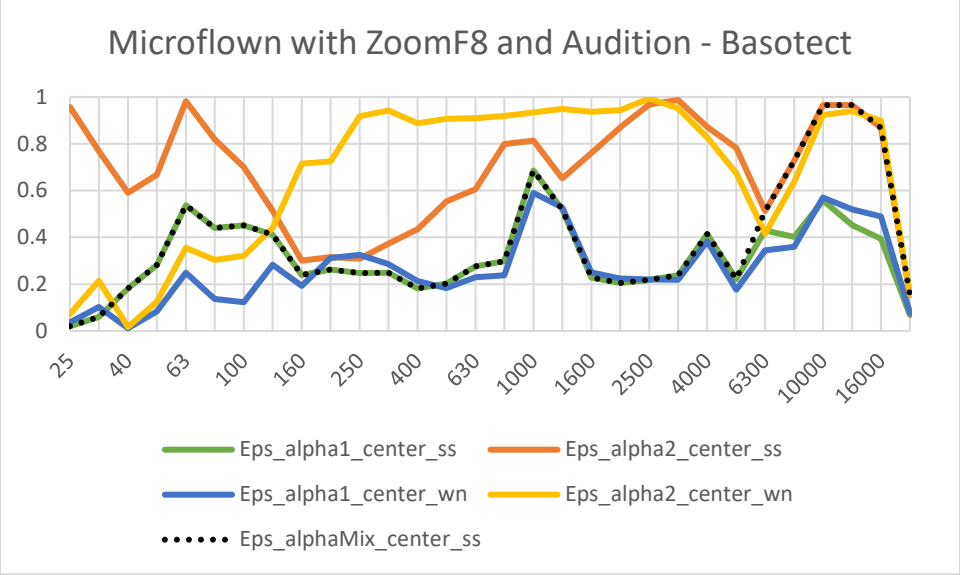

Figure 52: The combination of Farina-Fausti formula with Chung-Blaser allows obtaining an alphaMix that proves more representative also in the case of EPS.

Analyzing the acoustic behavior of EPS in the reliable frequency range (250-8000 Hz), the material shows typical behavior of a closed-cell predominantly reflective material, with generally low absorption coefficients, interrupted only by a significant peak between 1000 and 1600 Hz. Although both configurations of the complete Microflown system (alpha 3 and alpha 4) produce similar results, the configuration with Zoom F8 card and Audition provides results more consistent with expected EPS

characteristics. In particular, the hybrid alphaMix approach shows a more reliable solution, effectively combining the advantages of Farina-Fausti and Chung-Blaser formulas in their respective optimal frequency bands.

4.2.2 Car seat measurements in the laboratory

Analysis of the seat's acoustic properties required particular attention to both measurement configuration and the complex structure of the sample. Three different configurations were examined: elevated seat with air between seat and floor (and metal structure under the seat), seat placed directly on floor without metal structure, and complete seat placed on floor (with metal structure underneath).

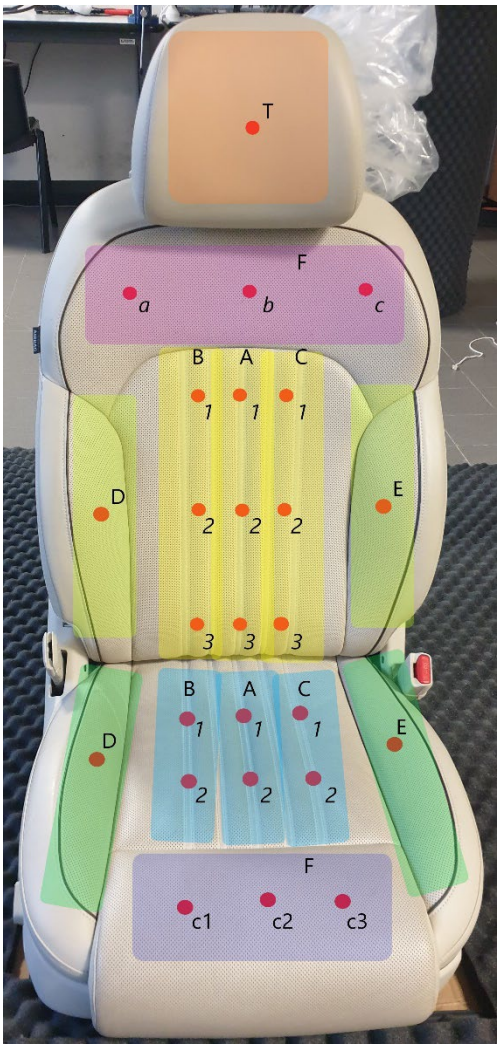

Figure 53: Mapping area of front seat.

Figure 54: Overlap of top and bottom parts of the seat to show what the sound wave encounters along its path.

The acoustic characterization of the seat was carried out through a systematic series of measurements at the points indicated in the figure above. The selection of measurement points followed two fundamental criteria: ensuring optimal coverage of previously identified zones and respecting the probe's operational constraint, which requires a measurement area of 20x20 cm fully contained within the seat. Consequently, measurement points were positioned at a maximum distance of 10 cm from the seat edge to avoid edge effects that could compromise measurement accuracy.

The robustness and reliability of the method were verified through two complementary approaches:

- Repetition of measurements at the same point, which showed excellent repeatability with very similar values between different acquisitions.
- Analysis of the surroundings of each point, performing additional measurements by moving 1 cm in the four cardinal directions, which confirmed the spatial stability of measurements as illustrated in figure below. However, it is important to note that at high frequencies some discrepancies were found, present in all three configurations, both in comparison between distant points and in analysis of adjacent points, suggesting an intrinsic limitation of the method in this region of the spectrum.

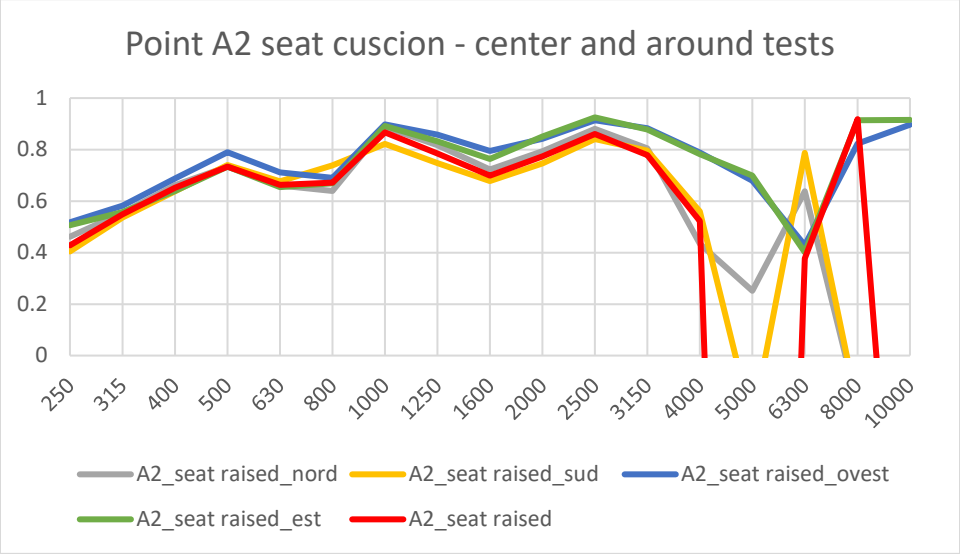

Figure 55: Point of area A compared with the 4 points measured around it moving 1 cm from it.

The choice of optimal configuration cannot disregard the complex structure of the seat, characterized by heterogeneous stratification in both materials and thicknesses. The seat presents different zones (A, B, C, D, E) that differ in both surface covering (smooth leather in zones D, E, C; perforated leather in zones A and B) and thicknesses (varying from 2 cm in the upper strip of zone A up to 11 cm in thicker parts). This structural variability has influenced some points as in the example below where two points in the same zone show some differences (in this case in the range 630 Hz-900 Hz).

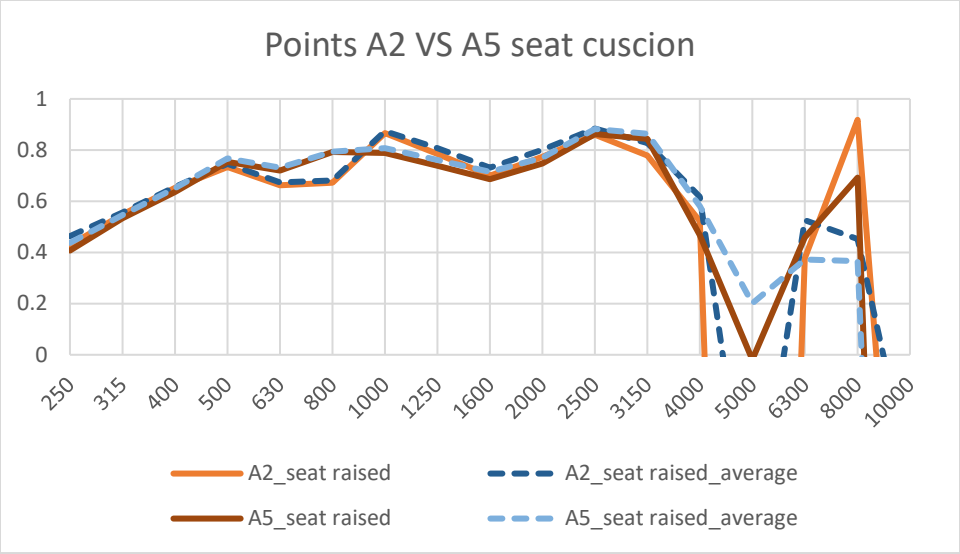

Figure 56: Comparison between two points in the same area A of the seat in the particular case of elevated seat.

However, a certain stability and repeatability remains confirmed particularly in the range between 250 and 4000 Hz, where all configurations have shown physically coherent results.

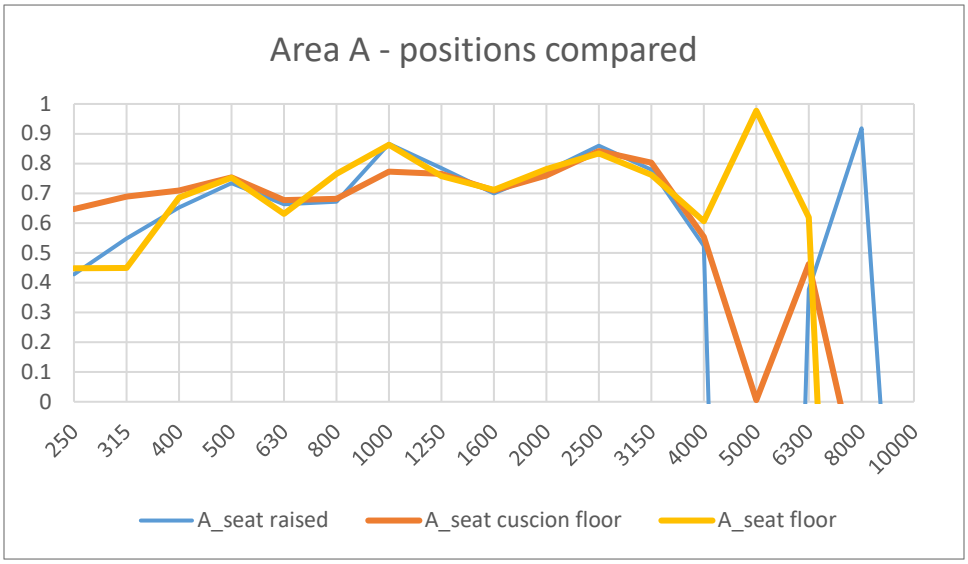

Figure 57: The three methods compared (raised seat, seat on floor, seat on floor) of area A.

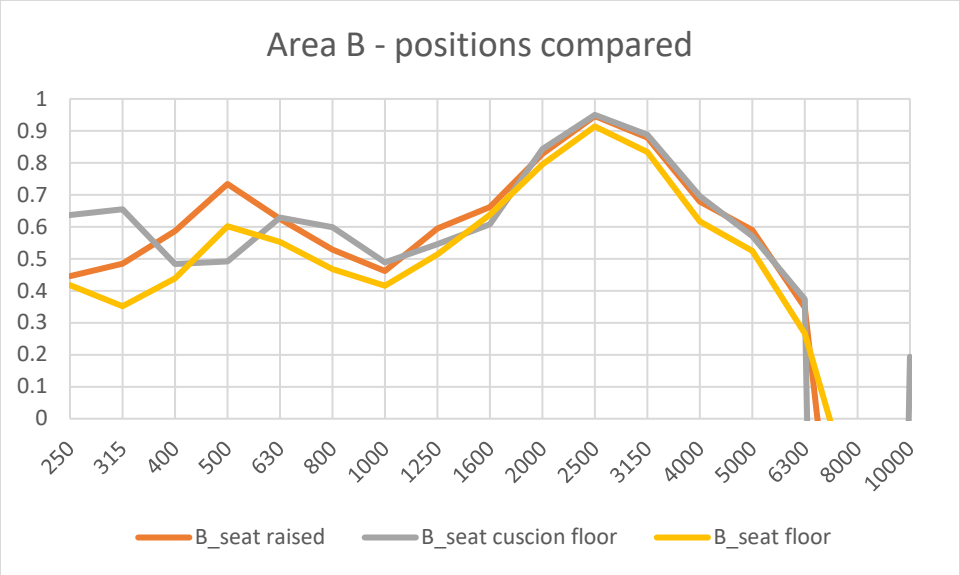

Figure 58: The three methods compared (raised seat, seat on floor, seat on floor) of area B.

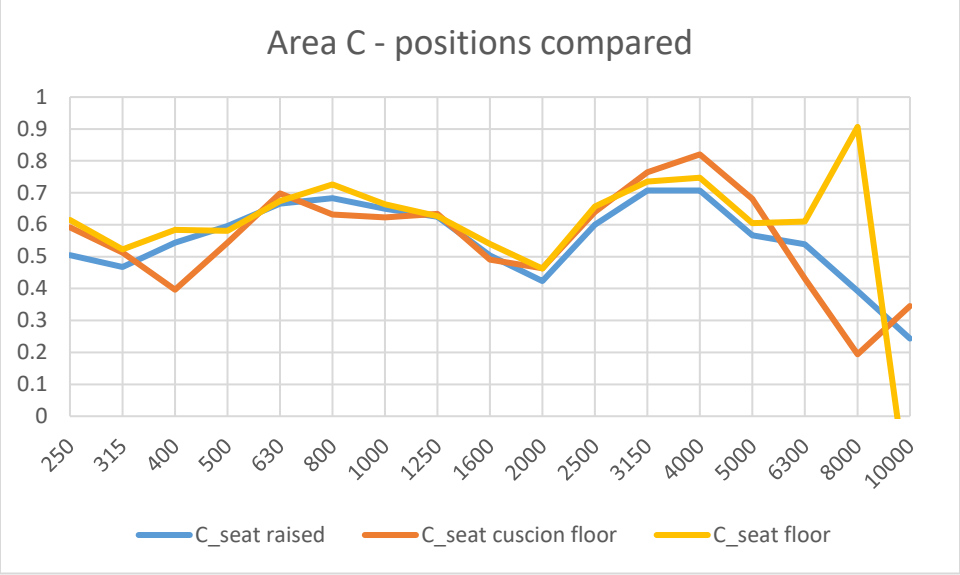

Figure 59: The three methods compared (raised seat, seat on floor, seat on floor) of area C.

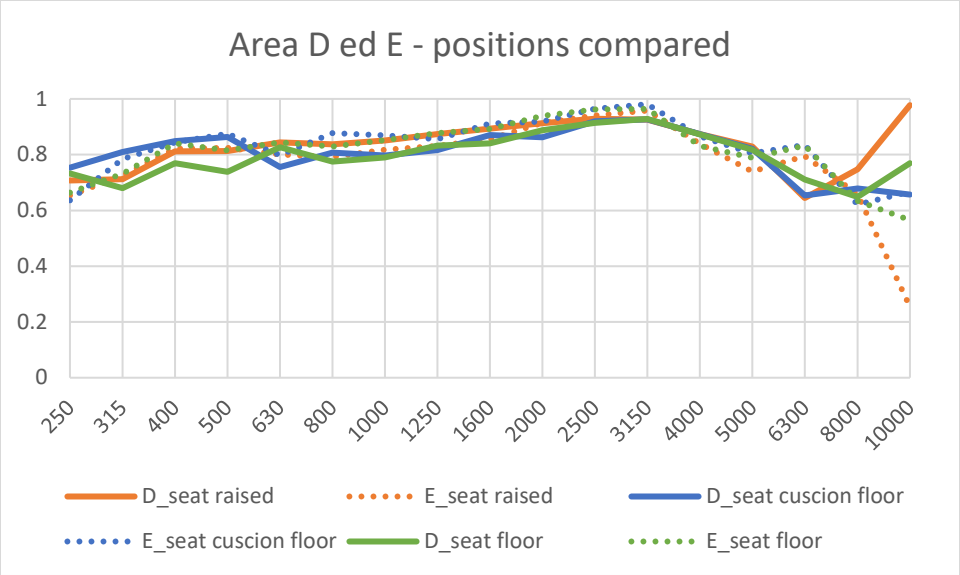

Figure 60: The three methods compared (raised seat, seat on floor, seat on floor) of areas D and E.

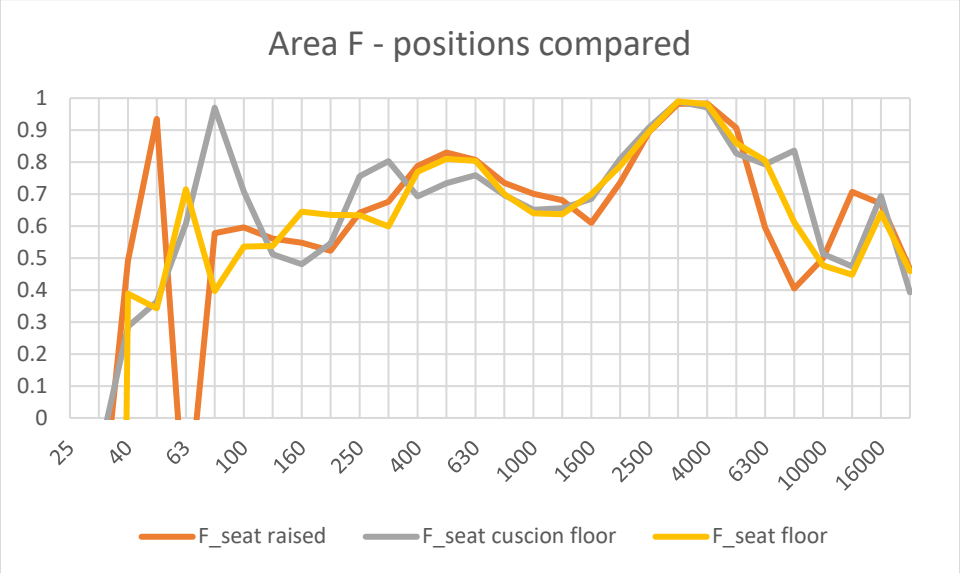

Figure 61: The three methods compared (raised seat, seat on floor, seat on floor) of area F (both F areas proved significantly similar to each other).

The raised seat configuration shows a characteristic behavior, with a gradual increase in absorption coefficient from low frequencies ($\alpha \approx 0.4$-0.5 at 250 Hz) up to reaching higher values in the medium frequency region ($\alpha \approx 0.7$-0.8 between 500-1000 Hz), then maintaining consistent absorption up to 3150 Hz. The seat positioned directly on the floor instead presents higher absorption at low frequencies ($\alpha \approx$

0.6-0.7 at 250-315 Hz) and more uniform behavior in medium frequencies, with values remaining stable between 0.7 and 0.8. The complete seat resting on the floor shows behavior similar to the raised configuration at low frequencies, but with greater stability in medium frequencies.

The raised seat configuration emerges as the most reliable for several reasons:

- It presents a more regular and physically plausible trend (especially at high frequencies where more problems occur).
- Shows less variability between different measurements within the same zone.
- When the seat is in contact with the reflective plane, the underlying metal structure introduces an additional contribution to reflections, complicating interpretation of results.
- More faithfully represents real conditions of seat use in the passenger compartment.

The metal structure can therefore generate:

- Multiple reflections between floor and metal parts.
- Possible resonances of the structure itself.
- Vibro-acoustic couplings between structure and sound-absorbing material.
- Resonant cavities between various metal parts.

Conversely, the presence of air under the seat in the raised configuration eliminates these additional reflections and resonances, allowing obtaining a measurement that more faithfully reflects the intrinsic acoustic properties of the seat itself, without interference from secondary phenomena due to interaction with the support structure. Although study of simple materials and panels has shown how the optimal configuration involves direct positioning of the sample on the floor, exploiting its reflective properties, in the specific case of the automotive seat it is necessary to adopt a different approach. The presence of the metal structure underneath the seat, which is itself a reflective element, requires modifying the measurement methodology. In this case, it is indeed preferable to raise the seat, interposing an air layer between it and the floor. This configuration allows eliminating interference due to double reflection (metal structure and floor), enabling a more accurate and representative acoustic characterization of the seat.

A critical issue that emerged during measurements even in the raised seat configuration concerns the presence of negative absorption coefficients at high frequencies, a physically impossible result when dealing with energy quantities. Comparison between the native Microflown system using only proprietary

software and the alternative configuration with Zoom F8 audio card has highlighted the superiority of the latter solution. This superiority is clearly demonstrated by analysis of a specific point in zone F of the seat, where the configuration with Zoom F8 manages to eliminate negative peaks that instead persist in the native system.

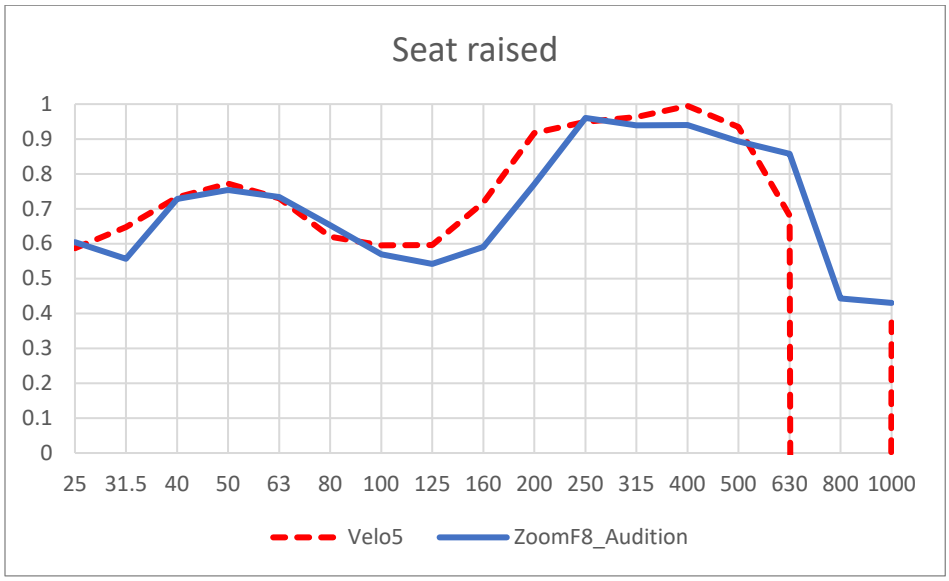

Figure 62: Example of a point where the negative peak at high frequencies is eliminated thanks to replacing native Velo5 software with ZoomF8 acquisition system and Audition.

This result not only confirms greater reliability of the Zoom F8 configuration but also emphasizes the importance of correct data acquisition and post-processing to obtain physically coherent results across the entire analyzed frequency spectrum.

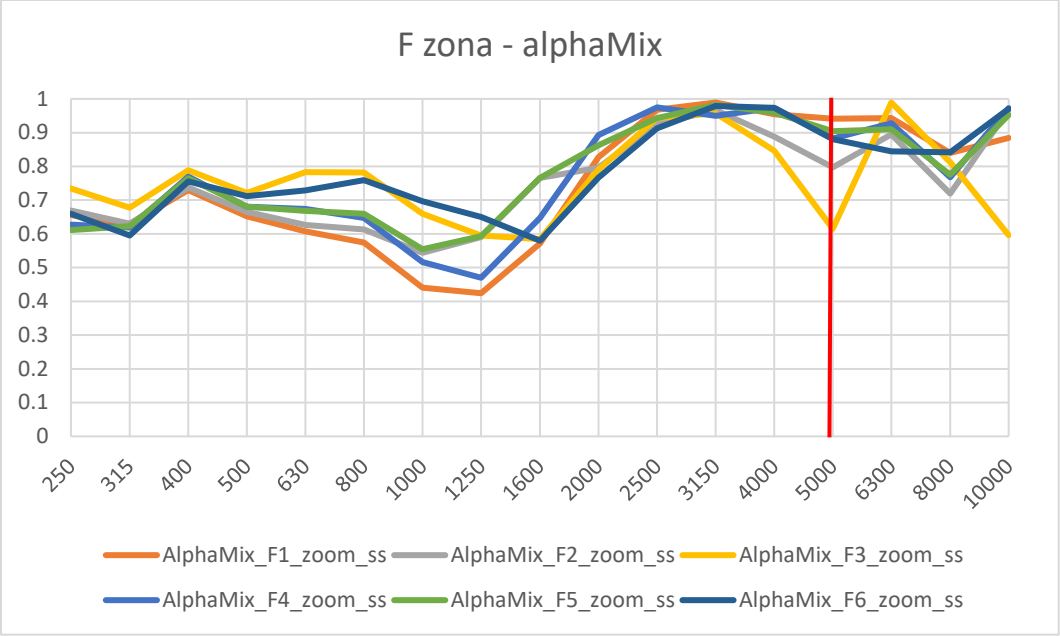

Figure 63: Behavior of six points measured in zone F (perforated leather without stitching) of alphaMix values (Farina-Fausti formula up to 5000 Hz, Chung-Blaser formula above 5 kHz).

In-depth analysis of the six measurement points in the perforated leather zone of the seat has revealed significant aspects regarding homogeneity of acoustic properties and influence of underlying structure. This zone, characterized by absence of stitching and presence of a metal structure below the polyurethane layer, represents a particularly interesting case study for evaluating uniformity of acoustic properties in presence of structural elements. The spatial distribution of absorption coefficients, measured at the six points, shows remarkable homogeneity in the frequency range between 250 - 4000 Hz. In particular, points on the same row (F1-F4, F2-F5, F3-F6) show very similar values, with differences typically less than 10%. This pattern maintains consistent using both the Farina-Fausti formula (alpha1) and Chung-Blaser formula (alpha2), with the latter tending to produce slightly higher values while maintaining the same spatial distribution. Precisely this consistency in spatial distribution, combined with complementary characteristics of the two formulas in different frequency bands, suggested the possibility of developing a hybrid approach (alphaMix) that exploits the strengths of both calculation methods.

Analysis in frequency bands reveals specific characteristics. At low frequencies (250-500 Hz), coefficients remain between 0.6 and 0.8, showing remarkable uniformity among different measurement points. In the medium frequency region (1000-2000 Hz), an absorption peak is observed with values between 0.8 and

0.9, accompanied by greater spatial variability. At high frequencies (2500-8000 Hz), a plateau is reached with very high values (0.9-1.0) and excellent spatial uniformity.

The significant variation observed in column F1-F2-F3, and particularly at point F3, provides an interesting correlation with the seat's underlying structure. Data analysis, when compared with physical arrangement of the "serpentine" mechanical structure, suggests a direct influence of relative position between measurement points and underlying structural elements. Points F1, F2 and F3, which show this distinctive behavior, are located in direct correspondence with the metal structure, while points F4, F5 and F6 are positioned in areas where they are more centered on the polyurethane alone and close to the structure (but not directly above it).

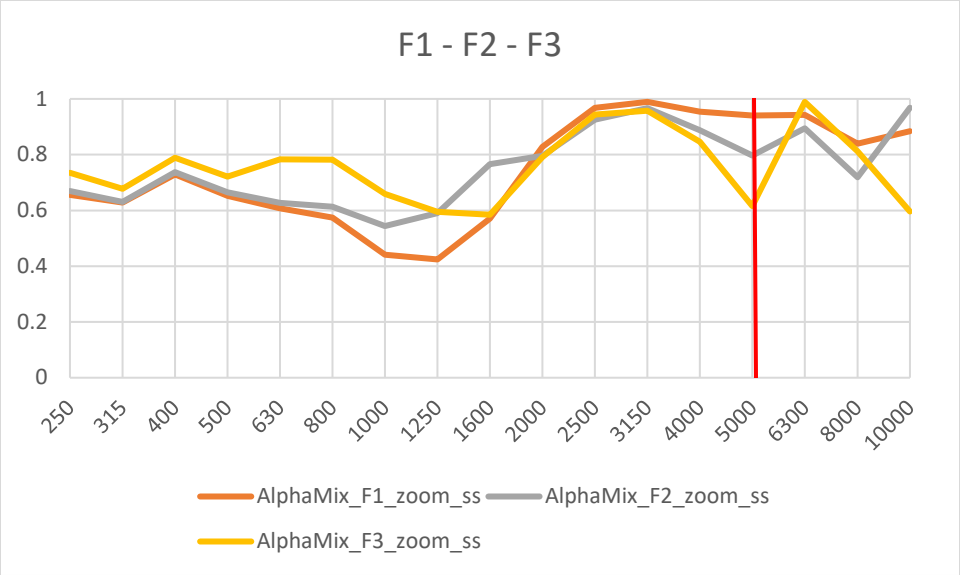

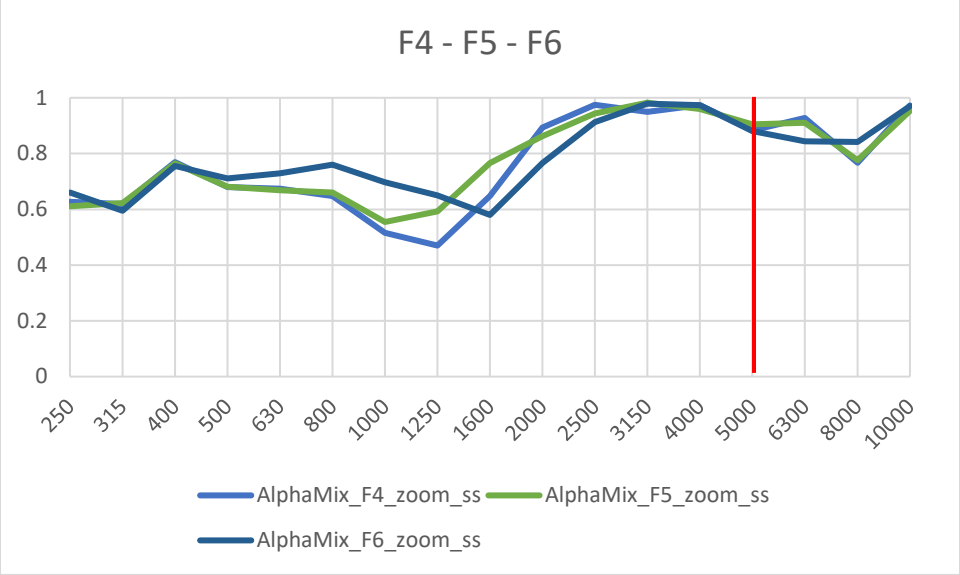

Figure 64: Zone F appears quite homogeneous, but still shows a slight difference since points in the column (F1,F2,F3) are more centered over the underlying mechanical structure compared to other points (F4, F5, F6).

This geometric difference seems to significantly influence absorption properties:

- Points above the structure (F1-F2-F3) show a downward absorption peak.
- Points near but not directly above the structure (F4-F5-F6) present more uniform values.

This observation confirms how, despite the apparent homogeneity of the perforated leather surface, local acoustic properties are influenced by the complex geometry of the underlying structure, highlighting the importance of considering the entire system (perforated leather-polyurethane-metal structure) in

acoustic characterization of the seat. This suggests that the raised seat configuration allows effectively characterizing acoustic properties of the composite perforated leather-polyurethane-metal structure system, maintaining good spatial coherence despite structural complexity. However, this variability at high frequencies does not compromise overall validity of measurements, which demonstrate how the perforated leather zone, despite presence of underlying metal structure, presents remarkably homogeneous acoustic characteristics in the frequency band of greatest interest. These results confirm not only effectiveness of the measurement method with raised seat, but also the technique's ability to reliably characterize acoustic properties of complex composite structures, providing coherent and physically significant results with a mix of the two absorption formulas. The choice to use the Farina-Fausti formula up to 5000 Hz and the Chung-Blaser formula beyond this frequency is not random, but derives from observation of specific behavior of the two formulas in different frequency bands. The Farina-Fausti formula shows particular reliability in the 250-5000 Hz band, where it provides stable and physically coherent results, with good ability to characterize both absorption properties at low and medium frequencies and absorption peaks typical of porous materials. Beyond 5000 Hz, however, this formula tends to produce more unstable and sometimes physically impossible results. The Chung-Blaser formula, on the other hand, shows complementary behavior: while at low and medium frequencies it may overestimate absorption, it becomes particularly accurate beyond 5000 Hz, where it maintains better stability and produces always physically plausible results.

The frequency of 5000 Hz emerges as optimal transition point between the two formulas, as it represents the limit beyond which the Farina-Fausti formula begins to show instability, while the Chung-Blaser formula reaches its reliability. This combination allows exploiting strengths of both formulas, obtaining more accurate characterization across the entire frequency spectrum. The validity of this choice is confirmed by analysis of data from all studied zones, where the hybrid approach reveals a homogeneity in acoustic properties that would be difficult to appreciate using a single formula.

Analysis of zone F, characterized by smooth leather, has shown how the underlying metal structure only partially influences acoustic properties, allowing this zone to be considered acoustically homogeneous and thus characterizable through an arithmetic mean of measured values. Attention then shifted to the central part of the seat, where presence of a more complex surface texture, characterized by alternation of smooth and perforated leather with stitching, requires in-depth analysis to evaluate its potential influence on absorption properties. In particular, this zone is characterized by alternation of smooth leather strips (1 cm wide) and perforated leather (3 cm wide), separated by stitching. This particular

configuration offers the opportunity to analyze how different surface finishes influence acoustic absorption properties of the composite system. At low frequencies (250-800 Hz), acoustic behavior appears substantially independent of surface finish. Absorption coefficients remain between 0.4 and 0.7, with minimal differences (on the order of 0.05-0.1) between smooth and perforated leather. This suggests that in this frequency band, absorption is mainly determined by deeper layers (expanded polyurethane) rather than surface finish.

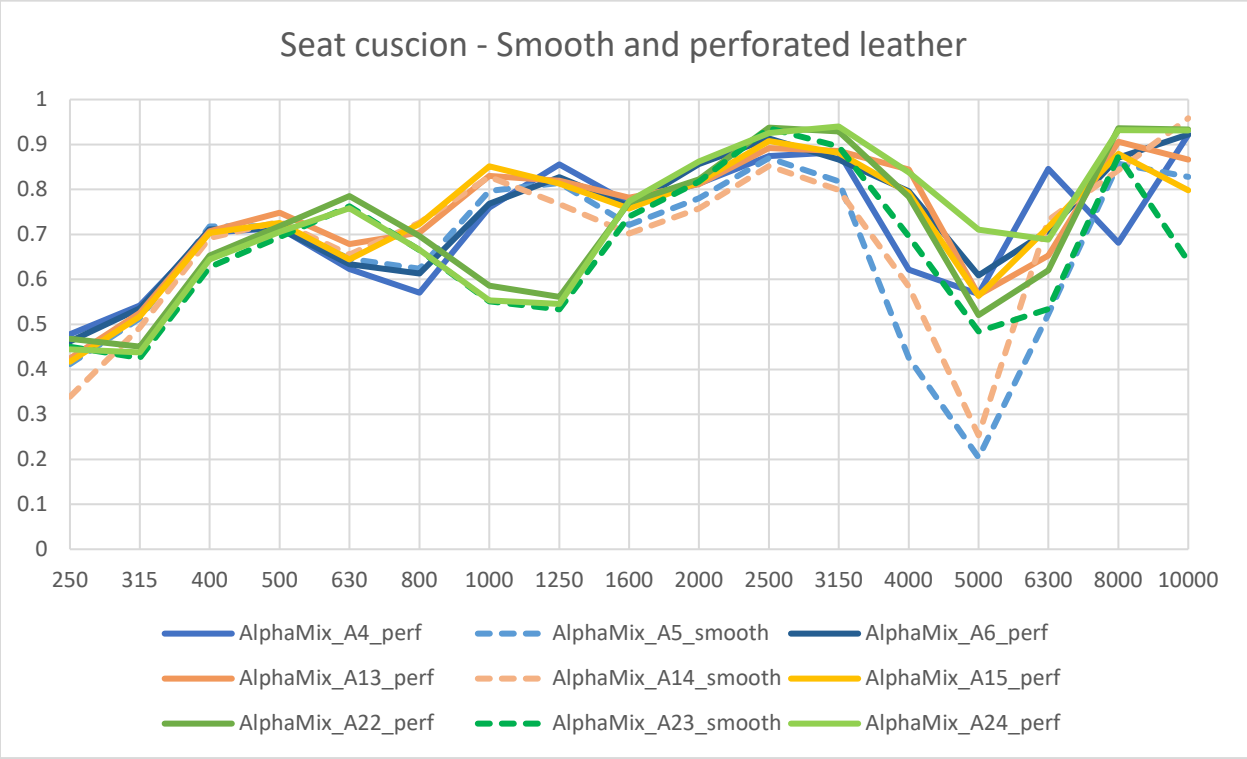

Figure 65: Comparison between smooth leather parts (solid line) and perforated parts (dashed line) on the three rows of points measured in the most favorable area of area A.

In the medium frequency region (800-2000 Hz), more marked differences emerge. Perforated leather shows slightly higher absorption coefficients (with differences on the order of 0.1-0.15) compared to smooth leather, and more pronounced absorption peaks are observed. This difference is probably due to greater acoustic permeability of perforated leather, which allows better interaction of sound wave with underlying absorbing layers. At high frequencies (2500-4000 Hz), convergence in behavior of the two materials is observed, with high absorption coefficients (0.8-0.95) for both finishes. In this region,

influence of surface texture becomes less relevant, suggesting that absorption mechanisms are dominated by overall properties of the multilayer system.

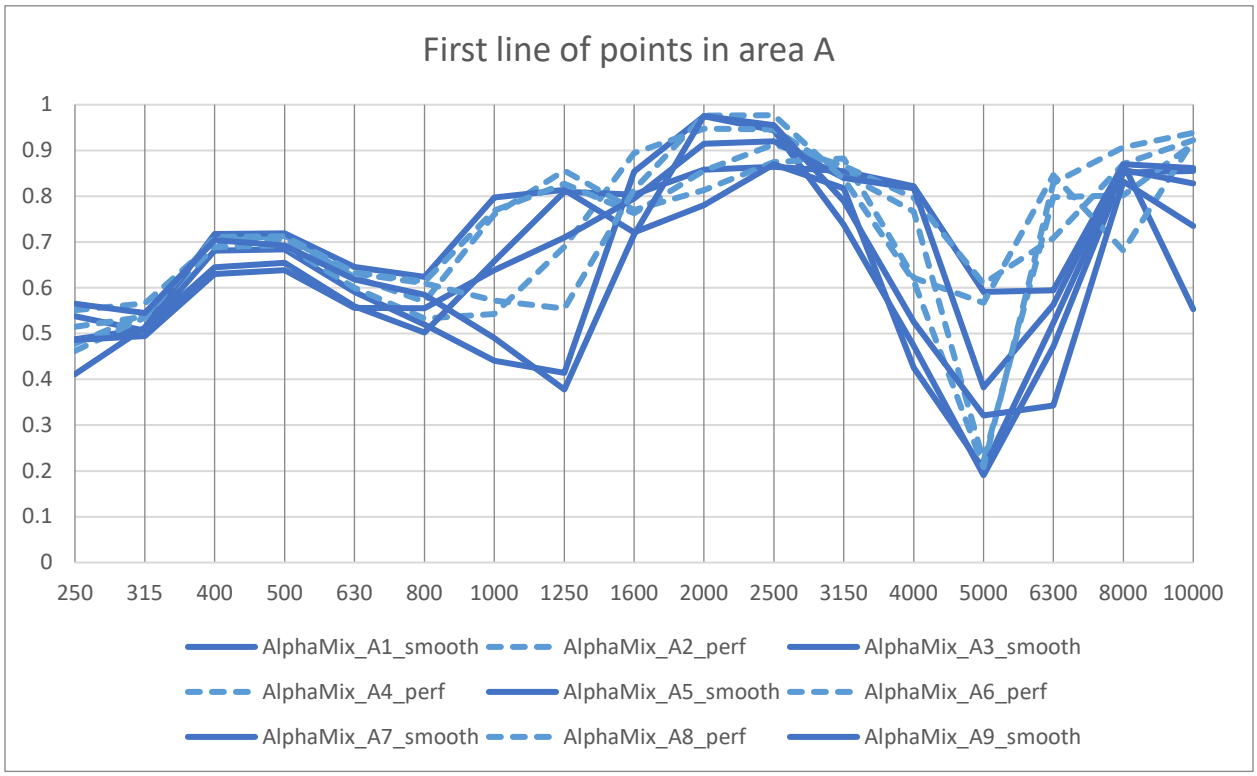

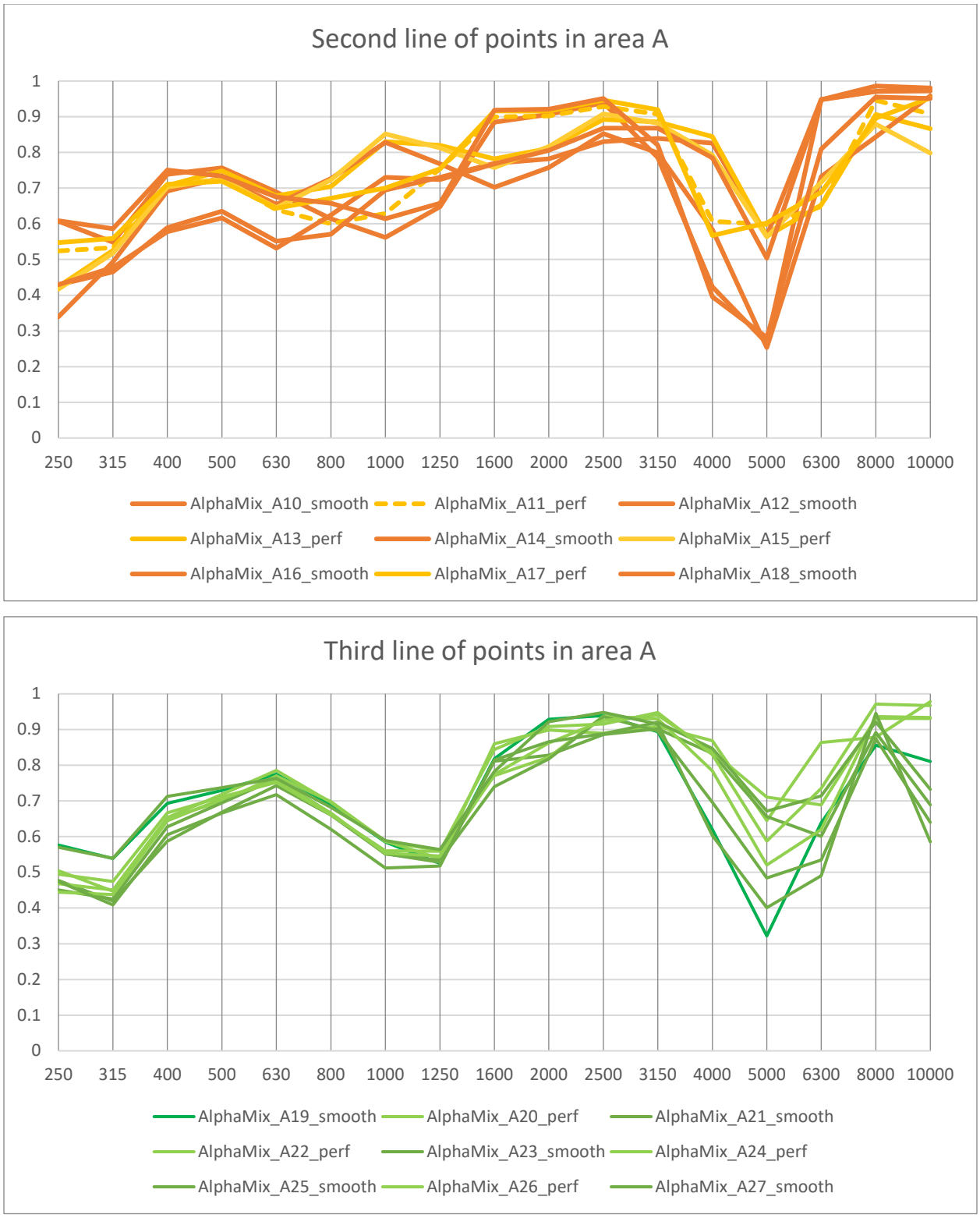

Figure 66: Measurements obtained in first, second and third rows (respectively) of area A (where smooth indicates that the point is on the smooth strip and perf indicates it is on the perforated strip).

In-depth analysis of seat's central zone, characterized by a regular pattern of alternation between smooth and perforated leather separated by stitching, has revealed complex interactions between different factors that influence acoustic behavior of the system.

Polyurethane thickness difference emerges as one of the most significant factors:

- 9 cm in first two rows.
- 7 cm in third row.

This difference is particularly evident in the 800-1600 Hz band, where:

- First two rows show a characteristic absorption peak
- Third row presents opposite behavior with a "valley".

However, this difference becomes less relevant at high frequencies (>2000 Hz), where all rows show high and similar absorption values. Comparison between zones with smooth and perforated leather reveals moderate but systematic differences. The influence of perforation becomes particularly evident at high frequencies (3150-8000 Hz), where points on perforated leather generally maintain higher absorption values compared to those on smooth leather. This suggests that perforation becomes a dominant factor when sound wavelength becomes comparable with hole dimensions. Stitching, despite its visible presence, shows marginal influence on acoustic properties. This can be attributed to their reduced dimensions compared to probe's measurement area (20x20 cm), which leads to an "averaging" of their effect with surrounding areas. Relative position with respect to other seat structures emerges as a significant factor:

- First two rows, closer to backrest (which presents the same alternation pattern), show greater variability in values, probably due to multiple reflections and interaction with backrest's acoustic pattern.
- Third row, more distant from backrest and closer to an area of unstitched perforated leather, shows more stable and coherent values, suggesting that a more "open" acoustic environment allows cleaner measurements.

At 5000 Hz, transition point between Farina-Fausti and Chung-Blaser formulas, a downward peak is systematically observed, suggesting that at this frequency leather effect becomes dominant compared to underlying polyurethane.

Despite observed variations, several factors support the possibility of considering the entire area as a single acoustic zone:

- Differences, although present, remain contained and follow predictable patterns.
- High-frequency behavior shows remarkable coherence across all zones.
- Observed variations are mainly due to structural factors (polyurethane thickness, relative position) rather than fundamental differences in acoustic properties.
- From a practical viewpoint, an average value can adequately represent acoustic behavior of entire area.

This unification is justified not only by relative homogeneity of results, but also by practicality in seat's acoustic modeling, where too detailed characterization could introduce unnecessary complexity without significant gain in accuracy. Detailed understanding of various factors influencing acoustic behavior supports this simplification, allowing maintaining optimal balance between characterization accuracy and model practicality.

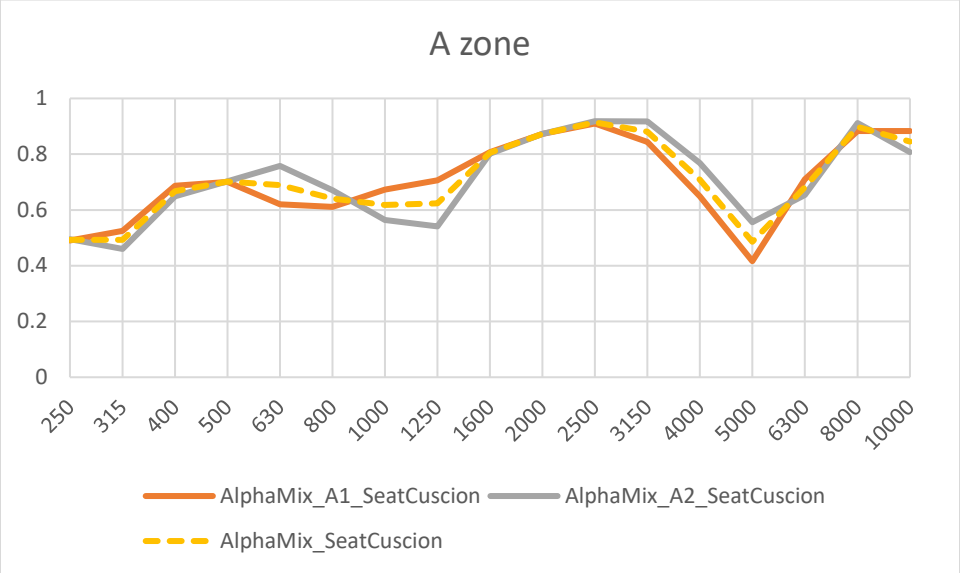

Figure 67: Comparison between averages of first two rows (A1) with average of third row (A2), and finally representative average of area A obtained by arithmetically averaging A1 with A2.

Analysis was extended to all seat measurement points, allowing identification and characterization of several acoustically homogeneous zones. For each identified zone, values of individual measurement

points were statistically processed through arithmetic mean, thus obtaining a representative value of acoustic properties for entire area. This zoning and averaging approach created a simplified but accurate acoustic mapping of entire seat, maintaining distinctive characteristics of each zone while reducing complexity of overall characterization. Furthermore, analysis of both seat and seating has revealed similar acoustic patterns that allow reasoned simplification of characterization. Measurements conducted on the seat and backrest, despite difference in total thickness (27 cm for seat and 21 cm for backrest), show surprisingly coherent behaviors when comparing zones with analogous surface characteristics.

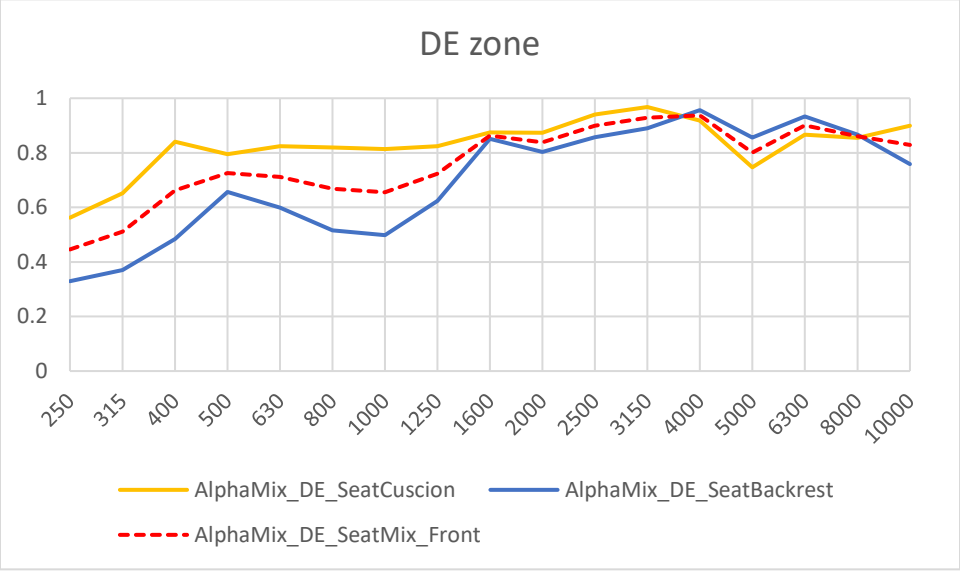

Figure 68: Comparison between seat and backrest in zone DE of front seat.

DE zones, characterized by smooth leather with stitching, show very similar acoustic behavior between seat and backrest. This coherence was particularly evident in 400-3150 Hz frequency band, where absorption coefficients follow parallel trends despite difference in overall thickness. This suggests that acoustic properties in these zones are primarily determined by surface characteristics rather than total thickness.

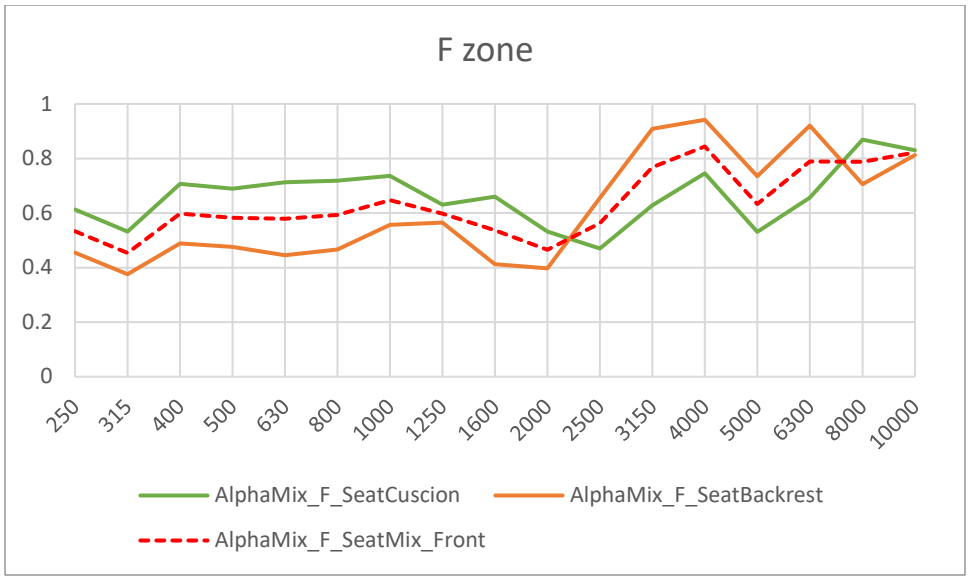

Figure 69: Comparison between seat and backrest in zone F of front seat.

F zones, distinguished by smooth leather without stitching, confirm this trend. Although slight differences are observed in medium frequencies, general absorption pattern remains coherent between seat and backrest, with particular uniformity at high frequencies. This coherence reinforces hypothesis that surface finish plays a dominant role in determining acoustic properties.

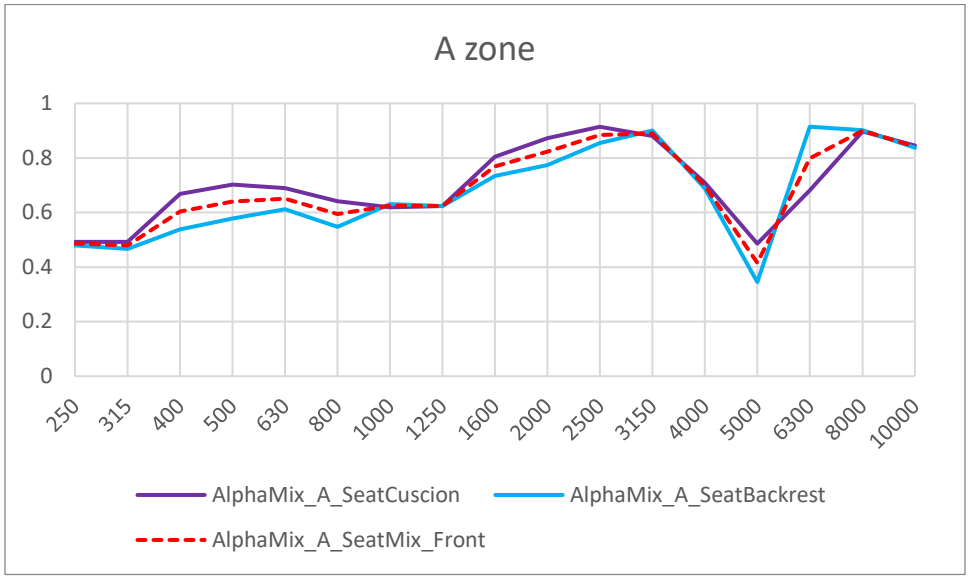

Figure 70: Comparison between seat and backrest in zone A of front seat.

Particularly interesting is behavior of A zones, which present alternation of smooth and perforated leather. Despite complexity of surface structure and difference in total thickness, these zones show very similar behavior between seat and backrest, with aligned absorption peaks and notable stability across most of spectrum.

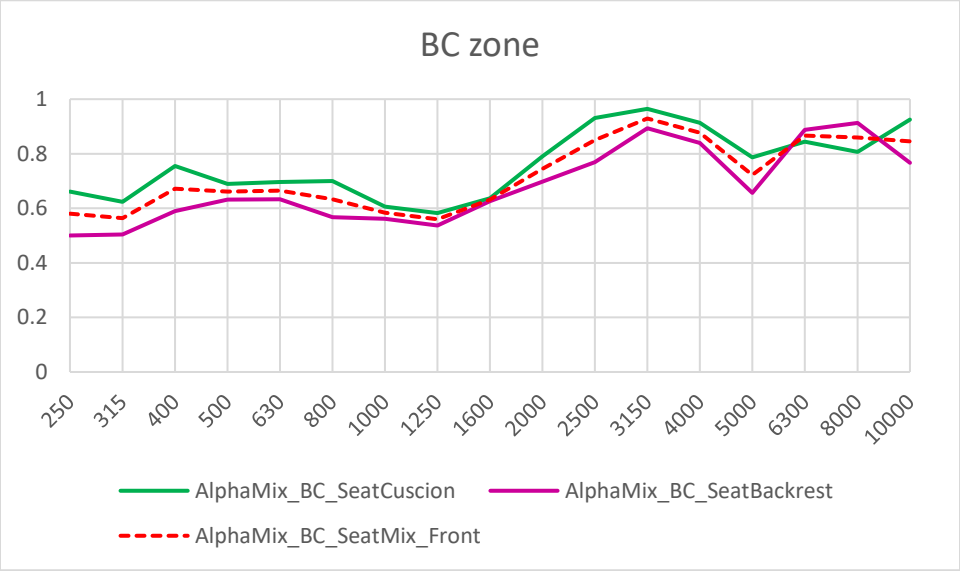

Figure 71: Comparison between seat and backrest in zone BC of front seat.

BC zones, which represent transition areas, also exhibit remarkable coherence between seat and backrest, with minimal differences despite different positions and structural contexts.

This homogeneity of behavior between analogous zones, regardless of their location on seat or backrest, seems to lead toward a significant hypothesis: type of surface finish (type of leather, presence of perforations, stitching) emerges as dominant factor compared to position or total structure thickness. The 6 cm difference in total thickness between seat and backrest (seat measures 27 cm, backrest 21 cm) has surprisingly limited impact on acoustic properties, suggesting that acoustic behavior is mainly determined by more superficial layers and that thickness, beyond a certain threshold, does not substantially modify absorption properties.

This evidence strongly supports possibility of unifying data from zones with similar surface characteristics, regardless of their position on seat or backrest. Such simplification not only maintains accuracy of acoustic characterization but also offers significant practical advantages in modeling overall acoustic behavior of seat. The possibility of basing characterization on type of surface material rather than position allows creating a more practical and manageable model, while maintaining accurate representation of system's acoustic properties.

This unification represents an important step forward in acoustic characterization of automotive seats, offering a more efficient approach that combines scientific accuracy and practical applicability.

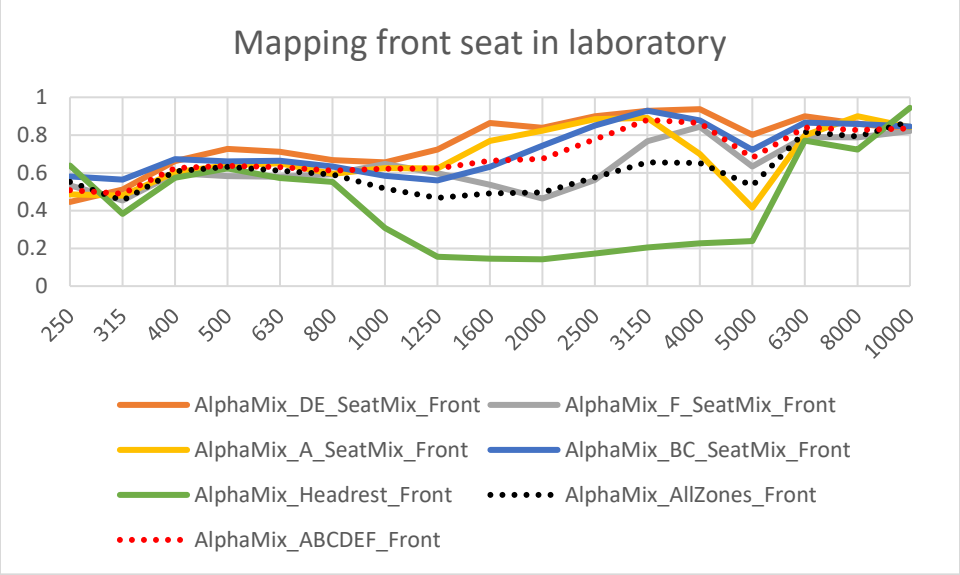

Figure 72: Comparison between various zones identified based on surface material and value of headrest zone of seat front, showing possible data averaged over entire compressive or non-compressive surface area including headrest.

There are still two fundamental questions regarding acoustic characterization: how to treat headrest and whether to maintain seat's division into zones or unify them.

Regarding headrest, its dimensions (26x18x18 cm) and peculiar acoustic behavior strongly suggest maintaining it as an independent zone. Although measurement area is at limit of minimum dimensions required by Microflown probe (20x20 cm), it still falls within range of measurement validity. Fewer measurements were made in this zone but still averaged together to have total trend of this zone. Acoustic behavior of this element differs significantly from other zones, particularly evident in medium-high

frequencies (1000-5000 Hz) where it presents notably lower absorption coefficients. This uniqueness can be attributed to several concurrent factors: surface uniformly covered in smooth leather without material variations or stitching, compact dimensions, likely different internal structure, and absence of alternation between different materials that instead characterizes other seat zones. Its isolated position and different exposure to sound field in passenger compartment further contribute to justifying separate characterization.

Regarding zonization of rest of seat, data analysis strongly supports maintaining division into distinct zones (DE, F, A and BC) rather than their unification. Each zone indeed presents characteristic and well-defined acoustic behavior. DE zone, characterized by smooth leather with stitching, shows distinctive absorption peaks between 1600 and 3150 Hz, with values reaching 0.86-0.93. F zone, with smooth leather without stitching, presents more uniform behavior with generally lower values in medium frequencies. A zone, with its alternation of smooth and perforated leather, shows intermediate behavior with characteristic peaks, while BC zones show a distinctive growing absorption pattern. These differences are not random but reflect different surface structures and underlying: presence or absence of stitching, alternation of smooth and perforated leather, variations in polyurethane thickness all contribute to creating specific acoustic behaviors for each zone. However, average excluding headrest presents rather coherent and gradual trend, maintaining characteristic patterns of seat's main zones. This average shows more natural progression of absorption coefficients across frequency spectrum and results more representative of seat's general acoustic behavior. Meanwhile, average including headrest shows significant distortions compared to seat's characteristic behavior. This is particularly evident in medium frequencies, where sharp decrease in absorption coefficients is observed. In critical range between 1600 and 4000 Hz, inclusion of headrest leads to significantly lower values compared to average of seat zones alone. For example, at 1600 Hz coefficient changes from 0.66 (average without headrest) to 0.49 (average with headrest), at 2000 Hz from 0.67 to 0.50, and at 3150 Hz difference becomes even more marked, with values of 0.88 and 0.66 respectively.

These substantial differences strongly support need to maintain headrest as independent acoustic zone. Its inclusion in general average (denominated AlphaMix_AllZones_Front in previous graph) not only significantly distorts values, but creates behavior that is not representative of any of seat's real zones.

Regarding unification of other seat zones into a single average, question is more nuanced. Although this operation inevitably involves some simplification of specific acoustic characteristics of each zone, results suggest it could be acceptable for some practical applications. Average of main zones (denominated

AlphaMix_ABCDEF_Front in previous graph) indeed maintains general representative trend and preserves main absorption characteristics of seat, providing more manageable characterization.

Choice between maintaining separate zones or using average will necessarily depend on specific application. For detailed acoustic modeling, where it is necessary to consider local variations of acoustic properties, it will be preferable to maintain separate characterization of different zones. For applications requiring more general characterization of seat's acoustic behavior, average of main zones might prove sufficient.

In conclusion, quantitative analysis supports two main recommendations: headrest must necessarily be maintained as independent zone to not compromise accuracy of overall acoustic characterization, while for other seat zones, choice between unified or separate characterization can be guided by specific application requirements, keeping in mind that average, while simplifying some aspects, maintains reasonably accurate representation of seat's general acoustic behavior.

The definitive validity of these two possible characterization strategies - use of separate zones with their respective averaged absorption coefficients or use of a single average for entire seat front - will be evaluated through numerical simulations in COMSOL. By implementing both solutions in simulated seat model, it will be possible to determine which approach provides most accurate representation of real acoustic behavior, balancing characterization precision and computational complexity.

Particular analysis was dedicated to seat back, a predominantly reflective surface previously characterized through Laser Doppler Vibrometer LDV method [9]. This part of seat represents an interesting case study for comparison between measurement methodologies, given its primarily reflective nature. LDV, being specifically designed for rigid and reflective surfaces, theoretically represents most suitable instrument for this characterization. On other hand, Microflown probe, while optimized for measuring absorbing materials, was nevertheless employed on seat back. This choice, apparently counter-intuitive, was motivated by need to validate robustness and versatility of developed measurement method. Application of Microflown probe to this surface, where theoretically it might show accuracy limitations, indeed allows:

- Verifying method limits under non-optimal conditions.
- Establishing direct comparison between two characterization techniques.
- Evaluating possibility of using a single instrument for entire seat.
- Validating overall reliability of developed methodology.

This comparative approach provides valuable information not only on acoustic characterization of seat back, but also on validity and limits of measurement method as a whole.

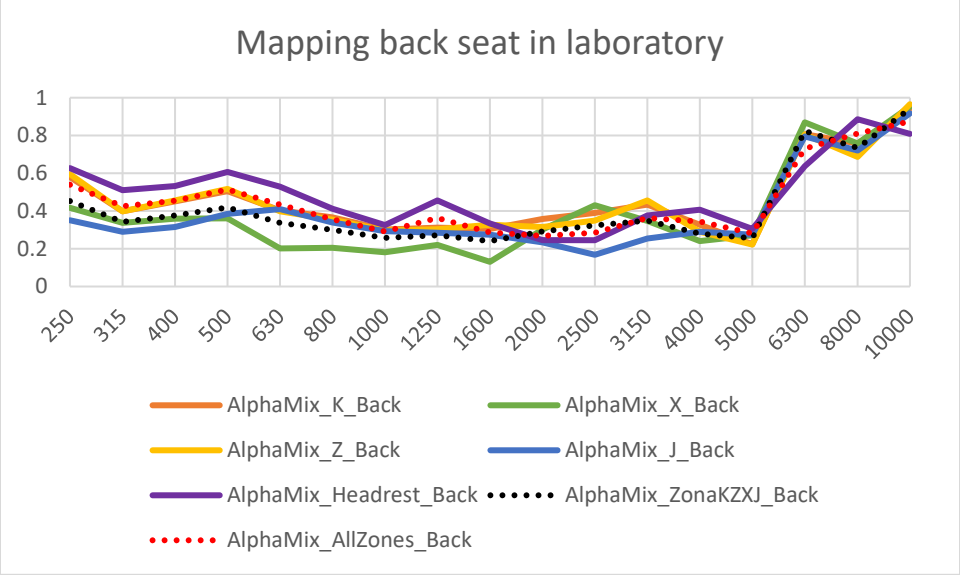

Figure 73: Comparison between various zones identified based on surface material and value of headrest zone of seat back, showing possible data averaged over entire surface area with or without headrest.

Detailed analysis of absorption coefficients of different seat back zones reveals significant patterns that guide characterization choices. Seat back structure can be divided into distinct zones: three central areas of backrest (K, X, Z), a lower zone characterized by presence of a door (J), and headrest back. Central backrest zones show very coherent acoustic behavior among themselves, characterized by moderate absorption at low frequencies (values between 0.4 and 0.6 in 250-500 Hz band), followed by significant decrease in medium frequencies (values between 0.2 and 0.3 from 800 to 2000 Hz), then rising significantly at high frequencies (0.7-0.9 above 6300 Hz). Zone X distinguishes itself slightly with lower values in medium frequencies, but maintains general pattern. Door zone (J), while following similar trend to central zones, presents some peculiarities: lower values in 200-500 Hz band, more uniform trend in medium frequencies, then converging with other zones at high frequencies. Headrest back instead shows rather distinctive behavior, characterized by generally higher values at low and medium frequencies, less variability in overall trend, and significant divergence from other zones beyond 10000 Hz. This difference is attributable to different surface nature: smooth leather for headrest versus rigid plastic for rest of back.

All zones show some common characteristics: absorption peaks at very low frequencies (40-63 Hz), very high values beyond 6300 Hz, and typical behavior of reflective surfaces in medium frequencies. Analysis of averages confirms opportunity to maintain separate characterization between headrest back and rest of structure. Average of rigid plastic zones (K, Z, X, J) shows coherent and representative behavior of surface, with values varying from 0.45 at 250 Hz, 0.27 at 1250 Hz, 0.28 at 4000 Hz, up to 0.73 at 8000 Hz. Including headrest in this average would introduce significant distortions, as evidenced by overall average values: 0.54 at 250 Hz, 0.36 at 1250 Hz, 0.34 at 4000 Hz and 0.81 at 8000 Hz. This analysis supports a characterization strategy that provides:

- Unification of central zones and door in a single characterization, given their common nature (rigid plastic) and similar acoustic behavior.
- Maintaining headrest as separate zone, justified by different surface nature (smooth leather) and distinctive acoustic behavior.

This approach allows effectively balancing need for accurate characterization with opportunity for model simplification, respecting physical and structural differences of materials. Choice is supported not only by numerical data but also by practical considerations about nature of materials and their structural function in seat. This optimized characterization provides solid basis for subsequent analyses and modeling, maintaining accuracy necessary to represent acoustic behavior of seat back in its complexity.

4.2.3 Automotive Seat Measurements in Car

The definitive validation of the Microflown probe measurement method was conducted through a series of measurements directly in the final destination environment: the car passenger compartment.

Figure 74: Setup of measruments inside the car.

This phase of research allows verifying effectiveness and robustness of method in real conditions, significantly different from those controlled in laboratory.

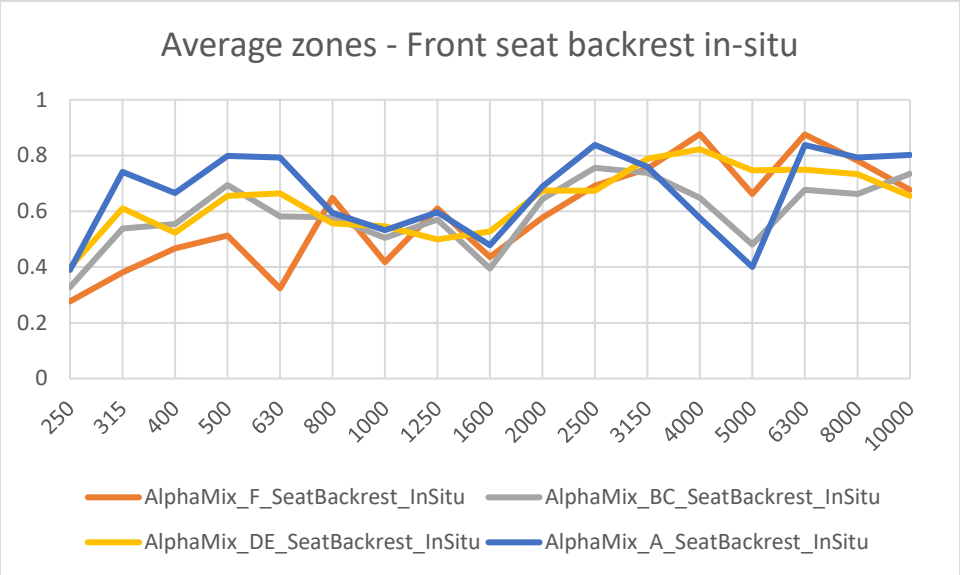

Figure 75: Representative averages of zones into which backrest was mapped with measurements directly inside passenger compartment (in situ) which prove to be the same delineated in laboratory measurements.

The methodological approach required some adaptations to operating conditions:

- Use of probe in manual mode with appropriate grip, instead of tripod mounting.
- Implementation of more frequent calibration protocol.
- Consideration of passenger compartment-specific environmental variables.

Particular attention was dedicated to system calibration. Given confined nature of passenger compartment, characterized by rapid variations in environmental parameters (temperature, humidity), a more frequent calibration protocol was adopted: every 10-15 measurements a new calibration was performed, emitting sine sweep signal in passenger compartment, taking care to orient probe away from seat to obtain reliable reference measurement. This allowed generating updated matching filters representative of real measurement conditions. Repeatability validation was maintained through usual

four repeated measurements at same point and four measurements in surrounding cardinal points, at all points previously studied during laboratory measurements. Although these measures showed slightly higher variability compared to laboratory measurements (predictable given manual measurement mode), they maintained coherence in general trend, confirming method robustness.

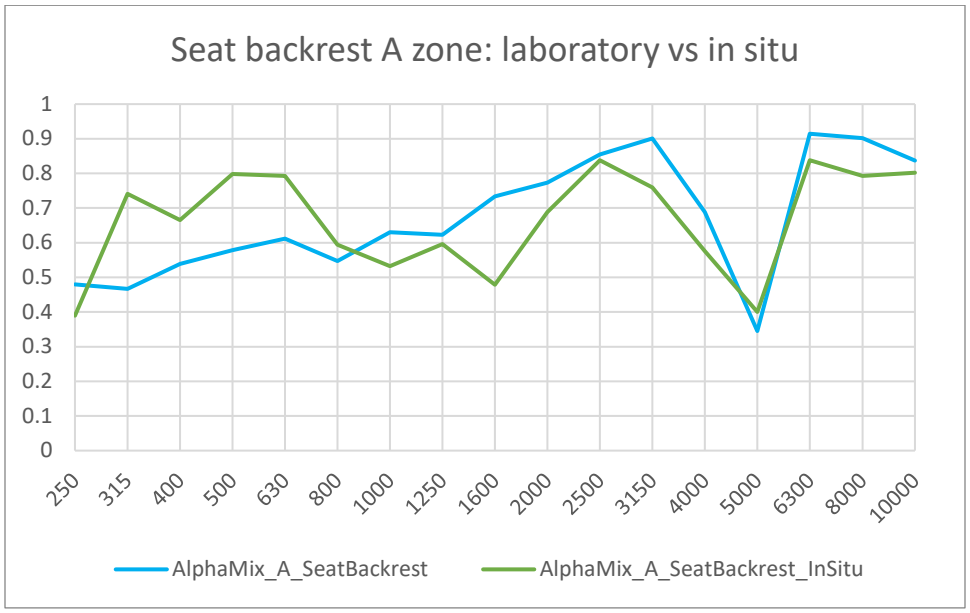

Figure 76: Comparison between results obtained in laboratory and in situ in zone A of backrest.

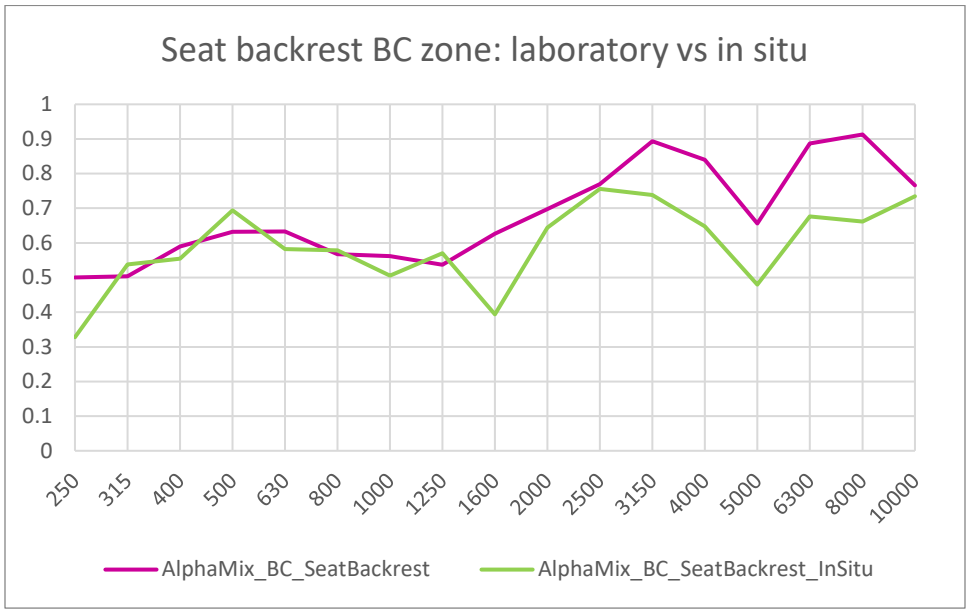

Figure 77: Comparison between results obtained in laboratory and in situ in zone BC of backrest.

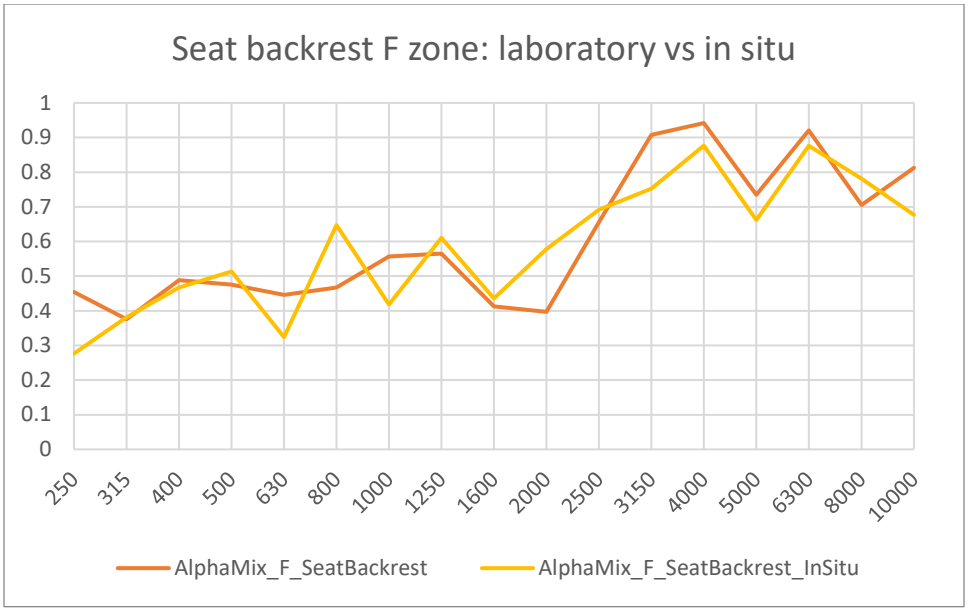

Figure 78: Comparison between results obtained in laboratory and in situ in zone F of backrest.

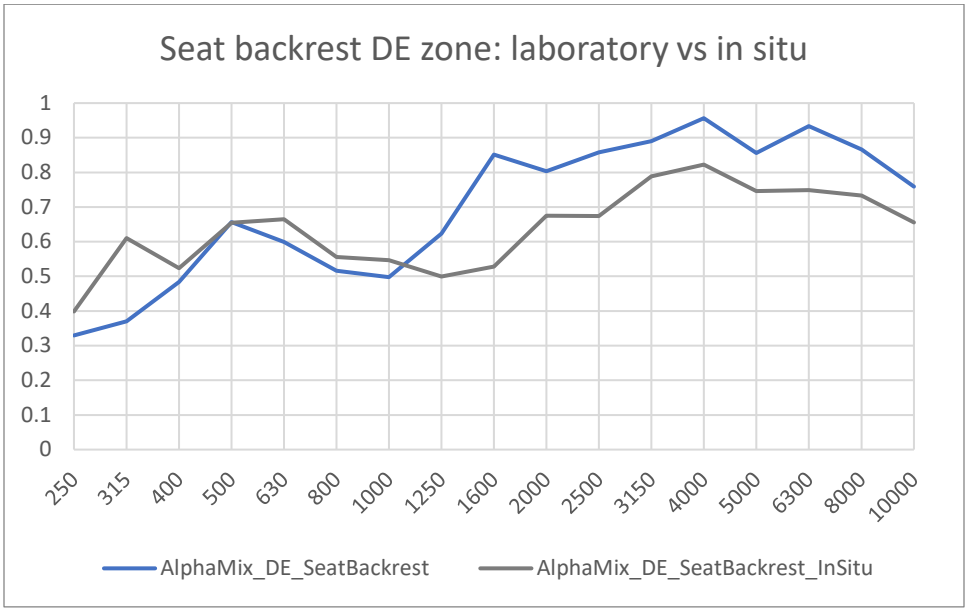

Figure 79: Comparison between results obtained in laboratory and in situ in zone DE of backrest.

The most significant result of this phase was correspondence between acoustic mapping obtained in situ and that previously developed in laboratory. Zones with different or similar acoustic characteristics recreated a similar pattern of spatial distribution, confirming that method is reliable even in real conditions and that measured acoustic characteristics are intrinsic properties of seat.

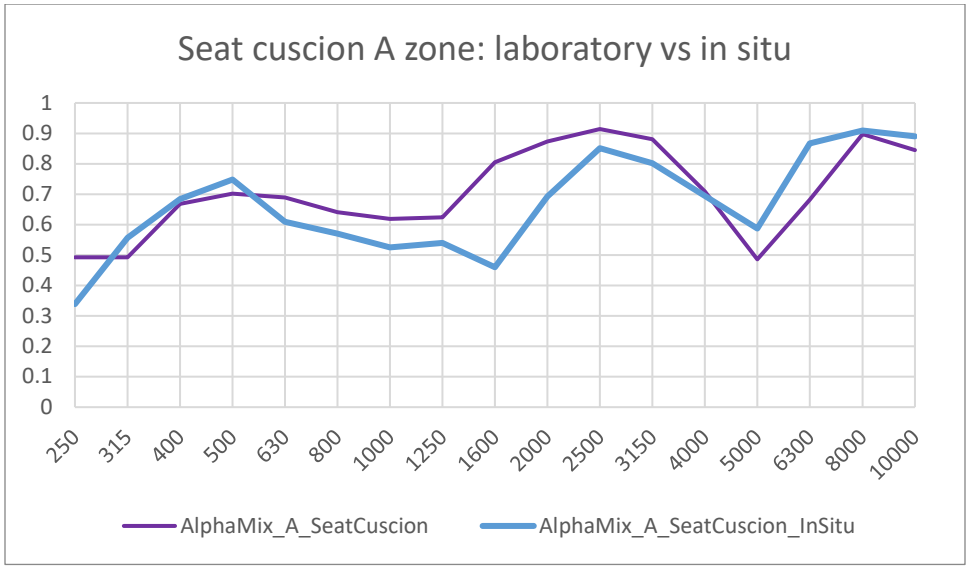

Figure 80: Comparison between results obtained in laboratory and in situ in zone A of seat.

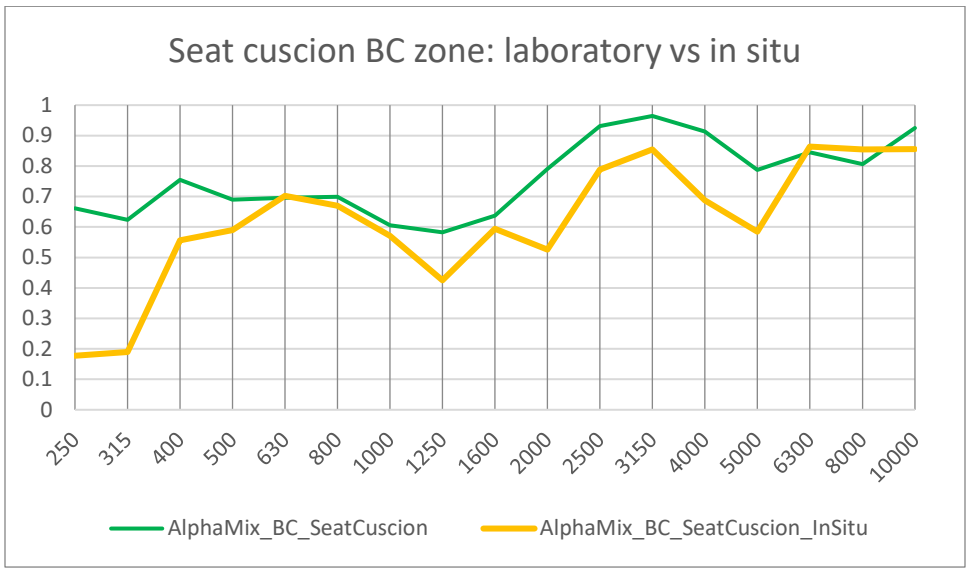

Figure 81: Comparison between results obtained in laboratory and in situ in zone BC of seat.

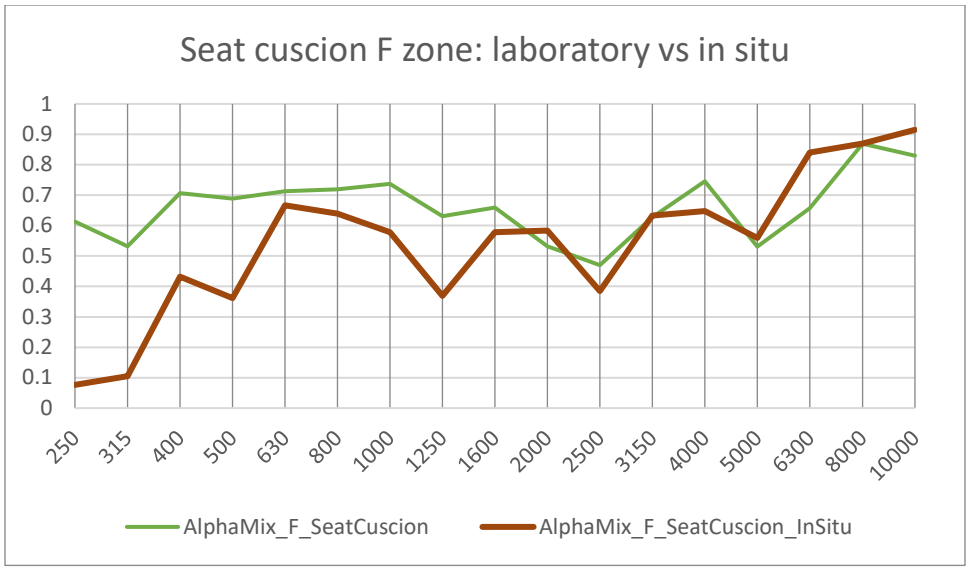

Figure 82: Comparison between results obtained in laboratory and in situ in zone F of seat.

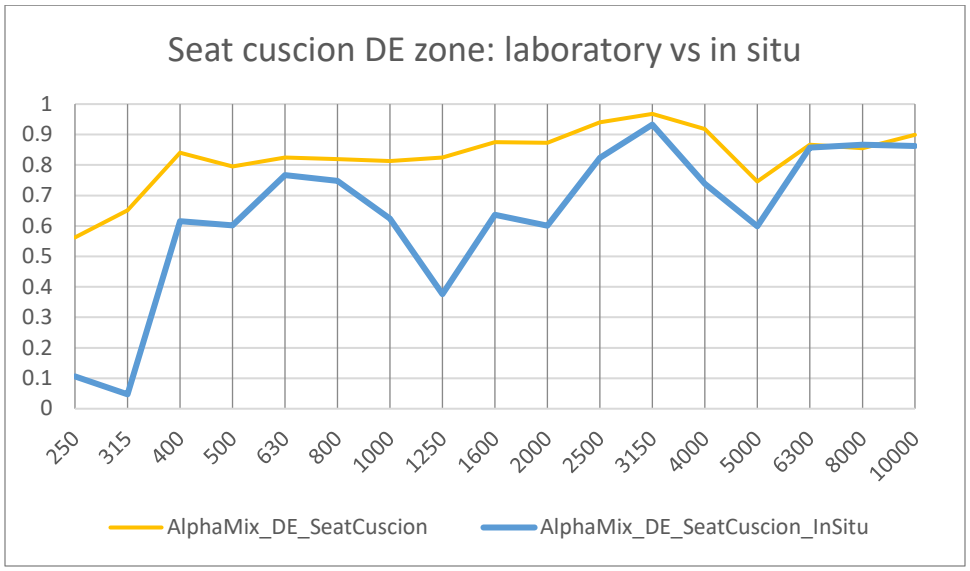

Figure 83: Comparison between results obtained in laboratory and in situ in zone DE of seat.

This in situ validation has particular relevance because:

- Confirms practical applicability of method.
- Demonstrates repeatability of measurements in real conditions.
- Validates acoustic characterization developed in laboratory.
- Supports overall reliability of methodology.

Correspondence between mappings obtained in two environments (laboratory and car) not only validates measurement method but also suggests that developed acoustic characterization is representative of real seat behavior in its context of use.

A similar correspondence between laboratory and in situ measurements was found in analysis of seat cushion. Acoustic characterization allowed identifying same distinctive zones in both measurement conditions: analysis of measurement points, while showing some variations in values between adjacent points or belonging to same zone, shows an overall coherent pattern that allows replicating same zonization identified in laboratory. Observed discrepancies can be mainly attributed to two factors: use of probe in manual mode, rather than mounted on tripod, necessary for practical reasons of accessibility in passenger compartment; and in situ measurement conditions, where car's confined environment introduces variables not present in controlled laboratory conditions. This coherence in acoustic mapping between two measurement conditions provides further validation of method's robustness and reliability, demonstrating how characterization developed in laboratory maintains its validity even in real conditions of seat use inside cabin.

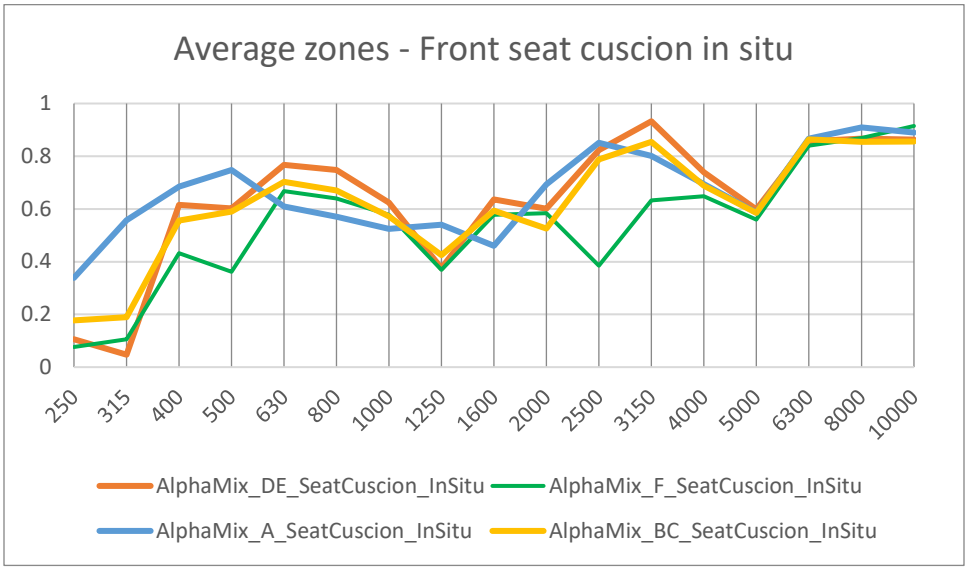

Figure 84: Representative averages of zones into which seat was mapped with measurements directly inside passenger compartment (in situ) which prove to be same delineated in laboratory measurements.

Zone A, characterized by alternation of smooth and perforated leather in central part of seat, was clearly identified. Average of these points excellently corresponds to values measured in laboratory, confirming robustness of characterization method even in real conditions. Zone BC where acoustic behavior shows same characteristic pattern identified in laboratory, with high values at low frequencies and significant

peaks at high frequencies. Zone DE shows characteristic pattern measured in laboratory: significant growth at low frequencies (250-630 Hz), stable and high values in medium frequencies (800-2000 Hz), and pronounced peaks beyond 2500 Hz. Zone F is characterized by more contained values and a distinctive pattern in medium frequencies, coherent with laboratory measurements.

Comparison between two measurement methods in this part of seat has revealed significant aspects:

- Laboratory measurements offer:
    - Greater control of environmental conditions.
    - Possibility of more precise probe positioning.
    - More stable measurements thanks to tripod use.
    - Less influence from unwanted reflections.
- In situ measurements present:
    - Real conditions of seat use.
    - Need for more frequent calibrations.
    - Greater variability in results.
    - Influence of confined passenger compartment environment.

Despite these differences, correspondence between zones identified in two measurement environments confirms validity of method.

This complete validation supports reliability of Microflown probe measurement method, confirming its ability to provide accurate and repeatable acoustic characterizations, regardless of measurement environment.

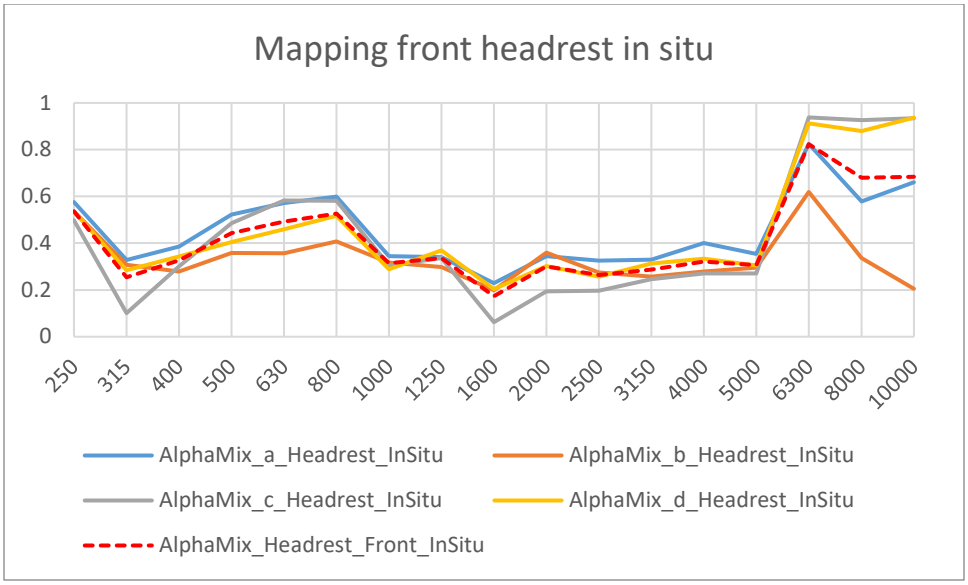

Figure 85: In situ measurement of headrest, measured 4 times at same point manually (a,b,c,d) and then averaged (front).

Analysis of four repeated measurements (a,b,c,d) of headrest central point in situ offers interesting insights on method repeatability in real conditions. At low frequencies (250-630 Hz), measurements show contained variability, with values oscillating around mean in reasonable way. For example, at 250 Hz values vary from 0.49 to 0.57, converging toward mean of 0.53, demonstrating good stability despite manual measurement. In medium frequencies (800-2000 Hz), greater variability is observed, probably due to method's higher sensitivity in this band and difficulty in maintaining exact probe position when held manually. However, values maintain a recognizable and coherent pattern. High frequencies (2500-10000 Hz) show greatest variability, particularly evident beyond 6300 Hz. For example, at 8000 Hz values vary from 0.33 to 0.92, a significant dispersion that reflects higher sensitivity of high frequencies to small variations in probe positioning. Despite these variations, calculated mean value provides a reasonable and physically plausible characterization of measured point's acoustic behavior. This suggests that, even in non-ideal measurement conditions like those in situ and with hand-held probe, method maintains sufficient reliability, especially when considering average of repeated measurements.

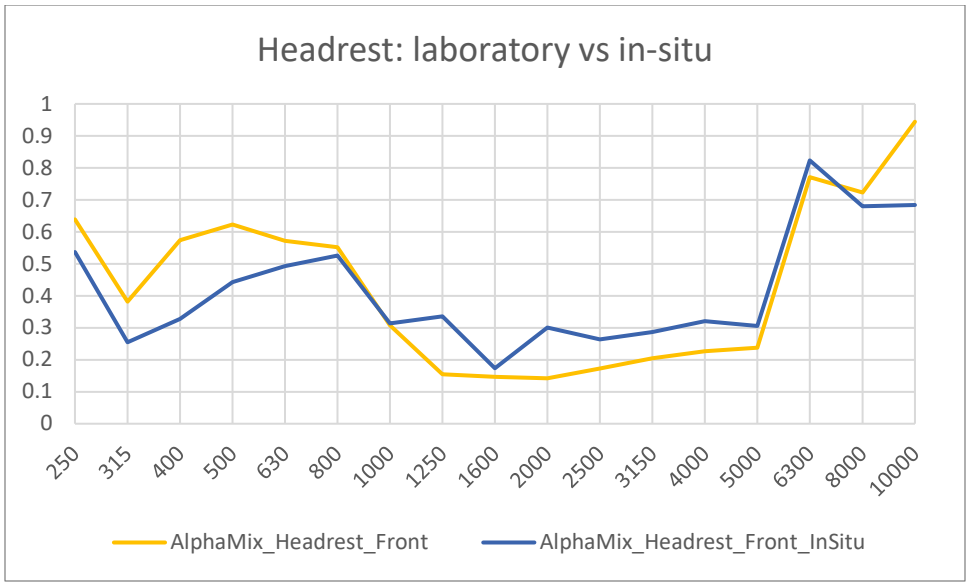

Figure 86: Comparison between trend obtained by averaging data recorded in headrest between those detected in laboratory and those in situ inside passenger compartment.

Comparative analysis between measurements made in laboratory and in situ reveals interesting patterns in different frequency bands. At low frequencies (250-630 Hz), laboratory measurements show generally higher values (0.38-0.64) compared to those in situ (0.25-0.54), with particularly marked difference at 400 Hz (0.57 vs 0.33), suggesting possible influence of car's confined environment. In medium frequencies (800-2000 Hz), convergence of values is observed around 800 Hz (0.55 vs 0.53), followed by interesting trend reversal after 1000 Hz, where in situ measurements show higher values, with significant difference at 2000 Hz (0.14 vs 0.30). At high frequencies (2500-10000 Hz), patterns remain similar up to 5000 Hz, with slightly higher values in situ, then diverge significantly beyond 6300 Hz, where laboratory measurements show higher peaks at very high frequencies (0.94 vs 0.68 at 10000 Hz). Both methods present specific advantages and limitations. Laboratory offers controlled environment, greater stability of environmental conditions and possibility to use precise supports, ensuring more repeatable measurements with less influence from unwanted reflections. However, these idealized conditions might not fully reflect real material behavior. In situ measurements, instead, provide more realistic representation of acoustic behavior in context of use, considering interactions with passenger compartment environment and effects of surrounding surfaces. Main challenges of this approach include greater operational complexity, influence of environmental variables and difficulty in maintaining precise positions.

Similarly to previous analyses, it was possible to unify data through an average between corresponding zones of seat and backrest, given coherence of values found between same areas in two components. This choice of unified characterization is supported by similarity in acoustic behavior of same types of materials and surface finishes, regardless of their location on seat or backrest. Validity of this zonal characterization is thus further confirmed.

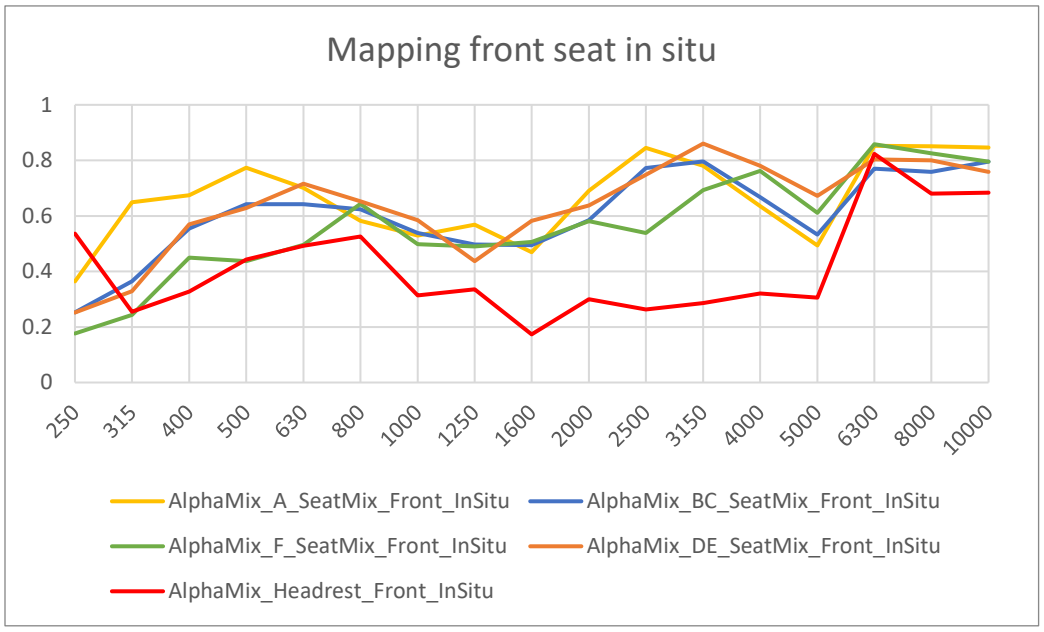

Figure 87: Comparison between various zones identified based on surface material and value of headrest zone of seat front in situ.

Comparative analysis of unified data between seat and backrest, obtained both in laboratory and directly in car passenger compartment, reveals interesting aspects about acoustic characterization of seat in different measurement conditions.

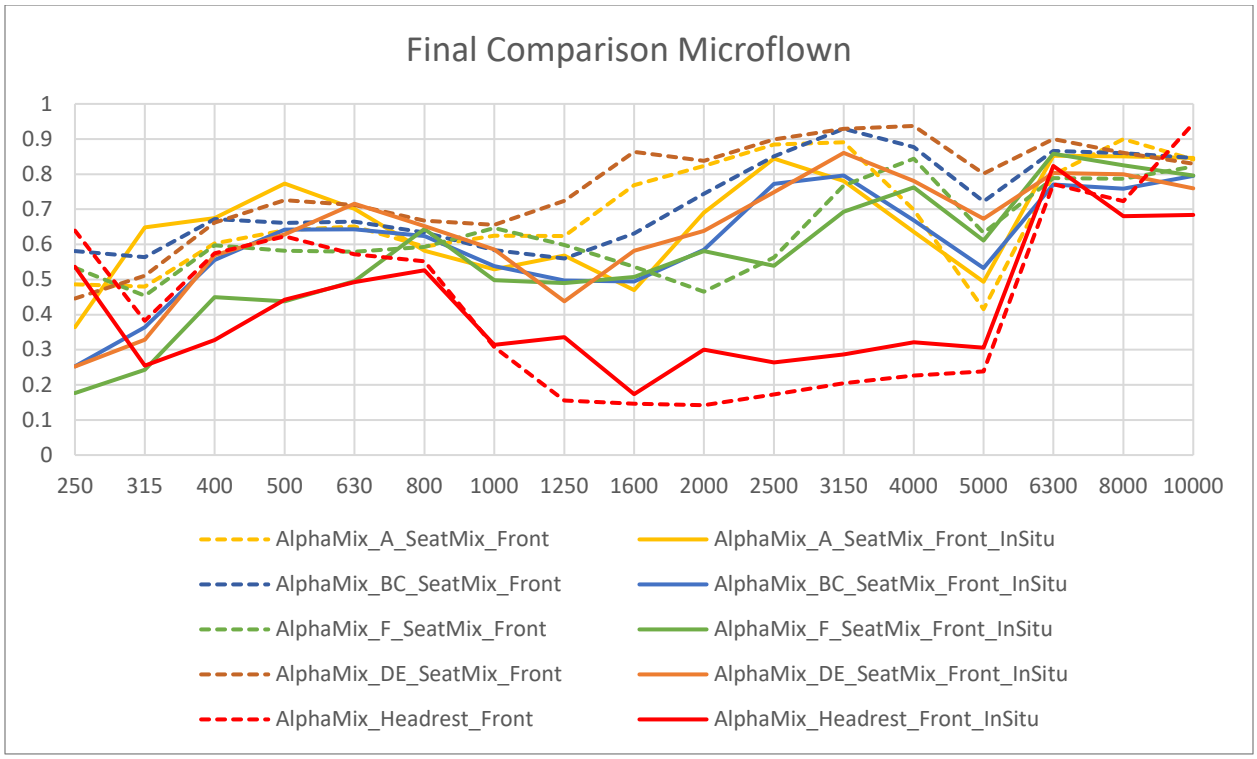

Figure 88: Comparison between various zones identified in laboratory (dashed) and in situ (continuous) of seat front part.

In central zone (zone A), characterized by alternation of smooth and perforated leather, in situ measurements show progressive increase in absorption coefficient from low frequencies, going from 0.36 to 0.77 between 250 and 500 Hz. Laboratory measurements follow similar trend, but with slightly higher values (0.48-0.64). Particularly significant is excellent correspondence between two measurement conditions at high frequencies, where both show coefficients between 0.84 and 0.89 in 2500-3150 Hz band. BC zone presents gradual growth at low frequencies during in situ measurements, with values increasing from 0.25 to 0.64. Laboratory measurements start from higher values (0.58-0.67), but show notable convergence beyond 2000 Hz, where patterns become very similar, with coefficients oscillating between 0.77 and 0.87 at high frequencies. Regarding F zone, in situ measurements show generally lower values at low frequencies (0.17-0.49) compared to laboratory measurements, which show more stable behavior (0.53-0.58). The two measurement conditions find good correspondence beyond 6300 Hz, with coefficients settling around 0.80. DE zone shows greatest variations between two measurement conditions, with differences particularly evident in medium frequencies. Although significant convergence is observed beyond 3150 Hz. Headrest, similarly, presents marked discrepancies between in situ measurements and laboratory ones, with generally lower values in car measurements and more regular

pattern and higher values in laboratory, however finding convergence point at 6300 Hz with coefficients around 0.77-0.82. Less controlled conditions of in situ measurements, influence of confined passenger compartment environment, effects of surrounding surfaces and different measurement mode (manual in car versus tripod in laboratory) may have contributed to formation of such differences. However, it is significant to note how, despite these variables, characteristic patterns of each zone remain clearly recognizable in both measurement conditions. General tendency of in situ measurements to show slightly lower values compared to laboratory ones is compensated by coherence of overall behaviors. This aspect, combined with maintenance of characteristic patterns of each zone, confirms not only robustness of characterization method but also validity of approach of unifying corresponding zones between seat and backrest, regardless of measurement conditions.

Choice of optimal method therefore depends on objective: laboratory is preferable for "pure" characterization of material, while in situ measurements provide more significant information for predicting actual behavior in context of use. Greater regularity of laboratory results suggests better reliability for basic acoustic characterization, while in situ measurements offer more realistic view of performance in application context.

4.3 Sonocat

4.3.1 Measurements of known materials

Considering that SonoCat can report negative values of absorption coefficient when measured reflected power exceeds incident power. This does not indicate negative energy (physically impossible), but signals that material is emitting sound energy instead of absorbing it. The software interprets this situation as an "emission coefficient", displaying it with negative sign.

This phenomenon can occur due to:

- Material vibrations.
- Multiple reflections in sound field.
- Violation of local plane wave hypothesis.

The negative sign thus functions as diagnostic indicator for operator, signaling measurement conditions that deviate from ideal assumptions of implemented mathematical model.

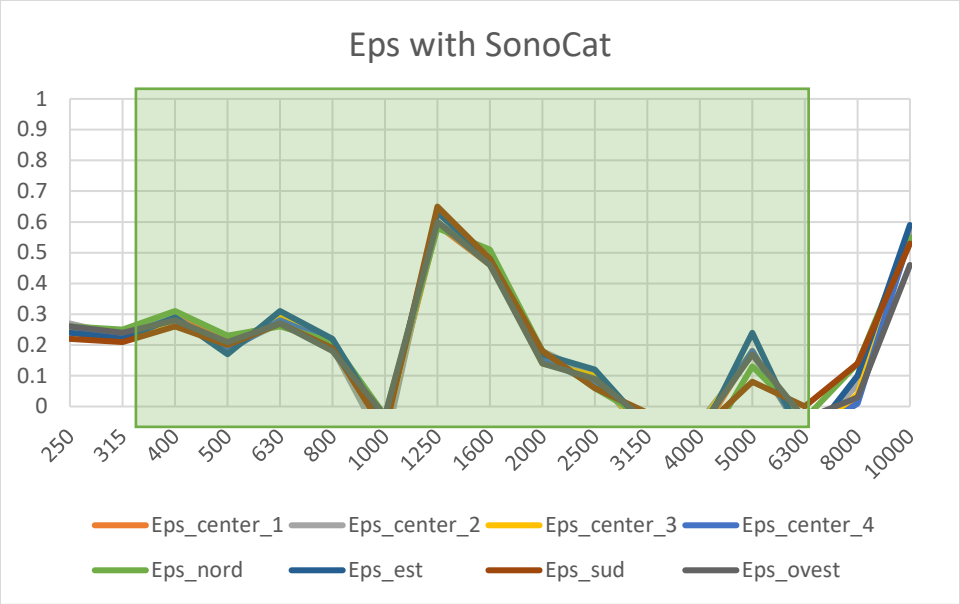

Figure 89: EPS behavior measured with SonoCat where position change and measurements at same point demonstrate its stability and robustness.

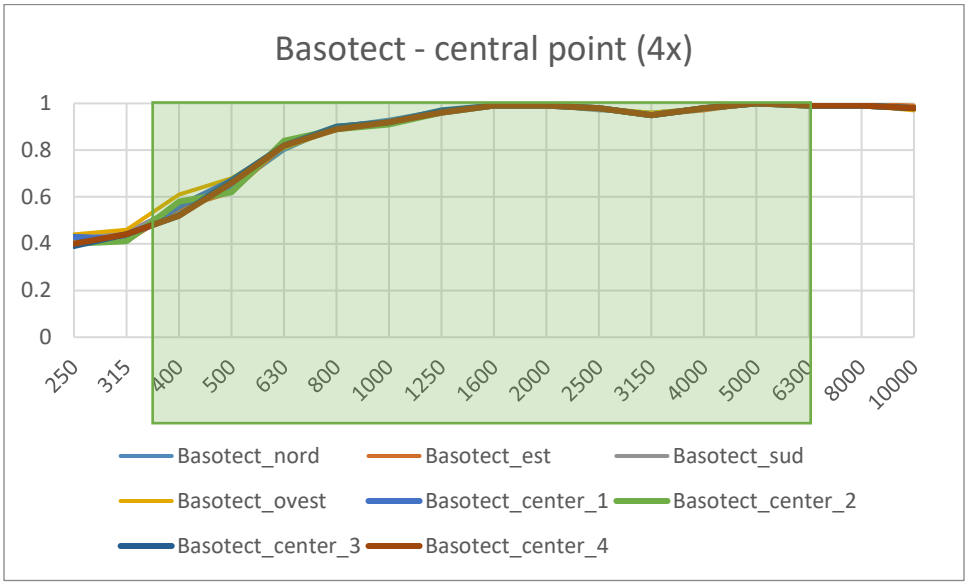

Figure 90: Basotect behavior measured with SonoCat where position change and measurements at same point demonstrate its stability and robustness.

Also for this type of probe, measurements of known materials found robust and concordant values both among themselves and with data obtained from other measurement instruments.

4.3.2 Automotive Seat Measurements in Car

Measurements were performed according to usual precise scheme: four repetitions at same central point and four additional measurements at 2 cm distance from center, in four cardinal directions.

Figure 91: Setup of measurements inside the car.

In frequency range up to 1600 Hz, results showed remarkable coherence and repeatability

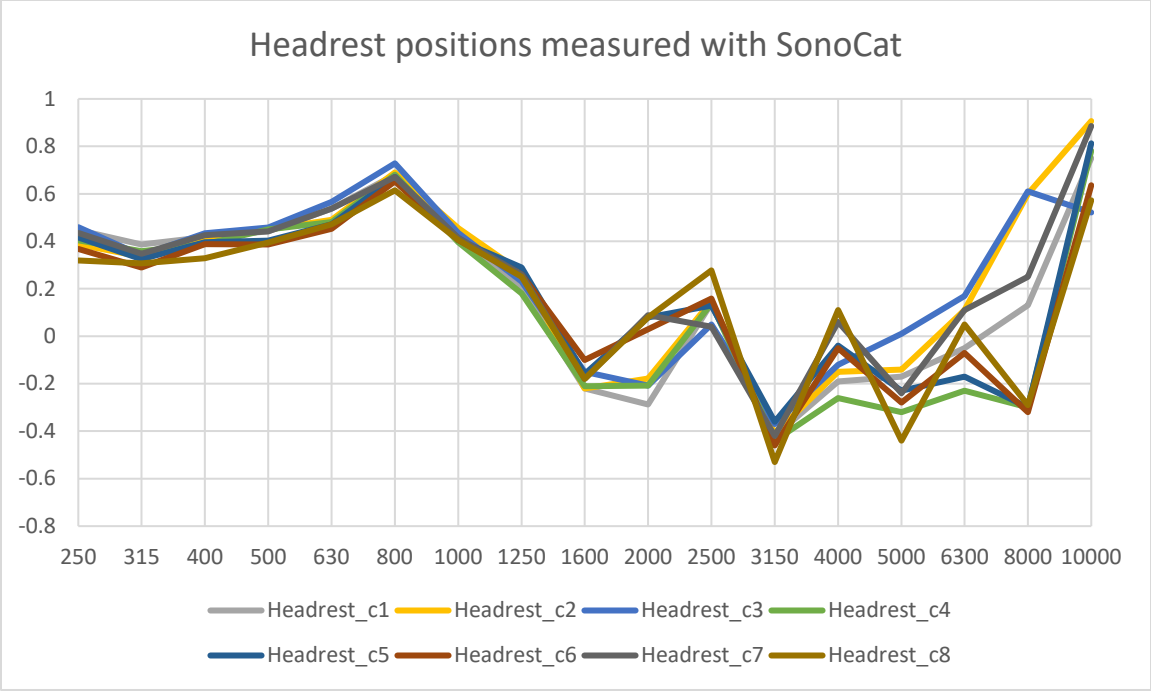

Figure 92: Measurement of headrest inside vehicle with Sonocat probe.

Absorption coefficients measured at different points present minimal variations, with differences on order of few hundredths. This stability is particularly significant because as it indicates that in this frequency band measurements are robust with respect to small position variations and influence of operator's hand movement holding instrument is negligible. Above 1600 Hz, however, progressive increase in dispersion of measured values is observed. This behavior can be attributed to the fact that at high frequencies, where wavelength becomes smaller, sound field becomes more sensitive to local variations and measurement system more reactive to small perturbations.

The persistence of same peaks and general trend, despite greater dispersion of values, suggests that measurements still maintain their statistical validity, while requiring more attention in interpretation of results at high frequencies.

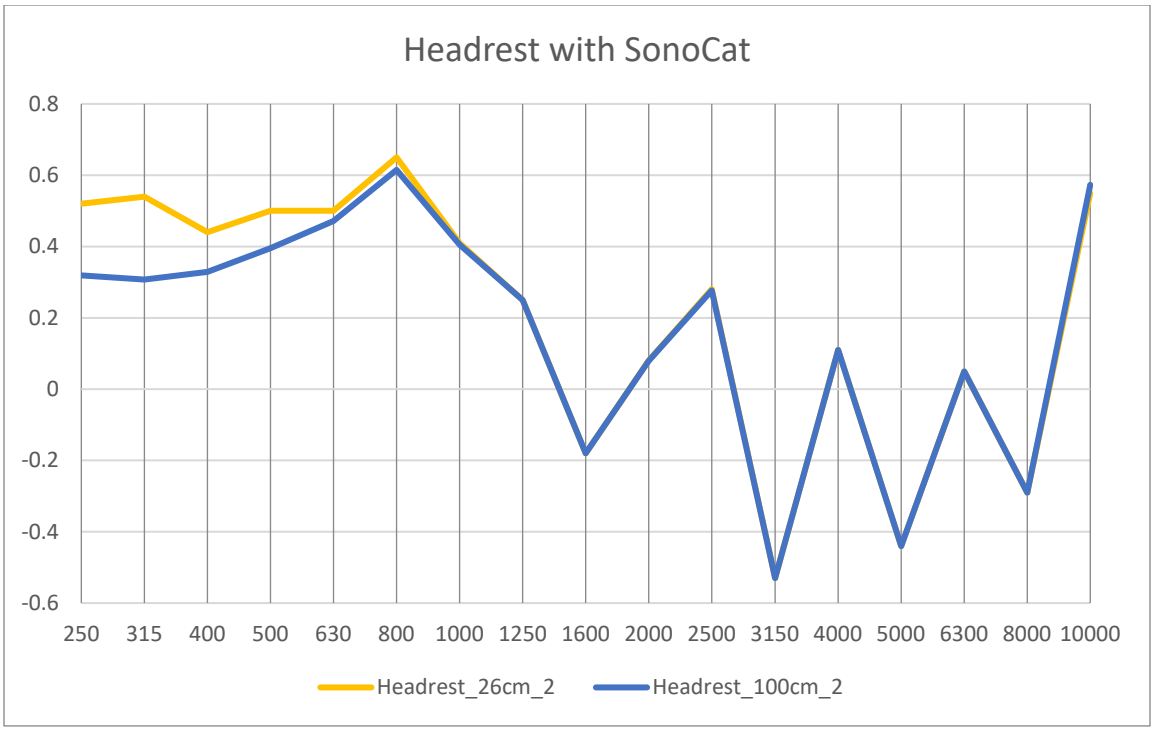

Figure 93: Measurement arithmetically averaged between various acquired measurements (at 26cm) compared to measurement that would have been obtained if speaker had been placed at distance of 100cm.

Following same methodology applied with Microflown probe, complete acoustic characterization of seat was carried out, mapping same areas previously identified starting from measurements of all identified points. Data shown relate to seat measurement directly in car to focus study on in situ environments rather than controlled ones like laboratory. Analysis of headrest revealed interesting aspect: absorption coefficients show remarkable stability and reliability up to 1600 Hz. At low frequencies (330-800 Hz), headrest shows significant absorption, with coefficients varying between 0.5 and 0.7. In medium frequencies (1000-1250 Hz), progressive decrease in absorption is noted in both configurations, with coefficients dropping to about 0.25-0.4. This trend suggests lower system effectiveness in this frequency band. Situation becomes particularly interesting beyond 1600 Hz, where several negative values are observed, especially pronounced at 3150 Hz (down to -0.53) and 5000 Hz (down to -0.44). These negative values do not indicate absence of absorption, but rather suggest that at these frequencies headrest behaves more like a reflector/resonator than an absorber. This complex frequency response can be attributed to composite nature of headrest, where interaction between absorbing materials (padding) and rigid structures (internal frame) creates articulated acoustic behavior that varies significantly with frequency.

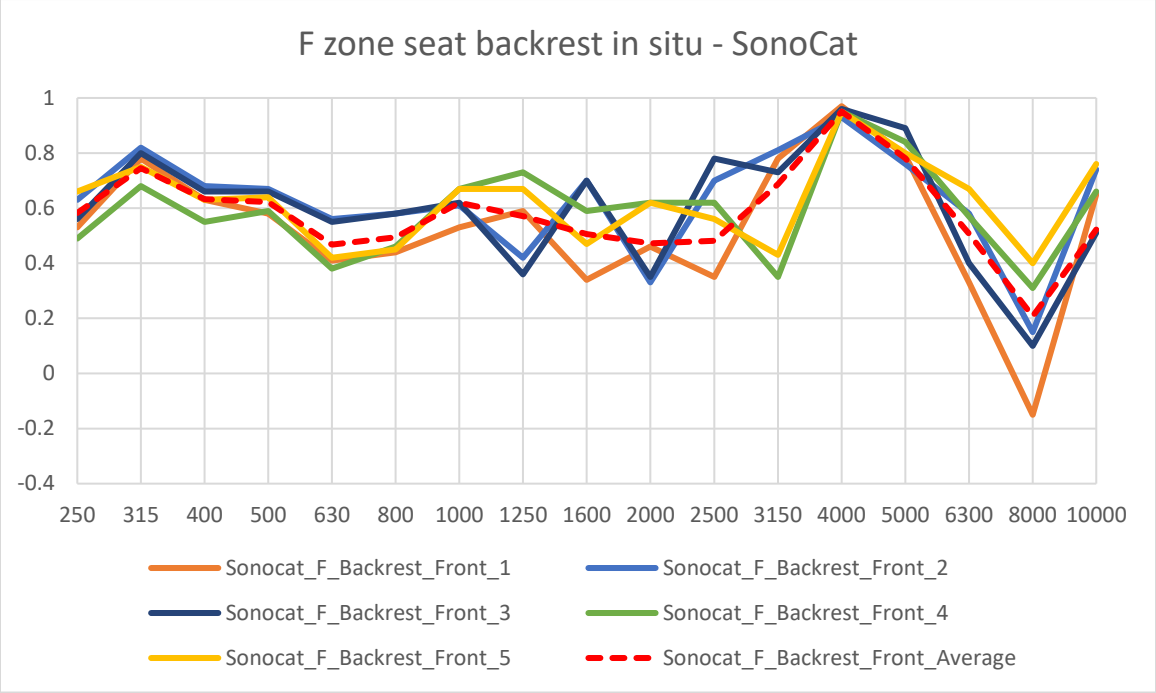

Figure 94: Comparative analysis between seat measurement points that showed most marked deviations from arithmetic mean calculated on all measured points.

In-depth analysis of seat's zone F reveals particularly interesting and complex acoustic behavior. Here too, all points necessary to best define zone were measured. The graph [fig 90] shows only some measurements that reveal representative deviation of all measurements and arithmetic mean obtained from all measured points of zone F. Behavior at low frequencies, up to 1000 Hz, shows particularly positive characteristic: measurements are coherent with each other despite some deviations. This stability in results gives us confidence in validity of measurements in this frequency band. Moving toward medium frequencies, between 1000 Hz and 2500 Hz, we observe slight decrease in absorption and greater influence of measurement conditions is observed, with more marked differences between different positions. At high frequencies we find concurrent peak in all measurements at 4000 Hz, where absorption coefficient consistently reaches values around 0.95. This concordance suggests we are observing intrinsic characteristic of structure or materials used in this zone of seat.

This response can be attributed to composite structure of this zone: perforated leather covering does not prevent action of underlying absorbing layers particularly at 4000 Hz peak. Variable values between 1000

Hz and 4000 Hz could represent combination of rigid materials (structure) and absorbing materials (padding).

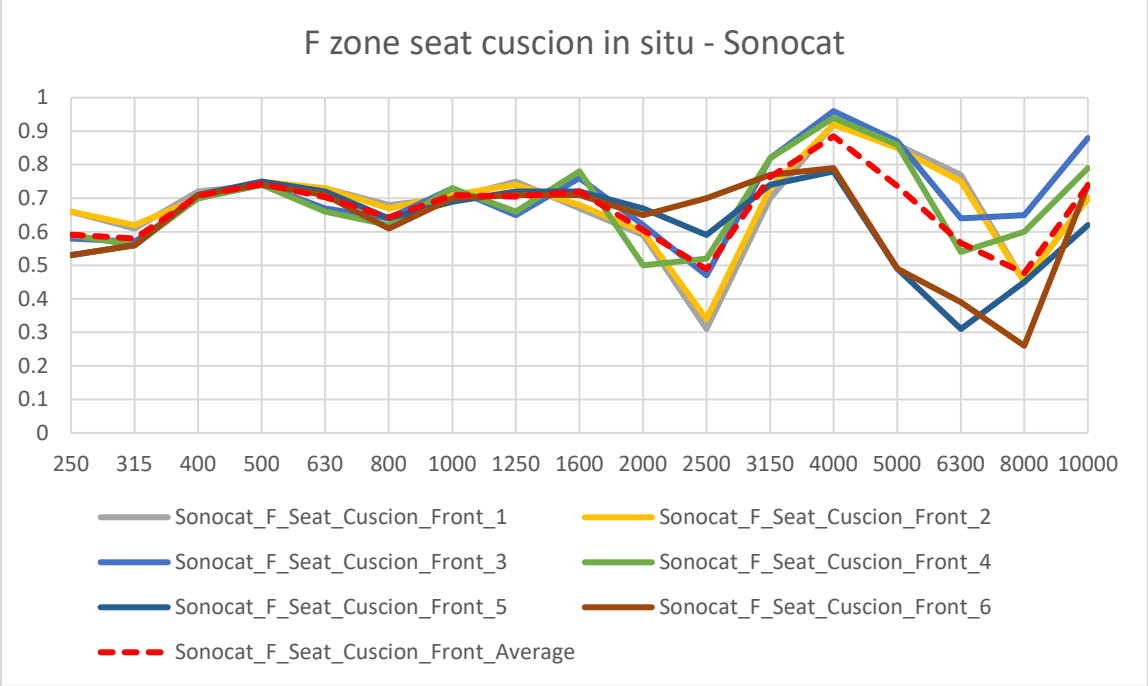

Figure 95: Comparative analysis between seat measurement points that showed most marked deviations from arithmetic mean calculated on all measured points.

Analysis of measurements made on seat zone covered in perforated leather F reveals at low frequencies (250-500 Hz) significant and very stable absorption, with coefficients progressively increasing from about 0.55-0.66 at 250 Hz up to reaching values around 0.74-0.75 at 500 Hz. Coherence of values between different positions suggests homogeneous behavior of entire seat surface in this frequency band. In medium frequencies (630-1600 Hz), material maintains remarkably stable performance, with absorption coefficients oscillating in narrow range between 0.65 and 0.75. This stability is particularly significant because it indicates effective action of padding underlying leather and demonstrates that perforated leather covering does not compromise even in this case absorbing properties of system. At high frequencies values continue to be non-homogeneous but with certain deviation, maintaining usual peak found also in backrest measurement of zone F at 4000 Hz. Of particular interest is repeatability of measurements in each position: pairs of repeated measurements show minimal differences, confirming reliability of measurement method and suggesting that variations observed between different positions

are actually due to local characteristics of seat rather than measurement uncertainties. This overall behavior suggests that seat system as whole works effectively as acoustic absorber, particularly in low and medium frequencies where performance homogeneity is more evident. Perforations, indeed, create system of micro-resonators that, in combination with underlying absorbing material, optimize conversion of sound energy into thermal energy through viscous losses. While variations at high frequencies could be attributed to subtle differences in leather tension or padding density in different seat zones.

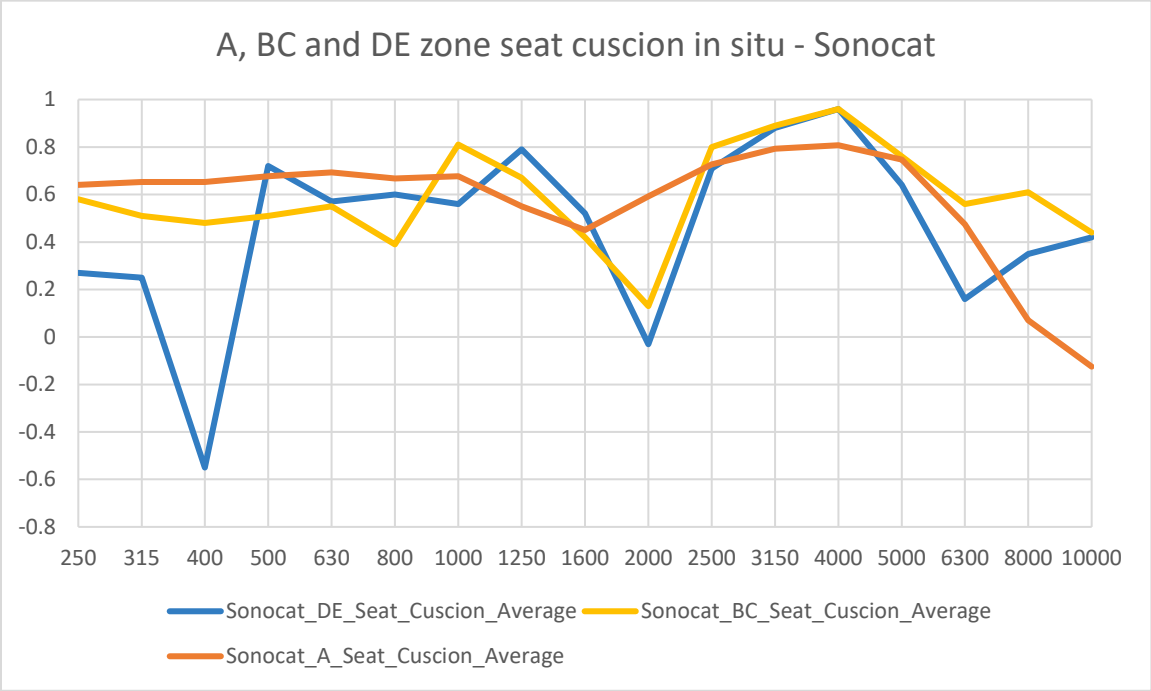

Figure 96: Three seat zones compared and measured in situ with SonoCat probe.

Comparative analysis of different seat zones reveals interesting patterns that reflect the influence of different surface treatments and underlying structures on overall acoustic behavior. Zone A, which recall is characterized by alternation of perforated leather and columns of smooth leather with stitching, shows particularly effective and stable behavior at low frequencies (250-800 Hz), with absorption coefficients consistently maintaining between 0.64 and 0.69. This stability suggests that in this frequency band alternation of materials does not compromise acoustic performance. Situation becomes more complex at high frequencies, where significant asymmetries emerge between right and left sides. These differences can be attributed to influence of stitching and surface alternations, which become acoustically more relevant at shorter wavelengths. Zones B and C, characterized by perforated leather without stitching,

maintain moderate but stable absorption at low frequencies, followed by more dynamic response at medium frequencies, with significant peak at 1000 Hz. Absence of stitching seems to contribute to more uniform and predictable behavior, especially at higher frequencies. This comparative analysis reveals common pattern at usual frequency of 4000 Hz and general stability in medium frequencies. Most marked differences manifest instead in stability of response at low frequencies (better in zone A), in presence of negative values (more frequent in armrests probably due to their reduced measurement surface), in variability at high frequencies (more pronounced in zone A with stitching). This detailed characterization suggests that, while different surface treatments significantly influence local acoustic behavior, underlying seat structure provides common base that manifests in recurring patterns, particularly evident in certain frequency bands. Presence of stitching and alternation of materials tend to introduce greater variability in response at high frequencies, while zones with perforated leather without stitching show more predictable and symmetric behavior.

4.3.3 Measurements of Automotive Seat Samples Outside

To complete acoustic characterization, samples measured in Kundt tube were also measured with SonoCat probe. This methodological choice was motivated by need for comparison with standardized method, considering that SonoCat shows different behavior from Microflown probe. In particular, SonoCat seems particularly effective in highlighting presence and interaction of absorbing and reflective materials, thus providing complementary information about composite nature of tested materials. Obviously test was done on sample pieces of larger size (not less than 20cm x 20cm surface area) compared to those used in Kundt tube (which were still cut from same measured material). Importance of choice of 26 cm measurement distance was verified through specific comparative analysis. In particular, perforated leather sample with polyurethane was chosen as significant case study, being one that showed greatest sensitivity to distance variations compared to other tested materials (which still showed same trends).

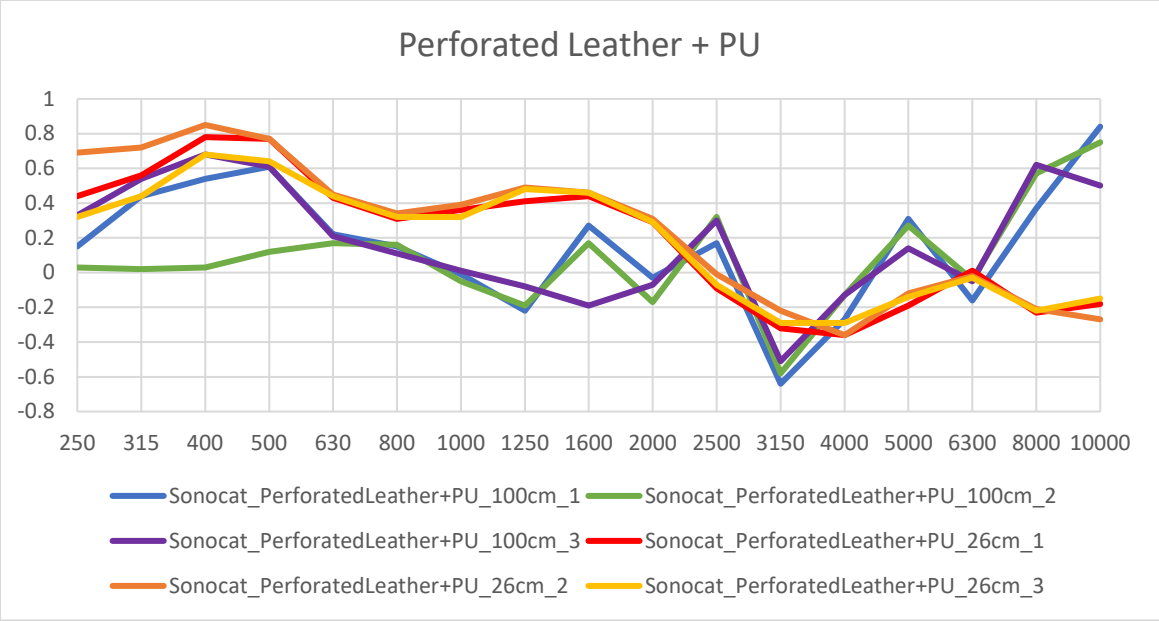

Figure 97: Comparison between trend of measurements taken at distance of 26cm (last three) and at 100cm (first three), of perforated leather and polyurethane sample with SonoCat probe.

This experimental evidence supports adoption of 26 cm as reference distance for measurements, confirming how this configuration provides more stable and representative results of real acoustic properties of material. At low and medium frequencies, measurements at 100 cm show greater variability between repetitions, while measurement repeatability appears better at 26 cm. At high frequencies both configurations show negative values in several bands, suggesting once again presence of reflective component in studied sample. Greater stability at 26 cm in low and medium frequencies could be due to better signal-to-noise ratio and less influence from environmental reflections. Measurements confirm that composite structure (perforated leather + polyurethane) creates complex acoustic system that proves absorbing at low frequencies up to about 2000 Hz, then becoming more reflective at higher frequencies. Fact that material shows best performance at low frequencies could be attributed to effective interaction between leather perforations and underlying polyurethane layer, which together create system of Helmholtz micro-resonators.

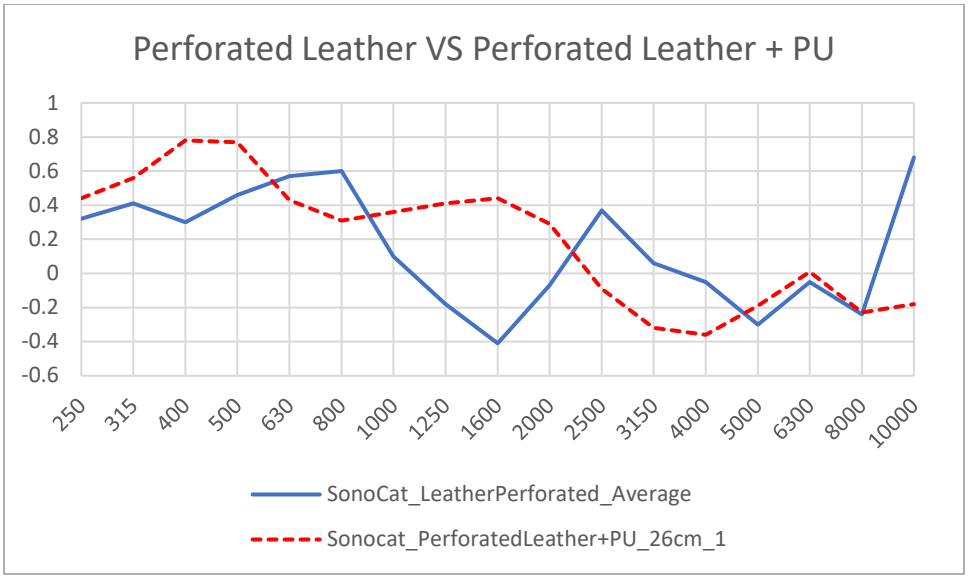

Figure 98: Trend calculated with arithmetic mean on all measured points of perforated leather sample, with SonoCat probe, compared with results obtained from perforated leather with polyurethane sample.

Analysis of perforated leather measurements alone, without polyurethane layer, reveals distinctive acoustic behavior and remarkable coherence between repeated measurements. The absorption peak observed at 800 Hz ($\alpha \approx 0.60$) deserves critical analysis. Despite coherence of repeated measurements, this relatively high value for predominantly reflective material like leather requires caution in interpretation. It could be influenced by resonance phenomena related to perforation geometry, interaction with measurement support, possible effects of local sound field.

More significant and probably more representative of material's real behavior is trend beyond 1000 Hz, where negative values predominate. This pattern clearly indicates leather's reflective nature, with characteristic peak at 2500 Hz that could be effectively indicative of material's intrinsic properties. This interpretation is supported by coherence with leather's known physical properties, stability of repeated measurements, consistent presence of negative coefficients indicating predominance of reflection over absorption. Abrupt transition between 800 - 1000 Hz could suggest presence of resonance phenomenon probably related to perforation geometry. While oscillations between positive and negative values could suggest series of perforated structure resonances.

Comparing these results with those of sample including polyurethane, significant differences emerge: presence of negative values is more pronounced and frequent in leather-only sample compared to one with addition of polyurethane, confirming leather sample as reflective element although perforated.

Latter also tends to have greater absorption probably due to underlying polyurethane that passes through leather holes and that such holes work as resonators only in specific frequency bands.

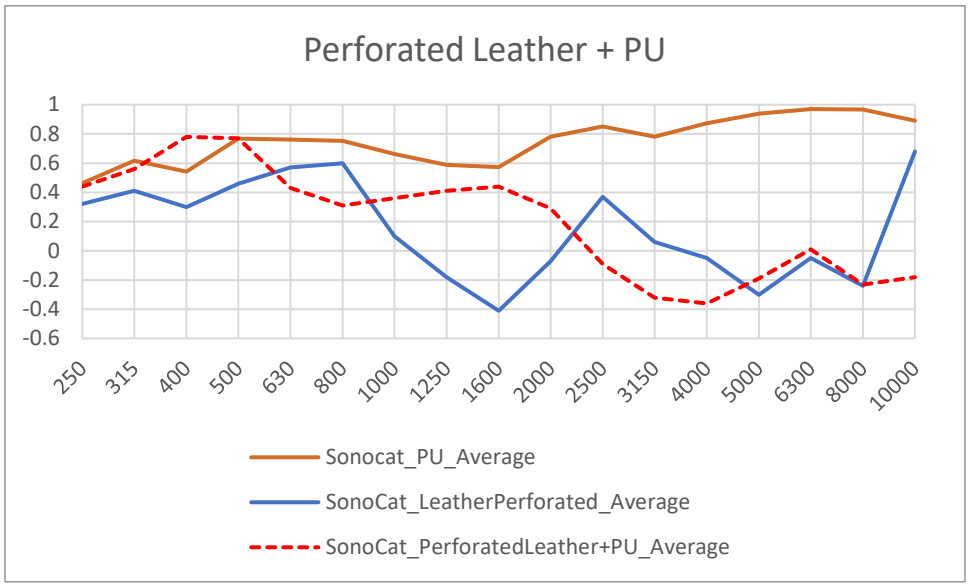

Figure 99: Comparison between three samples: perforated leather with polyurethane and then taken individually leather and polyurethane, measured with SonoCat probe.

Analysis of polyurethane measurements alone reveals notably different acoustic behavior from both perforated leather and composite perforated leather with polyurethane system, confirming that instrument is effectively characterizing material and not environment. Polyurethane shows characteristics of highly absorbing material, with performance that progressively improves with frequency. It is particularly significant to note absence of negative values, unlike what was observed in both perforated leather and composite system. Polyurethane alone shows generally more stable performance and is main responsible for acoustic absorption. Addition of perforated leather seems to reduce absorption effectiveness in many frequency bands and introduce resonance phenomena (evidenced by negative values).

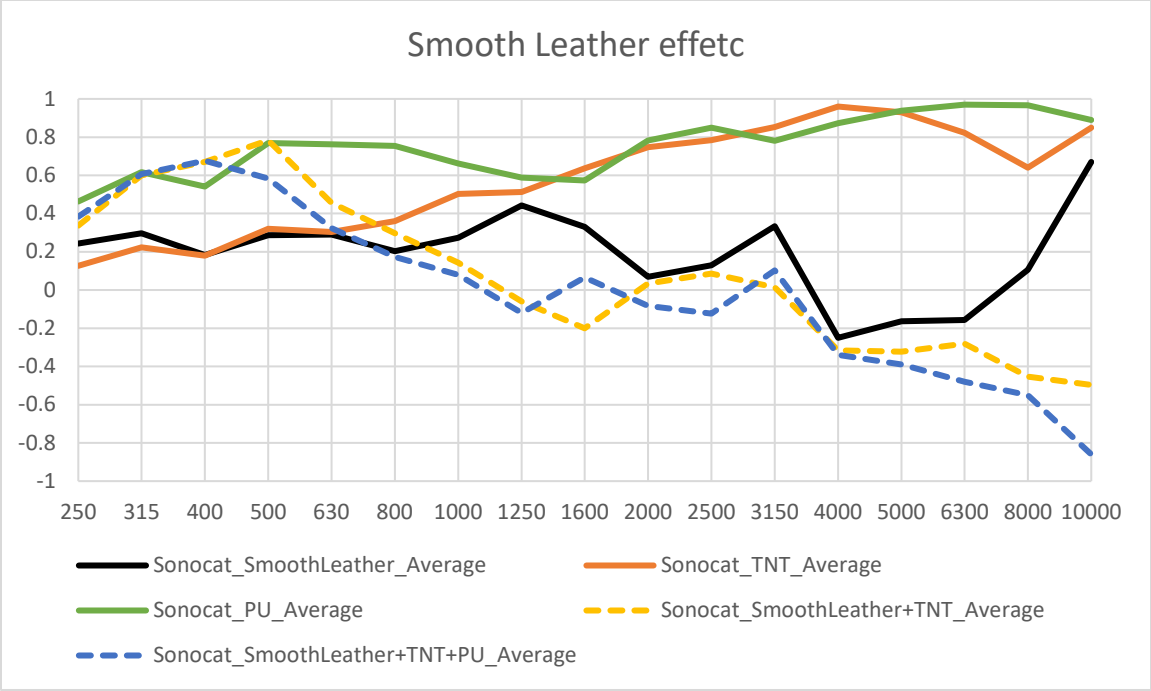

Figure 100: Action of smooth leather on other materials, all measured with SonoCat probe.

Smooth leather confirms its predominantly reflective behavior, characterized by low absorption coefficients at low-medium frequencies and negative values at high frequencies, indicative of its reflective nature. This behavior clearly distinguishes it from perforated version, which generally shows higher absorption coefficients. TNT system (which is actually 1 mm of TNT coupled with 4 cm of polyurethane) shows particular characteristics. At low frequencies (250-500 Hz), TNT shows lower performance compared to polyurethane in same band. This apparently counterintuitive behavior can be attributed to interaction between two materials, where TNT layer, despite its absorbing properties, modifies system's surface impedance and alters efficiency with which sound waves reach and are absorbed by underlying polyurethane. While in medium-high frequencies constant improvement in performance is observed with maximum peak at 4000 Hz. When smooth leather is coupled with TNT+polyurethane system, a mass-spring system is created where smooth leather acts as mass (favoring absorption at low frequencies). While at high frequencies, reflective nature of smooth leather becomes dominant, introducing resonance phenomena evidenced by negative values. This analysis highlights how in multilayer system, final acoustic properties are not simple sum of individual component properties, but result of complex interactions between materials. System effectiveness strongly depends on how these materials interact with each other and influence path of sound waves through composite structure.

5. In situ method validation and applications

Comparative analysis between in situ techniques and standardized Kundt tube method, described in detail in section 2.2.1, represented a fundamental step to validate effectiveness of new measurement methodologies. This comparison must considered multiple aspects, from intrinsic characteristics of materials to measurement conditions.

5.1 Comparison between Kundt Tube Method and In Situ Techniques

Overall analysis of measurements made with Kundt tube demonstrated reliability and potential of this instrument in acoustic characterization of materials, while also highlighting some specific limitations. Its effectiveness was particularly evident in measuring porous materials like Basotect and expanded polyurethane, where it showed excellent measurement repeatability and clear correspondence with expected theoretical behaviors.

For example, in case of Basotect, repeated measurements showed minimal variations, confirming method robustness for highly absorbing materials. On other hand, with more reflective materials like EPS, instrument showed greater measurement variability, suggesting need for particular attention in mounting and interpretation of results for this type of materials.

Measurements validity was further confirmed by analysis of more complex systems, like those with perforated and smooth leather. In case of perforated leather, correspondence between calculated theoretical resonance frequency (≈1720 Hz) and measured one (1600-2000 Hz) provided convincing validation of method. Even in analysis of multilayer systems, Kundt tube allowed clear identification of different absorption mechanisms at play, from viscous dissipation in porous materials to Helmholtz resonance in perforated systems, up to mass-spring effects in smooth leather systems. However, experience has highlighted critical importance of sample preparation and mounting: small variations in dimensions or positioning can significantly influence results, as demonstrated by variability observed in some measurements of multilayer systems. This suggests necessity of always performing multiple measurements of same sample and paying particular attention to preparation and installation phase of specimens.

Although Kundt tube proves effective in characterizing and quantifying different acoustic behaviors, from porous dissipations to resonance phenomena, its measurements are intrinsically limited to small portion

of material, determined by tube diameter. This aspect represents significant limitation, as measurement point might not be representative of material's average characteristics or, conversely, might provide optimistic results based on particularly performing area. To overcome this limitation, use of in situ measurement techniques becomes fundamental: these allow characterizing larger material surfaces, if not entire surface, providing more complete and statistically significant evaluation of acoustic performance. This broader approach allows mapping any material inhomogeneities, local variations in performance, and effect of different mounting or installation conditions, thus offering more realistic and complete characterization of system's acoustic behavior as whole.

5.1.1 Comparison of Known Materials

Validation begins with analysis of reference materials, Basotect and EPS, whose characteristics have been extensively discussed in section 2.1.1. These materials were chosen as references for their contrasting nature: one highly absorbing and other predominantly reflective. This choice allows:

- Verifying accuracy of in situ measurements on well-characterized materials.
- Evaluating ability to discriminate between opposite acoustic behaviors.
- Establishing measurement repeatability in different conditions.

Measurements made with Kundt tube (section 4.1) provide standardized reference against which to compare results obtained with in situ techniques (sections 4.2 and 4.3). While specific data on acoustic absorption of EPS are not available in literature, as this material is typically characterized through its insulating power, theoretical calculations based on material thickness and density indicated that optimal absorption value should occur around 1417 Hz. This theoretical prediction was confirmed by experimental measurements, showing an absorption peak at 1000 Hz.

Comparative analysis shows strong correlation between Kundt tube measurements and in situ ones, particularly in frequency range 500-4000 Hz. For Basotect, measurements made with both Microflown probe and SonoCat show significant agreement with Kundt tube results, with maximum deviations of 5-10% in medium frequencies. The results also confirmed the theoretical prediction that ideal frequency of maximum absorption occurs around 1700 Hz, visible in the graph as a marked increase starting from 1600 Hz.

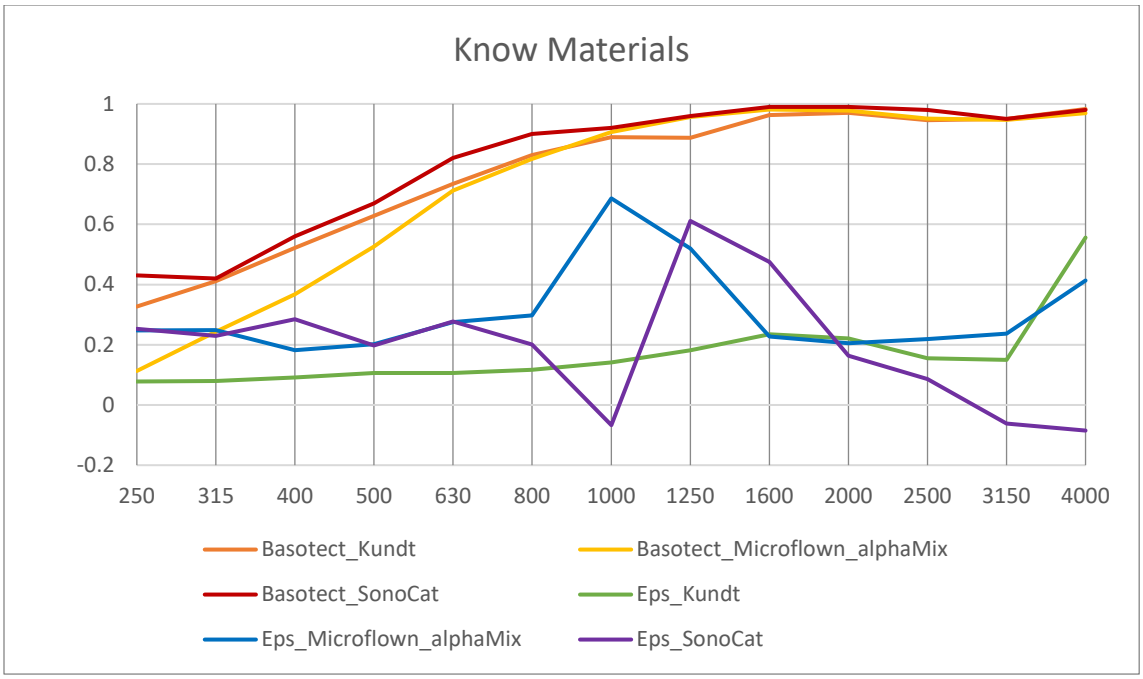

Figure 101: Comparisons between the classical Kundt tube method and in situ methods (Microflown and Sonocat) for measurements of known materials (Basotect and Eps) in laboratory.

Main differences between methods emerge:

- At low frequencies (<300 Hz), where in situ techniques show greater variability.
- At high frequencies (>5000 Hz), where Kundt tube presents intrinsic limitations due to its diameter.

Direct comparison between Sonocat and Microflown reveals complementary strengths:

- Microflown characteristics:
  - Excellent stability in range 800-5000 Hz.
  - Greater sensitivity to environmental conditions.
  - Need for frequent calibration.
  - High precision in point measurements.
- Sonocat characteristics:
  - Effective operating range 300-6300 Hz.
  - Greater robustness to environmental variations.
  - Ability to characterize directional behavior.

- Better management of environmental reflections.

Through extensive testing, an optimized protocol for Microflown measurements was developed, avoiding the complete system with Velo5 software (which produced physically impossible negative absorption values) in favor of using only the probe with Zoom F8 audio card and Adobe Audition post-processing. The optimal configuration requires:

- Probe parallel to surface at 8-13 mm distance.
- Fixed gain deactivated with gain at 4.38V.
- Sine sweep excitation signal.
- Minimum measurement surface of 20x20 cm on reflective support.
- Hybrid data processing approach combining Farina-Fausti formula (250-5000 Hz) and Chung-Blaser formula (5000-10000 Hz).

This configuration demonstrated excellent repeatability and robustness, providing a solid methodological basis for application to more complex cases like automotive seats.

5.1.2 Comparison of Automotive Seat Performance

The automotive seat case study, analyzed through Kundt tube (section 4.1.2), Microflown (4.2.2) and SonoCat (4.3.2), presented a particularly complex challenge due to:

- Complex multilayer structure (described in section 2.1.2).
- Impossibility of direct coring for Kundt tube measurements.
- Presence of curves and complex geometries.

To address these challenges, an innovative three-part approach was developed:

1. Creation of representative samples replicating seat material stratification.
2. Direct comparison between laboratory and in situ measurements in identical positions.
3. Cross-validation between different measurement techniques.

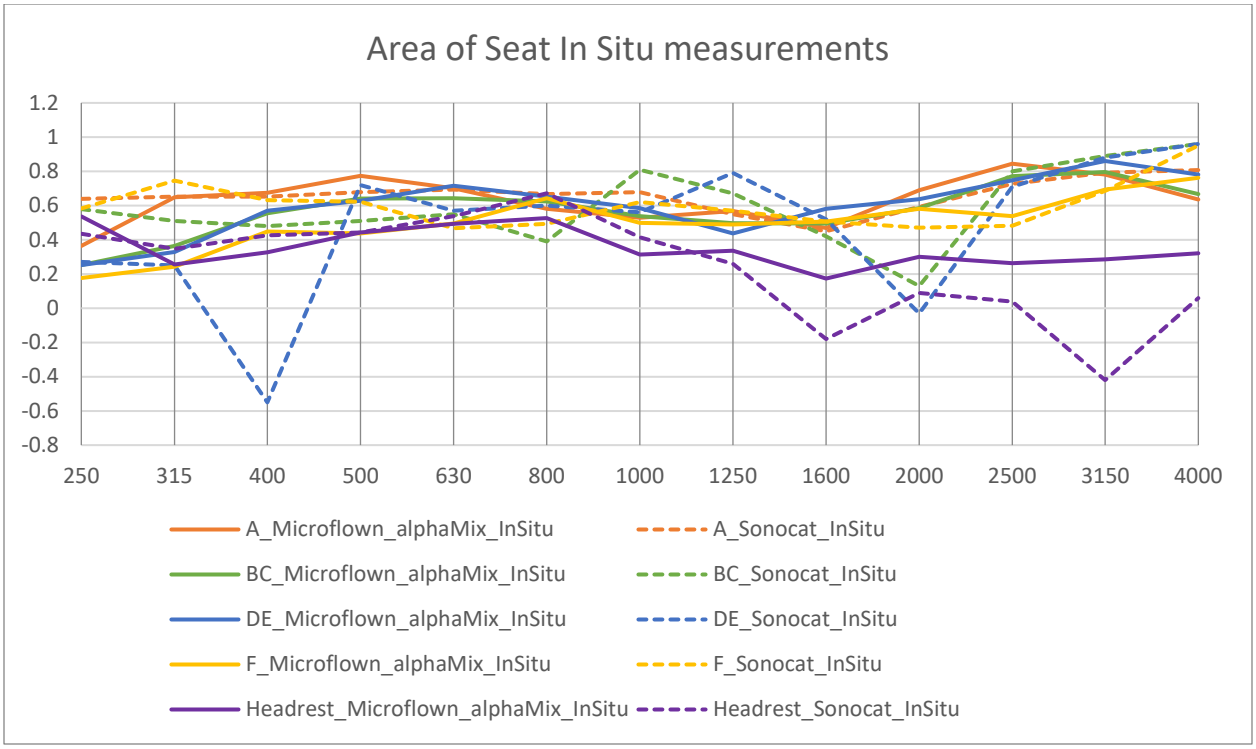

Figure 102: Comparison of seat areas between Microflown and Sonocat measurements taken in situ (inside the car).

The in situ comparison of seat measurements taken directly inside the vehicle revealed interesting patterns across different zones when comparing Microflown and Sonocat techniques. In zone A, characterized by alternating perforated and smooth leather with stitching, both techniques showed good agreement in medium frequencies, with absorption coefficients ranging from 0.6 to 0.7. However, Sonocat demonstrated slightly higher values at low frequencies (around 0.64) compared to Microflown (0.36).

The BC transition zones showed notable differences between the two techniques, with Sonocat generally indicating higher absorption values, particularly in the 500-1000 Hz range. This difference might be attributed to Sonocat's better handling of complex geometries and edge effects in these transition areas.

Zone F, featuring smooth leather without stitching, demonstrated the most consistent agreement between both techniques, especially in medium frequencies (1000-2000 Hz). However, Microflown showed more sensitivity to local variations, while Sonocat provided more stable measurements across the zone.

The DE zones, characterized by smooth leather with stitching, revealed interesting disparities. Microflown measurements showed lower absorption coefficients (around 0.25-0.35) compared to Sonocat (0.5-0.6) at low frequencies, but both techniques converged at higher frequencies.

The headrest measurements presented the most significant differences between the two techniques, particularly at high frequencies. Sonocat showed more stable results, while Microflown exhibited greater variability, possibly due to the headrest's compact dimensions and complex geometry.

Both techniques demonstrated complementary strengths when characterizing different seat areas, with Sonocat generally showing more stable results across larger areas and Microflown providing more detailed local characterization. This comparison validates the reliability of both methods for in-vehicle measurements while highlighting their specific advantages for different seat zones.

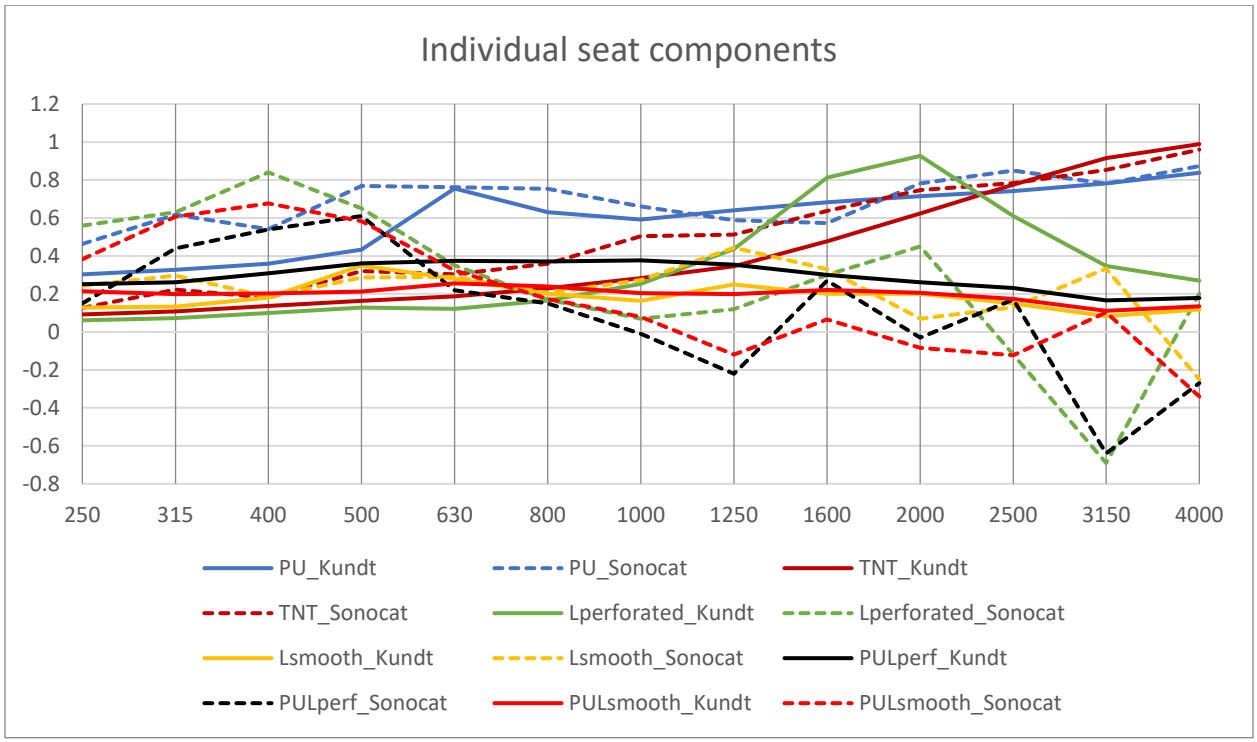

Figure 103: Individual seat components measured with Kundt's tube and SonoCat.

The comparative analysis of individual seat components reveals interesting patterns across different materials and measurement methods. Starting with the basic components:

Smooth Leather (Lsmooth): Shows relatively low absorption across all frequencies with both methods, as expected for a reflective material. The Sonocat measurements show slightly higher values than Kundt tube at low frequencies (250-315 Hz), but both methods confirm the material's reflective nature. Notable discrepancies appear at higher frequencies (>3150 Hz), where Sonocat shows negative values, indicating its limitations in measuring highly reflective materials.

Polyurethane Foam (PU): Demonstrates consistent absorption behavior across both methods, with particularly good agreement in the mid-frequency range. Both techniques show increasing absorption with frequency, though Sonocat generally indicates higher absorption values, particularly in the 400-800 Hz range. The material shows peak performance around 4000 Hz with both methods.

Textile Non-Woven (TNT): Shows progressive improvement in absorption with increasing frequency, a characteristic captured by both methods. Sonocat measurements tend to show higher values than Kundt tube, particularly in mid frequencies, but both methods agree on the overall trend of increasing absorption at higher frequencies.

Perforated Leather (Lperforated): Presents the most significant differences between methods, particularly at low frequencies where Sonocat shows notably higher absorption values. Both methods capture the characteristic peak around 1600-2000 Hz, likely related to Helmholtz resonance effects, though with different magnitudes.

Complex Combinations: The multilayer combinations (PU_Lperf and PU_Lsmooth) show more complex behavior. The perforated leather with polyurethane (PU_Lperf) demonstrates better absorption characteristics than the smooth leather combination, though both measurement methods show some disagreement on absolute values. The smooth leather with polyurethane (PU_Lsmooth) shows generally lower absorption values, with both methods indicating similar trends but different magnitudes.

This comprehensive comparison validates both measurement techniques while highlighting their specific strengths and limitations in characterizing different material types and combinations. The results particularly emphasize the complementary nature of these methods in understanding complex acoustic systems.

5.1.3 Comparison of Innovative Materials Performance

The validation of in situ methods extended beyond standard materials through testing on innovative materials, with particular focus on a compelling case study: IsolMix M35. This 50cmx50cm sample, made from recycled textile factory waste, provided a unique opportunity to evaluate our measurement techniques on a non-standard, heterogeneous material while simultaneously exploring sustainable acoustic solutions.

The measurement campaign across all three instruments revealed interesting patterns in their performance. In the critical low-frequency range (250-500 Hz), the Kundt tube and Microflown showed remarkable agreement, validating the reliability of in situ measurements in this challenging region. While the SonoCat initially showed higher values below 330 Hz (a known limitation of the instrument), the application of specially developed correction factors successfully brought its results in line with the other methods. As measurements moved into medium frequencies (630-1000 Hz), all three methods showed progressive convergence, culminating in excellent agreement at high frequencies (1250-4000 Hz).

Each measurement technique revealed distinct strengths in characterizing different aspects of the material. The SonoCat probe, with its spherical microphone array, proved particularly adept at capturing directional variations in absorption properties across larger areas. In contrast, the Microflown probe excelled at detailed point-by-point analysis, especially in identifying viscous dissipation mechanisms between 500-2000 Hz. These complementary capabilities proved especially valuable given the inherent

heterogeneity of IsolMix M35, where variations in density and fiber distribution posed significant measurement challenges.

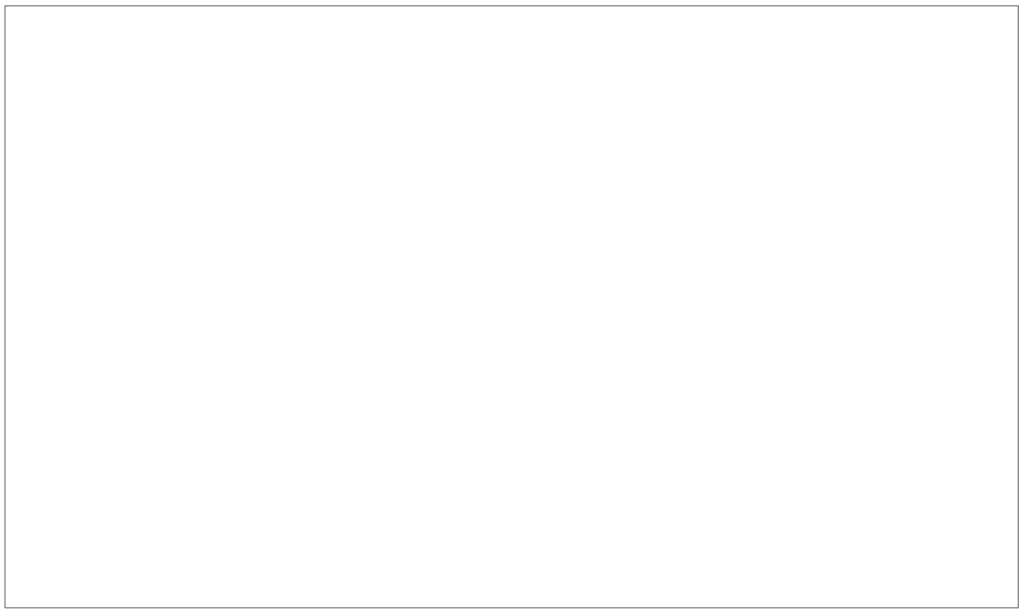

Figure 104: Comparison of various methods used, measuring a central point of new IsolMix M35 sample.

Perhaps most significantly, IsolMix M35 demonstrated acoustic performance comparable to Basotect, a reference material in the sector. This finding carries particular weight given current environmental concerns about textile waste. The successful characterization of this recycled material, despite its heterogeneous nature, not only validates our measurement methodologies but also opens promising avenues for sustainable acoustic solutions. Furthermore, the material's successful completion of building use certification tests (including fire resistance, humidity, and wear) suggests real practical potential for such recycled materials in acoustic applications.

The complementary nature of the different measurement techniques proved crucial in building a comprehensive understanding of the material's acoustic behavior. While each method had its strengths in particular frequency ranges or measurement scenarios, their combined use provided robust validation of results and deeper insights into absorption mechanisms. This multi-method approach proved

particularly valuable for characterizing complex, non-homogeneous materials derived from recycling processes.

These findings suggest that in situ techniques can not only effectively characterize innovative materials, but they can also play a crucial role in developing and validating sustainable acoustic solutions for the future.

5.1.4 Advantages and Limitations of In Situ Technique

In-depth analysis of both measurement techniques has highlighted how Microflown and Sonocat, while aiming at same acoustic characterization objective, present complementary characteristics that make them particularly effective in different scenarios.

Microflown probe demonstrated remarkable precision in point measurements, particularly excelling in frequency range between 800 and 5000 Hz. This characteristic made it ideal for detailed characterization of layered materials and complex structures, as evidenced in automotive seat measurements. Its high sensitivity in detecting local variations in acoustic properties proved particularly valuable in analysis of perforated systems, where it has shown exceptional ability to characterize Helmholtz resonator effects. A significant advantage was also the possibility of operating on relatively small sample areas, with minimum of 20x20 cm, making it particularly suitable for measurements in confined spaces.

However, this high sensitivity also translated into some significant limitations. Probe requires frequent calibrations to compensate for variations in environmental conditions and shows limited performance at low frequencies, below 300 Hz. Need to maintain precise distance control, ideally between 8 and 13 mm, can make measurements more complex in non-ideal conditions. Furthermore, limitations of native software required development of alternative solutions for data post-processing.

The Sonocat system, on other hand, distinguishes itself through greater operational robustness, particularly evident when characterizing larger measurement areas. Its superior ability to manage environmental reflections and provide superior directional characterization makes it particularly suitable for measurements in non-ideal conditions. Its native software, unlike that of the Microflown, offered reliable processing procedures that do not require external tools, with integrated validation procedures that increase results reliability.

However, the Sonocat also presents its limitations. Its effectiveness was reduced below 330 Hz, requires larger minimum measurement areas compared to Microflown, and presents greater complexity in data interpretation at high frequencies. Particularly critical is optimal measurement distance of 26 cm, which required development of specific correction factors to ensure results accuracy.

A particularly interesting aspect that emerged from the study was how these two techniques, apparently competing, can actually complement each other effectively. While Microflown excels in detailed point analysis, Sonocat offers better characterization of surface as whole. Combined use of both techniques has allowed obtaining more complete understanding of acoustic behavior of tested materials, with each system compensating for limitations of other.

The choice between these two techniques should therefore be based on specific application requirements: material nature (homogeneous or heterogeneous), measurement environment (controlled or in situ), required frequency range, dimensions of area to be characterized, and need for directional information. This thorough understanding of the advantages and limitations of each technique allowed selecting most appropriate approach for each specific application, ensuring accurate and reliable acoustic characterization results.

5.2 Analysis of Sound Levels in Comsol Simulation

Following analysis presents comparison between three distinct approaches: experimental measurements, numerical simulations based on Finite Element Method (FEM) and simulations based on Ray Tracing.

For each microphone position, four main configurations were analyzed:

- Speaker in front position with seat present.
- Speaker in rear position with seat present.
- Speaker in front position without seat (reference measurement).
- Speaker in rear position without seat (reference measurement).

Measurements without seat serve as reference to validate accuracy of numerical models and quantify effect of seat on sound propagation.

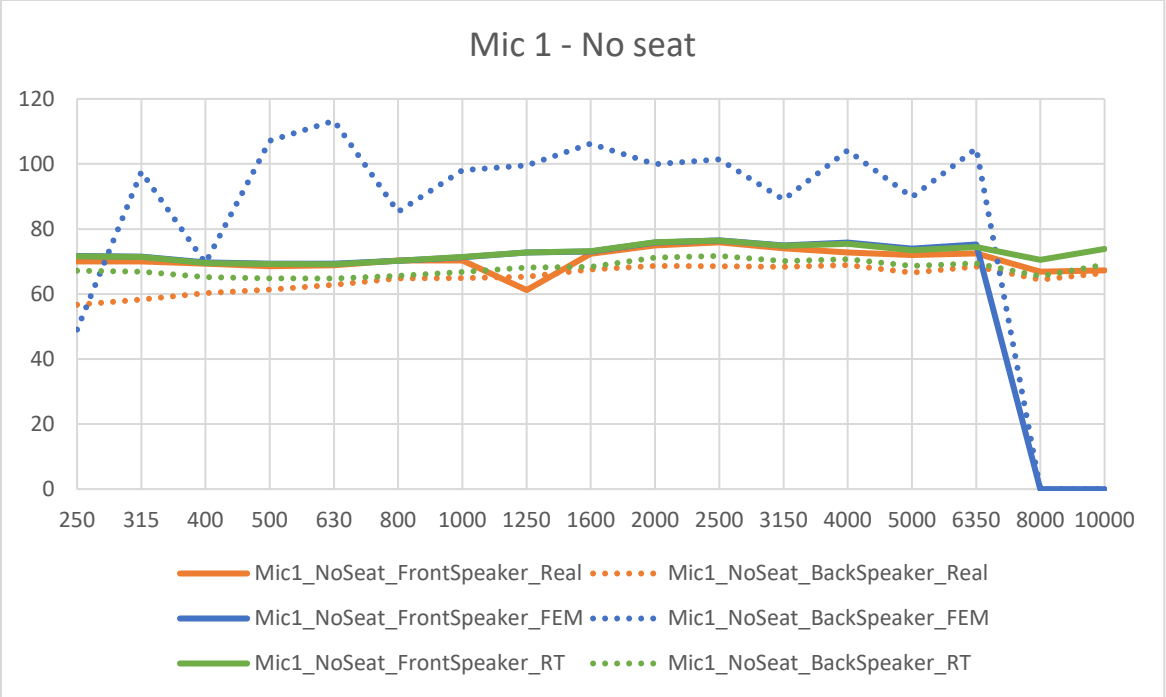

Figure 105: Comparison between trends detected during real measurement, simulated in FEM and simulated in Ray Tracing, in microphone 1 position with speaker both in front of and behind seat, in absence of seat itself.

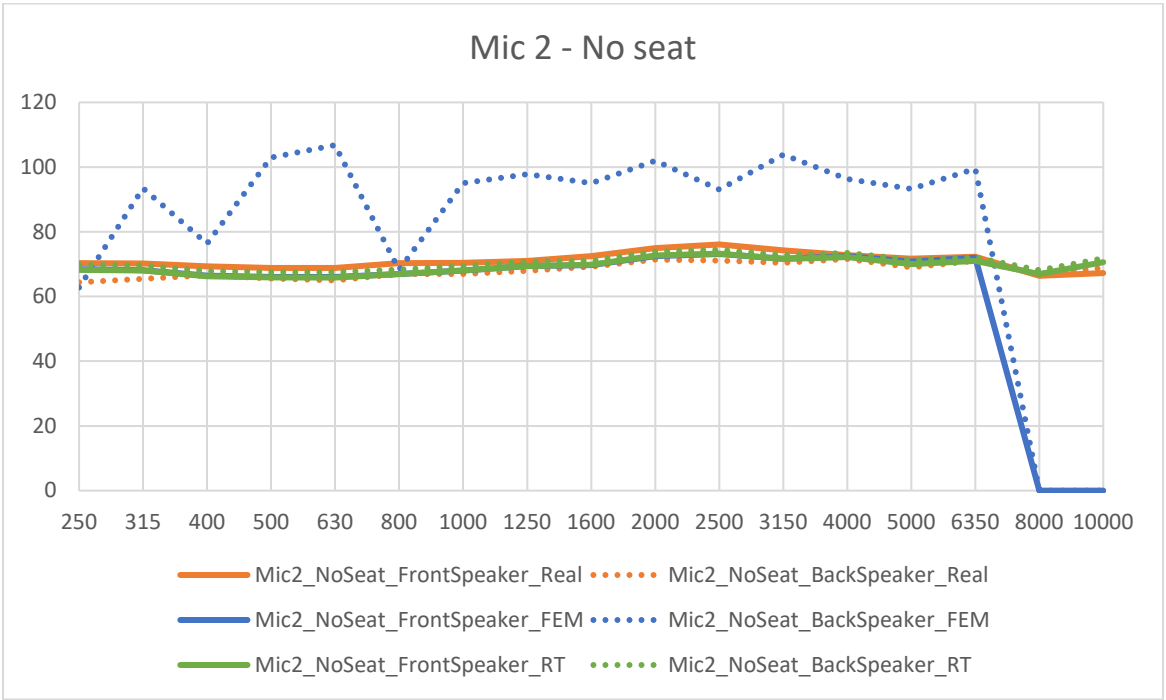

Figure 106: Comparison between trends detected during real measurement, simulated in FEM and simulated in Ray Tracing, in microphone 2 position with speaker both in front of and behind seat, in absence of seat itself.

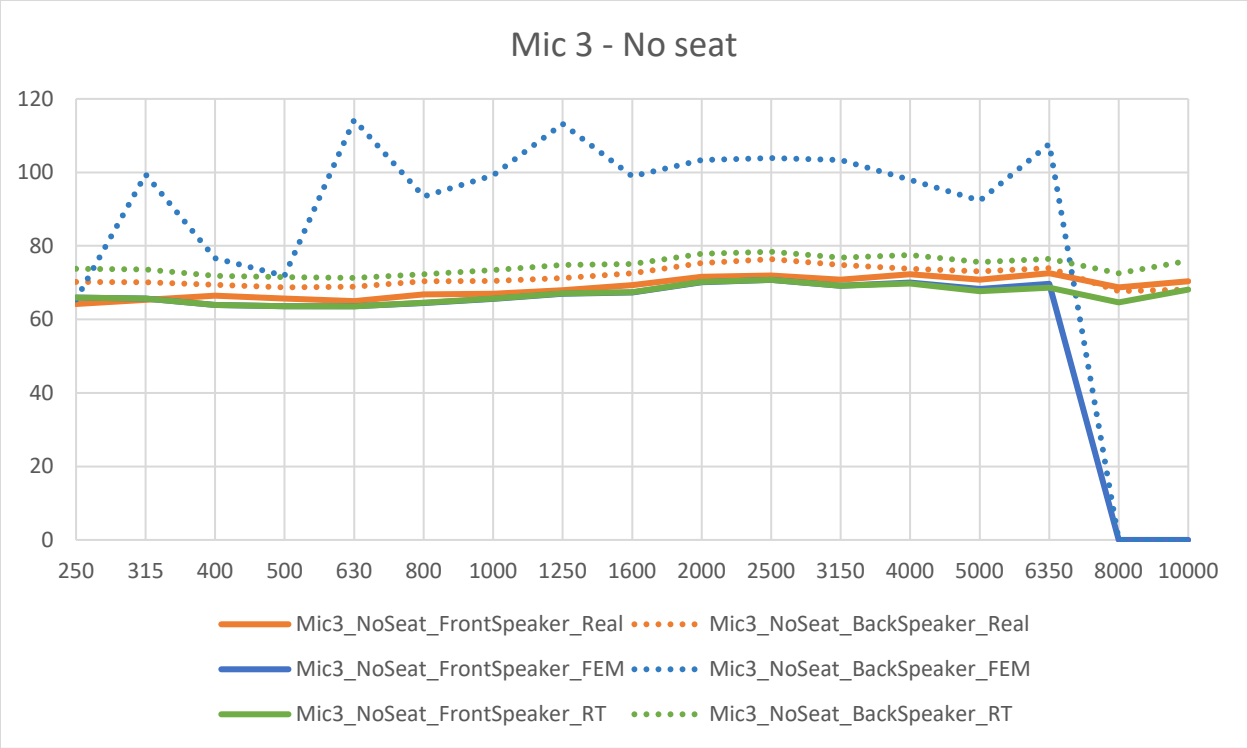

Figure 107: Comparison between trends detected during real measurement, simulated in FEM and simulated in Ray Tracing, in microphone 3 position with speaker both in front of and behind seat, in absence of seat itself.

It is easily observed how all models respond same way in environment without seat. Exception is anomalous response of FEM simulation in configuration with speaker placed behind seat. In empty environment, FEM must model wave propagation in open domain, and this is achieved through implementation of specific boundary conditions, particularly PML (Perfectly Matched Layer). When source is positioned posteriorly, particular interaction occurs between: direct waves from source, reflections from computational domain surfaces and interaction with PML. This leads to possible overestimation of acoustic energy in calculation domain for several reasons:

- Boundary conditions might not be optimized for posterior source position.
- PML might not work effectively when source is closer to its boundaries.
- Proximity of posterior source to computational domain boundaries could generate numerical instabilities.
- Acoustic energy might accumulate in non-physical way due to multiple reflections not properly attenuated.
- Source modeling itself might be less accurate in this position.

This problem does not manifest in other tests, suggesting problem is specific to FEM implementation and does not reflect real physical phenomenon. Ray Tracing simulation, based on different wave propagation principles, does not suffer from these numerical limitations and provides more realistic results even in posterior configuration. However, it is important to note that this FEM limitation does not compromise its overall usefulness, as it provides accurate results in other configurations and remains valid tool for acoustic analysis when appropriately used.

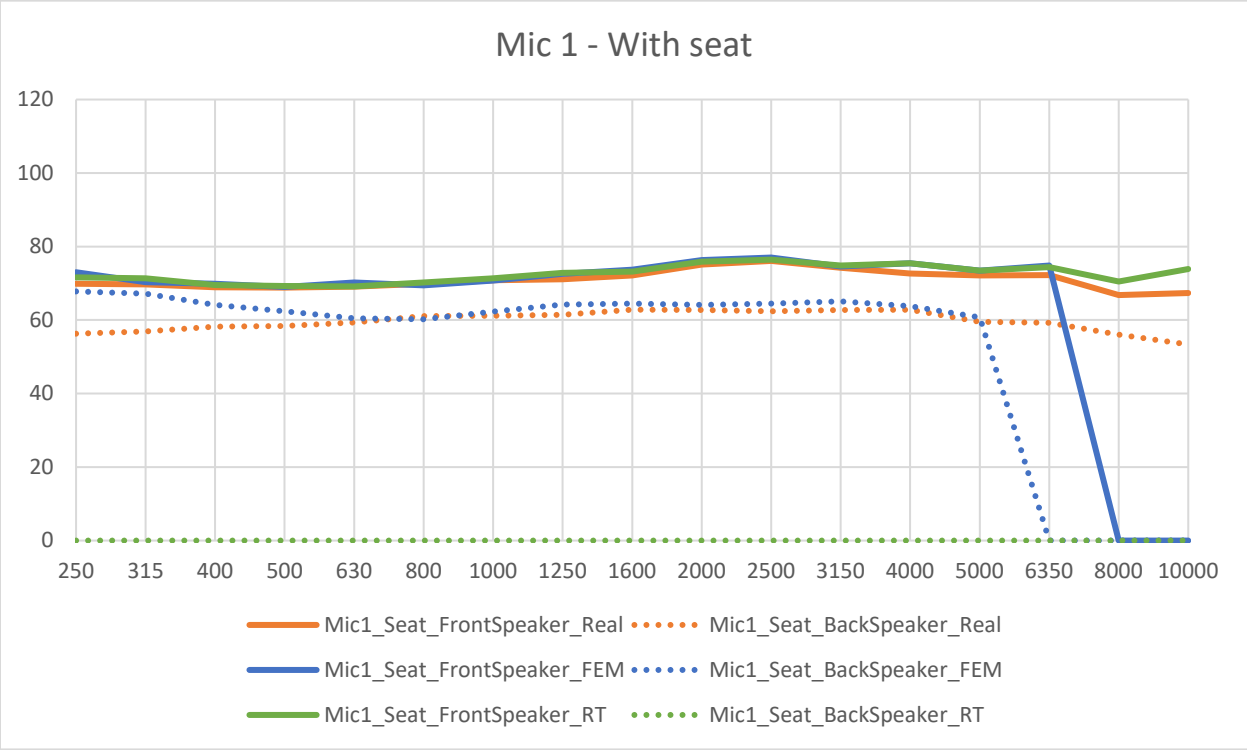

Figure 108: Comparison between trends detected during real measurement, simulated in FEM and simulated in Ray Tracing, in microphone 1 position with speaker both in front of and behind seat, in presence of seat.

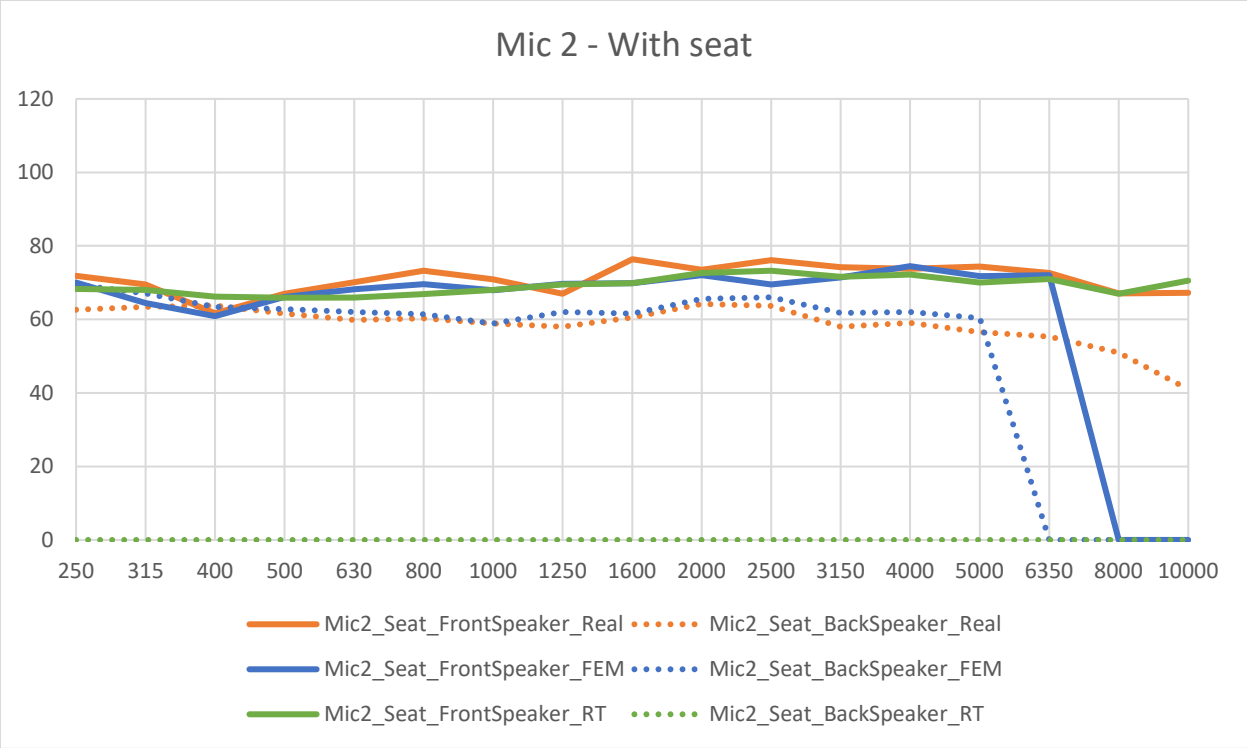

Figure 109: Comparison between trends detected during real measurement, simulated in FEM and simulated in Ray Tracing, in microphone 2 position with speaker both in front of and behind seat, in presence of seat.

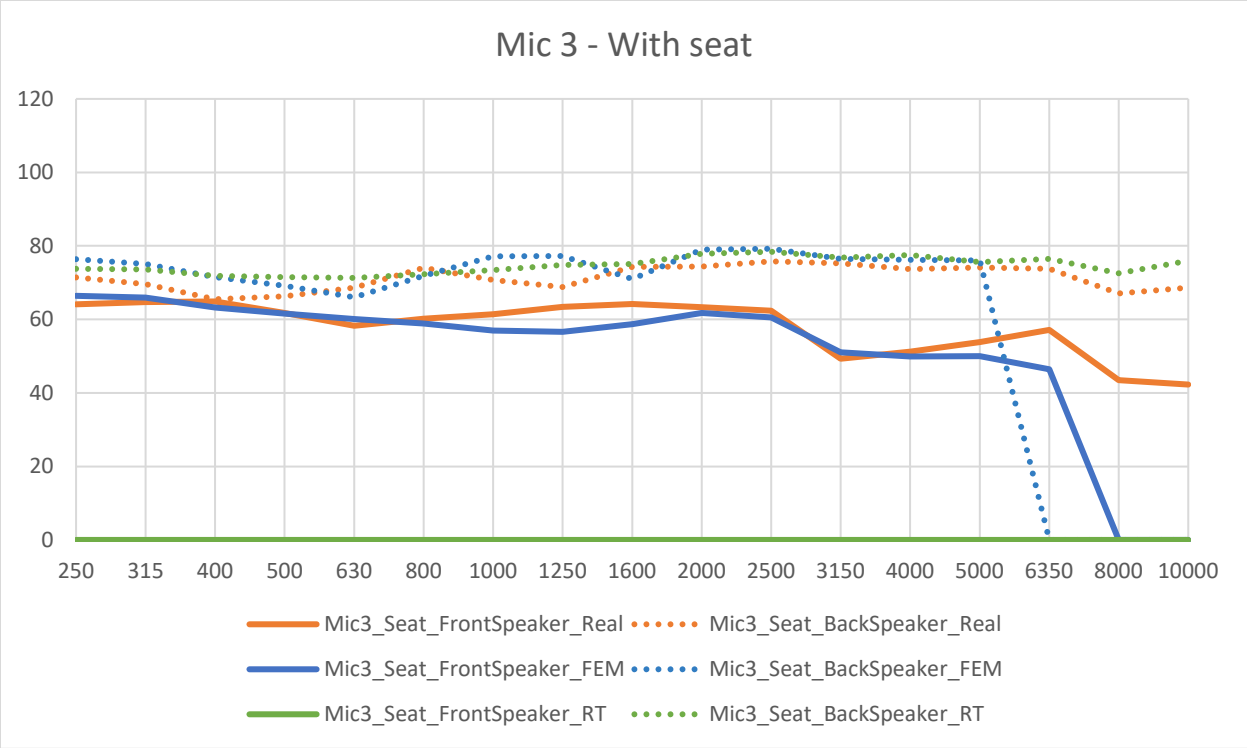

Figure 110: Comparison between trends detected during real measurement, simulated in FEM and simulated in Ray Tracing, in microphone 3 position with speaker both in front of and behind seat, in presence of seat.

Measurements in presence of seat instead show certain differences between methods. Real measurements show coherent and physically plausible behavior, clearly evidencing seat's shielding effect and certain coherence of results between different microphone positions. FEM method shows good ability to predict seat's shielding effect up to 5000 Hz, extraordinarily approaching values actually measured both in case of speaker in front of seat and behind. Ray Tracing demonstrates notable superiority over FEM method: not only does it reproduce real measurement results with high accuracy, but maintains this precision even beyond 5000 Hz, frequency that represents practical limit for FEM simulations. This ability to extend analysis to high frequencies represents significant advantage for applications requiring complete characterization of acoustic spectrum. However this occurs only in case where speaker is in front of microphone, showing inability to model transmission through physical obstacles like seat (results -Inf). This limitation is intrinsic to nature of Ray Tracing itself, which models sound as rays that propagate in straight lines and can be reflected or absorbed, but not transmitted through materials. Such behavior underlines how choice of simulation method must be guided by specific requirements of acoustic analysis to be performed and characteristics of phenomenon to be studied. A hybrid approach, combining FEM for

low and medium frequencies with Ray Tracing for high frequencies, could provide best results in overall modeling of seat's acoustic behavior.

6. Conclusions

6.1 Summary of Main Results

The research conducted has allowed performing an in-depth evaluation of three different acoustic characterization methodologies, each of which has revealed specific peculiarities and potential in its field of application. The comparative approach has allowed us to understand not only the strengths of each technique, but also how these can integrate to provide more complete characterization of acoustic materials.

The Kundt tube, used as a standardized reference, has confirmed its position as a fundamental instrument in acoustic characterization, demonstrating exceptional reliability in the 125-4000 Hz range, particularly in the measurement of homogeneous materials. However, the study has highlighted how this precision comes at a significant cost in terms of practical applicability. The need to core samples not only makes the method destructive, but can also alter the properties of the material to be analyzed, as clearly emerged in the case of composite materials and automotive seat. Moreover, the impossibility of performing in situ measurements significantly limits understanding of the acoustic behavior of materials in their real conditions of use.

The Microflown probe has demonstrated that it represents a significant step forward in acoustic characterization, offering previously unimaginable versatility. Its ability to perform non-destructive and in situ measurements, combined with excellent repeatability in point measurements in the 800-5000 Hz range, has made it particularly valuable in the study of complex systems. Its sensitivity in the characterization of specific absorption mechanisms, like Helmholtz resonators, has provided fundamental insights into the acoustic behavior of tested materials. However, the research has also highlighted how this sensitivity is accompanied by greater vulnerability to environmental conditions, requiring frequent and accurate calibration procedures.

The SonoCat has introduced innovative capabilities that have significantly expanded the possibilities of acoustic characterization. Its effective operating range between 300 and 6300 Hz, combined with the ability to characterize directional behavior of absorption, has opened new perspectives in understanding acoustic materials. Its ability to manage environmental reflections and map extended areas has made it particularly suitable for measurements in real conditions. However, this sophistication translates into greater complexity in the interpretation of results, requiring specific expertise for optimal use.

6.2 Critical Evaluation of In Situ Techniques Compared with Traditional Methods

The comparative analysis conducted in this study has highlighted how in situ techniques represent not only an alternative to traditional methods, but a real paradigm shift in the acoustic characterization of materials. While the Kundt tube continues to represent the reference for measurements in controlled conditions, new techniques have demonstrated the ability to provide valuable and complementary information, particularly relevant for understanding the behavior of materials in their actual conditions of use.

A fundamental advantage of in situ techniques, which clearly emerged during the study of the automotive seat, is the ability to preserve the integrity of tested materials. This characteristic has proved particularly valuable in the analysis of complex composite systems, where coring required by the Kundt tube would have significantly altered the system's properties. The possibility of performing direct measurements, without the need for sample preparation, not only simplifies the characterization process but provides results more representative of real acoustic performance.

The ability to map extended surfaces has opened new perspectives in understanding the acoustic behavior of materials. During measurements, it was possible to observe how acoustic properties can vary significantly across the same surface, an aspect impossible to detect with traditional methods. This characteristic has proved particularly useful in the analysis of non-homogeneous materials or those with directional properties.

However, the implementation of these techniques has required particular attention to several critical aspects. Accurate control of measurement conditions and management of environmental reflections have proved fundamental for obtaining reliable results. Experience acquired during the research has demonstrated how the appropriate choice of measurement configuration can significantly influence the quality of results.

A particularly interesting aspect that emerged from the study is the complementarity between the Microflown and the SonoCat. The two techniques, while based on different physical principles, have shown how they can reciprocally compensate for their limitations. The possibility of validating results through two independent methodologies has provided a higher level of confidence in acoustic characterization, also allowing the selection of the most suitable technique for specific applications.

6.3 Limitations Emerged from Research and Possible Future Improvements

The research has highlighted how, despite significant progress in in situ measurement techniques, some fundamental limitations remain that require further developments. The most significant challenge remains the accurate characterization of low frequencies (below 300 Hz), a limitation particularly critical in the automotive sector where low frequency noise control is fundamental for acoustic comfort. This limitation mainly derives from physical constraints related to instrument dimensions compared to wavelengths involved, suggesting the need for innovative approaches in instrumentation design.

Sensitivity to environmental conditions, particularly evident in the Microflown probe, and the complexity of calibration procedures represent further obstacles to widespread adoption of these techniques. The experience acquired during this study suggests the possibility of developing a proprietary probe that could combine advantages of different technologies: the SonoCat's stability with the Microflown's point precision.

A critical aspect that emerged during the research concerns data interpretation. The absence of a specific standard for in situ measurements makes complex the validation of results and their comparison with traditional methods. The development of more robust algorithms, possibly based on machine learning techniques, could automate and standardize the interpretation of results, reducing dependence on operator experience.

The research opens interesting prospects for application of these techniques in new fields. The building sector, for example, could significantly benefit from continuous monitoring systems of acoustic performance, while the automotive industry could use these techniques for optimizing interior acoustic comfort, particularly by characterizing complex composite materials used in cabin interiors. Moreover, the manufacturing industry could use these techniques for quality control of acoustic materials during production. Integration with numerical simulation techniques, already explored in this study, could be further developed to create more accurate predictive tools.

Particular attention deserves the study of innovative materials, especially those derived from recycling processes. In situ techniques have proved particularly suitable for characterizing these materials, often non-homogeneous and with variable properties. This capability opens new possibilities for the development of sustainable materials with optimized acoustic performance, an increasingly relevant research field in the perspective of circular economy.

Acknowledgements

I would like to express my sincere gratitude to all those who have supported and contributed to this research journey.

My deepest appreciation goes to my supervisor, whose guidance and expertise have been invaluable throughout this work. My sincere gratitude extends to those colleagues who actively participated in my research projects and with whom I developed valuable professional collaborations. Our exchange of ideas, resources, and expertise has been crucial to the development of this work. I am also grateful to research partners who shared their knowledge and time, enriching this study with their valuable insights.

Special thanks to the University of Parma and all the academic and technical staff who provided support and resources essential for this research. I would also like to acknowledge the financial support received through the National Operational Programme Research and Innovation 2014-2020.

Finally, I extend my heartfelt thanks to my husband, family and friends who have believed in me and supported me throughout this journey. Their constant encouragement and understanding have been fundamental to the completion of this work.

This achievement would not have been possible without the contribution of each one of you.

BIBLIOGRAFIA

[1] L. Saccenti, J. Ferrari, D. Pinardi and A. Farina, "Noncontact Measurements of Sound Absorption Coefficient with a Pressure-velocity Probe, a Laser Doppler Vibrometer, and a Microphone Array.," in *I3DA International Conference - Immersive and 3D Audio*, Bologna, DOI:10.1109/I3DA57090.2023.10289528, 2023.

[2] L. Saccenti, E. Armelloni, A. Farina, A. Bevilacqua and L. Lavagna, "In-Situ Measurements of Normal Impedance and Sound Absorption Coefficient of Hard Materials by using a Laser Doppler Vibrometer," in *Audio Engineering Society Convention 153*, New York, 2022.

[3] H.-E. d. Bree, "The Microflown E-book," 2009. [Online]. Available: https://www.microflown.com/resources/e-books/e-book-the-microflown-e-book.

[4] P. Soto, M. Herráez, A. González e J. d. Saja, «Acoustic impedance and absorption coefficient measurements of porous materials used in the automotive industry,» *Polymer Testing,* pp. 77-88, Volume 13, Issue 1, 1994.

[5] F. Pompoli e C. Marescotti, «Misura del coefficiente di assorbimento acustico apparente in campo diffuso secondo la norma UNI EN ISO 354:2003,» Ferrara, 2021.

[6] I. 10534-1:2001, «"Acoustics - Determination of sound absorption coefficient and impedance in impedance tubes - Part 1: Method using standing wave ratio",» International Organization for Standardization (ISO), Geneva, 2001.

[7] I. 10534-2:1998, «"Acoustics - Determination of sound absorption coefficient and impedance in impedance tubes - Part 2: Transfer-function method",» International Organization for Standardization (ISO), Geneva, 1998.

[8] E. Tijs, «Study and development of an in situ acoustic absorption measurement method,» PhD thesis, University of Twente, Enschede, The Netherlands, 2013.

[9] L. Saccenti, «In-Situ Impedance Measurement with Microflown and Laser Doppler Vibrometer,» Università degli Studi di Parma, Parma, 2022.

[10] E. T. a. D. F. C. Peter Cats, «Exploration of the differences between a pressure-velocity based in situ absorption measurement method and the standardized reverberant room method,» *Acoustical Society of America,* pp. Vol19, DOI: 10.1121/1.4798958, 2013.

[11] H.-E. d. B. E. B. Emiel Tijs, «High resolution absorption mapping with a pu surface impedance method,» in *NOISE-CON 2010*, Baltimore, Maryland, 2010.

[12] A. Farina e P. Fausti, «Standing wave techniques for measuring normal incidence absorption coefficient: comparison of different experimental setups,» in *proc. of FASE congress*, Valencia, pp.3-6, 15-17 november, 1994.

[13] T. P. A. P. J. S. D. F. C. Maro Puljizević, «Comparative analysis of acoustic testing methods of a multi-layered material: uncovering the membrane effect,» in *Inter.Noise*, Nantes, France, 2024.

[14] E. T. a. H.-E. d. B. Daniel Fernández Comesaña, «Exploring the properties of acoustic particle velocity sensors for near-field noise source localisation applications,» in *Forum Acusticum*, Krakow, 2014.

[15] T. M. S. D. F. C. Fanyu Meng, «Error analysis of the pu in-situ absorption measurements in terms of background noise,» 2021. [Online]. Available: https://hal.science/hal-03233974v1.

[16] D. F.-C. T. M. S. E. Güven, «Sound intensity-based panel noise contribution analysis for improving the acoustic performance of a vehicle interior,» *Aachen Acoustics Colloquium,* pp. 205-214, 2021.

[17] E. T. M. J. a. G. C. P. Daniel Fernandez Comesana, «A novel in-situ calibration method for acoustic particle velocity sensors based on surface velocity,» in *The 22nd International Congress on Sound and Vibration*, Florence, Italy, 2015.

[18] H.-E. d. B. Tom G. H. Basten, «Full bandwidth calibration procedure for acoustic probes containing a pressure and particle velocity sensor,» *Acoustical Society of America,* pp. 264-270, DOI: 10.1121/1.3268608, 2010.

[19] S. C. R. W. W. Wang, «A Fast Irregular Microphone Array Design Method Based on Acoustic Beamforming,» *IEEE Sensors Journal,* Vol. %1 di %223, no.6, n. DOI: 10.1109/JSEN.2023.3240888, pp. 6156-6168, 2023.

[20] B. R. J. Rathsam, «Analysis of absorption in situ with a spherical microphone array,» *Applied Acoustics,* pp. 273-280, 2015.

[21] P. M. E. A. A. C. Angelo Farina, «Arraydi microfoni per registrazioni musicali in formato 5.1 Surround ed Ambisonics,» Parma, 2006.

[22] L. C. F. C. A. V. P. Brambilla Giovanni, «Visualizzazione 3D del campo acustico mediante un sistema ad array microfonico sferico.,» in *Associazione Italiana di Acustica 34° Convegno Nazionale*, Firenze, 2007.

[23] H. H. C. H. Q. C. H. L. K. Bies A. David, Engineering noise control - sixth edition, Boca Raton (FL): CRC Press, 2024.

[24] F. M. Sipei Zhao, «A circular microphone array with virtual microphones based on acoustics informed neural networks.,» *J. Acoust. Soc. Am,* pp. 405-415, 2024.

[25] G. H. E. S. Artur Paszkiewicz, «Microphone array measurement for the determination of the absorption coefficient,» in *BeBeC Berlin Beamforming Conference*, Berlin, 2020.

[26] F. O. Lorenzo Ferri, Il metodo del beam-forming acustico, Università di Bologna, A.A.2014/2015.

[27] M. M. A. B. Samuel Dupont, «Measurement of sound absorption with a dual-plane array of microphone by an optimization approach.,» in *Forum Acusticum*, Lyon, 2020.

[28] A. B. M. P. F. A. T. A. A. S. M. Olivieri, «Acoustic Imaging With Circular Microphone Array: A New Approach for Sound Field Analysis,» *IEEE/ACM Transactions on Audio, Speech, and Language Processing,* vol. 32, n. DOI: 10.1109/TASLP.2024.3369533, pp. 1750-1761, 2024.

[29] S. S.r.l, «Soundinsight,» [Online]. Available: www.spectra.it.

[30] ". U. M. Soundinsight BV, «Soundinsight,» 2023. [Online]. Available: www.soundinsight.nl.

[31] M. Á. N. D. d. l. P. L. I. A. D.-C. Antonio Pedrero, «On the accuracy of the sound absorption measurement with an impedance gun,» *Applied Acoustics,* vol. 158, n. Doi.org/10.1016/j.apacoust.2019.107039, p. 107039, 2020.

[32] C.-X. B. M. V. Y.-B. Z. R. O. Wang-Lin Lin, «In Situ Measurement of the Absorption Coefficient Based on a Time-Domain Subtraction Technique with a Particle Velocity Transducer,» *Acta Acustica united with Acustica,* vol. 102, n. DOI 10.3813/AAA.919009, pp. 945-954, 2016.

[33] A. Amendola, Analisi spaziale della propagazione del suono nelle sale, Parma: PhD Thesis University of Parma, 2010-2011.

[34] soundinsight, 2024. [Online]. Available: https://soundinsight.nl/wp-content/uploads.

[35] C. M. r. m. 6.1, «Comsol,» 2023. [Online]. Available: https://doc.comsol.com/.

[36] M. H. Jensen, «Acoustics modeling in Comsol Multiphysics,» 2020. [Online]. Available: https://www.comsol.com/blogs.

[37] Z. Enrico, «Design, construction and test of three-dimensional microphone arrays employing MEMS and A2B technologies,» Politecnico Milano, A.A. 2021-2022.

[38] C. t. A. s. o. a. ellipsoid, «Comsol,» [Online]. Available: https://www.comsol.com/models.

[39] D. &. P. R. &. S. F. Pilon, «Behavioral criterion quantifying the edge-constrained effects on foams in the standing wave tube.,» *The Journal of the Acoustical Society of America,* Vol. %1 di %21980-7, n. DOI: 10.1121/1.1598193, p. 114, 2003.

[40] R. P. F. S. Dominic Pilon, «Behavioral criterion quantifying the effects of circumferential air gaps on porous materials in the standing wave tube.,» *The journal of the Acoustical Society of America,* vol. 116(1), n. DOI: 10.1121/1.1756611, pp. 344-356, 2004.

[41] J. C. L. D. R. W. D. Mansour Alkmim, «Angle-dependent sound absorption estimation using a compact microphone array,» *J. Acoust. Soc. Am.,* pp. 2388-2400, 2021.

La borsa di dottorato è stata cofinanziata con risorse del
Programma Operativo Nazionale Ricerca e Innovazione 2014-2020, risorse FSE REACT-EU
Azione IV.4 “Dottorati e contratti di ricerca su tematiche dell’innovazione”
e Azione IV.5 “Dottorati su tematiche Green”

The doctoral scholarship was co-funded with resources from the National Operational Programme
Research and Innovation 2014-2020, FSE REACT-EU resources
Action IV.4 "Doctoral and research contracts on innovation themes"
and Action IV.5 "Doctoral programs on Green themes""